NEUROTOXICITY SCREENING USING HUMAN PLURIPOTENT STEM CELL DERIVED NEURONS AND ASTROCYTES FOR ADVERSE OUTCOME PATHWAY MAPPING

by

XIAN WU

(Under the Direction of Steven L. Stice)

ABSTRACT

There is overwhelming evidence that environmental factors play a role in the development and progression of a host of central nervous system disorders. Of over 80,000 chemicals are commercially available now, only about 200 have undergone developmental neurotoxicity (DNT) testing according the established guidelines. Human embryonic stem cells based DNT assays mimic neuron development in vitro and have become an alternative to expensive and time consuming animal DNT models. The main focus on this study was to establish in vitro human models for adverse outcome pathway mapping. For this main purpose, first study involved mimicking events associated with early human neurogenesis beginning with proliferating human neuron progenitor cells (hNP), progressing through differentiation and maturation of post mitotic neurite extending neurons at 14 days in vitro. The neuron in vitro differentiation model demonstrated neurotoxicant exposure during a maturation continuum affected human neurogenesis including neuron maturation and neurite outgrowth at substantially lower levels than previously known. The 14 day in vitro neuron was further differentiated to a

pure neuron population for high throughput neurite outgrowth toxicity screening. A training set of chemicals including pesticides and endocrine disruptors were tested and their neurotoxicity were validated in the screening, showing the promise of this human model at cellular level for adverse outcome pathway mapping. Finally, these pure neurons were co-cultured with hNP derived astrocytes to study the role of cytochrome P450 in astrocyte neuroprotection. The hNP derived neuron and astroyte co-culture model identify critical role of cytochrome P450 in chlorpyrifos metabolism and indicated cell type specific neurotoxicitity for chlorpyrifos in brain. The hNP derived in vitro cell models in this study showed broad application of hNP derived neurons and astrocytes for DNT study and in the future the cells should be used to replace animal models in order to decrease the uncertainty associated with extrapolating toxicity across species.

INDEX WORDS: Human embryonic stem cells, human neuron progenitor cells, developmental neurotoxicity, astrocyte, cytochrome P450

NEUROTOXICITY SCREENING USING HUMAN PLURIPOTENT STEM CELL DERIVED NEURONS AND ASTROCYTES FOR ADVERSE OUTCOME PATHWAY MAPPING

by

XIAN WU

B.S., Anhui University, P.R.China, 2008

M.S. East China Normal University, P.R.China, 2011

A Dissertation Submitted to the Graduate Faculty of The University of Georgia in Partial Fulfillment of the Requirements for the Degree

DOCTOR OF PHILOSOPHY

ATHENS, GEORGIA

2016

NEUROTOXICITY SCREENING USING HUMAN PLURIPOTENT STEM CELL DERIVED NEURONS AND ASTROCYTES FOR ADVERSE OUTCOME PATHWAY MAPPING

by

XIAN WU

Major Professor:	Steven L. Stice
Committee:	Mary Alice Smith
	Nikolay Filipov
	Franklin West

Electronic Version Approved:

Suzanne Barbour
Dean of the Graduate School
The University of Georgia
December 2016

ACKNOWLEDGEMENTS

I cannot express enough thanks to my committee for their continued support and encouragement: Dr. Steven L. Stice, my committee chair; Dr. Mary Alice Smith; Dr. Nikolay Filipov; and Franklin West. I offer my sincere appreciation for the learning opportunities provided by my committee. My completion of this dissertation could not have been accomplished without the support of my labmates: Anirban Majumder, Robin Webb, Raymond Swetenburg, Forrest Goodfellow, Edith Marie Mckenzie and Christina Elling.

This work would not have been possible without the financial support of US EPA STAR Grant 25-21-RC287-557 and University of Georgia Interdisciplinary Toxicology Program. I would also like to thank Dr R. Tripp's Lab for providing Cellomics ArrayScan VTI HCS reader high-content imaging system and Dr. Michael G. Bartlett and Xiangkun Yang for their participation in the LC-MC metabolite analysis work.

I would specially give my thanks to Dr. Stice for bringing me in UGA toxicology program. As my teacher and mentor, he has taught me more than I could ever give him credit for here. He has shown me what an enthusiastic and patient scientist should be. I would like to thank my parents, whose love and guidance are with me in whatever I pursue.

TABLE OF CONTENTS

Page

LIST OF TABLES

Page

LIST OF FIGURES

Page

CHAPTER 1

Introduction and literature review

Environmental factors affect the development and progression of a host of central nervous system disorders and are likely due to a continuum of exposure in windows of susceptibility (WOS) during and post neural development. Human stem cell based assays may prove to be an alternative in vitro model, mimicking different WOS. The main focus of this study was to characterize endocrine disruptor and pesticide effects during different in vitro neural developmental stages. Characterization began with division and migration of neural progenitor (NP) cells to human Hu protein C and Hu protein D (HuC/D) positive expression early post mitotic neural cells. Homogenous microtubule-associated protein 2 (MAP2) neurons with neurite outgrowth were also characterized for endocrine disruptor and pesticide neurotoxicity screening. Human neural progenitor (hNP) cells are capable of directed independent differentiation into astrocytes, oligodendrocytes and neurons and offer a potential cell source for developmental neurotoxicity (DNT) assays. The hNP cells derived astrocytes and neurons can be co-cultured at ratios to mimic human brain cell composition and interaction. In this study, we developed a defined astrocyte and neuron co-culturing model to study endocrine disruptor and pesticide neurotoxicity and their molecular mechanisms.

Developmental neurotoxicity models

Developmental neurotoxicity is defined as the adverse effect of compounds or xenobiotics on the nervous system associated with exposure during neuron development [1].

Exposure to these compounds or xenobiotics perturb commitment of neural stem cells (NSCs), cell proliferation, cell death, migration or neurite outgrowth. Functional neuronal activity such as synaptogenesis, formation of neurotransmitters and receptors, trimming of connections, myelination, and development of blood-brain barrier (BBB) are all affected [1]. Impairment of the nervous system by developmental neurotoxins lead to a variety of birth defects such as altered behavior, mental retardation, and other neurodevelopmental disabilities [2]. Current in vivo test methods for detecting neurotoxicity and DNT are based on a number of end points including behavioral ontogeny, motor activity, motor and sensory function, learning and memory [3, 4]. Regulators consider behavioral testing crucial for neurotoxicity risk assessment according to Organization for Economic Co-operation and Development (OECD) and USEPA DNT guideline [3].

A resource-intensive traditional toxicity test is the US EPA DNT guideline for identification of chemicals that may pose a hazard to the developing nervous system. The protocol recommends testing for neurobehavioral deficits and neuropathological changes in rats after in utero and lactation exposure, and requires a substantial number of animals and time to complete [5]. However, traditional animal-based models are impractical for screening due to the resource requirements associated with testing large numbers of chemicals. According to the DNT guidelines for the current regulatory test strategy, approximately $1.4 million per substance is needed for a routine DNT assessment of drugs and chemicals [6]. Importantly animal models for neurotoxicity may not be representative of human condition. For example, interspecies differences in central nervous system (CNS) development between animals and human may impair the use of rodents in these models since some of the targets for neurotoxic chemicals are developed postnatally in rodents but prenatally in humans [7]. Developmental neurotoxicants

such as lead, methylmercury, and polychlorinated biphenyl (PCB) induces DNT at lower dose levels in humans than in laboratory animals [8].

Alternative non mammalian models zebrafish and *C. elegans* are particularly suited to address neurotoxicity and DNT endpoints [9]. The ease of obtaining high numbers of progeny, the availability of neuronal tissue specific in vivo reporter strains and the inherent transparency of the embryos make the two model organisms amenable to high-throughput screening (HTS) in vivo. Zebrafish embryo develops rapidly and development of specific neurons and axon tracts can be visualized in live embryos using differential interference contrast (DIC) microscopy or by injecting live dyes [9]. Zebrafish are exceptionally well suited for developmental studies that combine cellular, molecular, and genetic approaches [10]. Quantitative assays can be used to assess a broad range of potential neurological endpoints at cellular level. Assays include brain-specific cell death (apoptosis), commissure patterns and size of axon tracts in the brain and caudal third of the embryo (the tail region of the embryo responsible for movement of the animal), specific toxicity on motor neuron development and number of catecholaminergic neurons in the brain [9].

Adverse outcome pathway (AOP) in developmental neurotoxicity

Animal models provide important information on the effects of toxins at the organ and whole organism level. However, animal models may not be optimal for determination and connection of molecular and cellular events to a toxin or group of toxins. The AOP is a conceptual framework that portrays existing knowledge concerning the linkage between a direct molecular initiating event and an adverse outcome at a level of biological organization relevant to risk assessment [11]. AOP can be used to identify alternative, high-throughput predictive

assays and testing strategies that facilitate identification of uncertainties and corresponding research gaps [12]. Moreover, linked with computational tools for concentration-response extrapolation across multiple levels of biological organization. These alternative assays, once developed and validated will likely provide flexibility in testing based on risk-management needs while at the same time, reduce animal use and study costs [13]. Following is a diagram showing each step in AOP study.

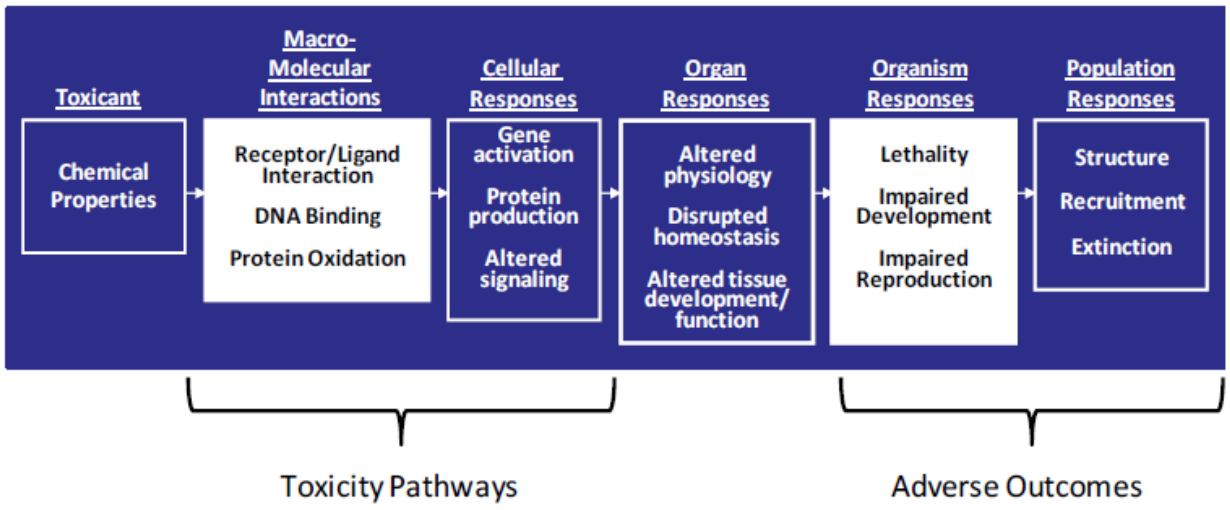

Fig 1.1. A schematic representation of the Adverse Outcome Pathway (AOP) [14, 15]

At the cellular level, human embryonic stem cell (hESC) provides cell sources for cellular decision to proliferate or differentiate as well as migrate [16]. Stem cell in vitro models provide tools to identify toxicity pathways at molecular and cellular level after chemical exposure. Combining existing knowledge of key cellular events with neural disorders or malfunction at the organism level allow the use of stem cell models in DNT AOP. For example, in a retinoic acid–neural tube/axial patterning adverse outcome pathway (RA–NTA AOP) framework, molecular interaction with RA homeostasis are defined as molecular initiation

events. RA then disrupts cell proliferation, migration and neural differentiation using hESC cell model. The cellular events are related to adverse outcomes regarding (dys)morphogenesis of the body axis accompanied by gene down regulation of CYP26a1 and up regulation of Aldh1a2. RA–NTA AOP may allow the detection of a major subset of developmental toxicants targeting on RA homeostasis. All the patterning related genes are regulated by RA exposure in cell culturing models and potentially used as biomarkers of neural tube developmental effects [17].

In vitro DNT assays increase throughput but reduce tissue complexity

To reduce the complexity of the developing nervous system to specific cell and/or molecular events and lower the cost of the HTS model, numerous alternative in vitro methods of DNT testing have been developed including organotypic cultures, re-aggregating brain cell culture, primary dissociated culture, immortalized human and rodent cell lines and stem cell model. Advantages and disadvantages of these models are summarized in the following paragraph. These in vitro alternative methods were incorporated for DNT study and used as international hazard and risk assessment strategies [3, 18].

In organotypic cultures, in vivo–like three-dimensional anatomic and functional organization such as tissue-specific cyto architecture are preserved, neuronal connectivity, electrophysiologic activity, complex glial–neuronal interactions are also present for analysis. Limitations of the models are low throughput comparing to cell models and limited period of culture due to necrosis in the tissue center by limited oxygen and nutrient supply [3, 19-21]. In re-aggregating brain cell culture, neuronal cell types are present corresponding to the original tissue, and all glial cell types and functions are preserved, i.e., astrocytes, oligodendrocytes, microglia, glial cell proliferation and maturation, synaptogenesis, and myelination recapitulate in

vivo development, formation of natural extracellular matrix [3, 22]. The cultures exhibit spontaneous and evoked electrical activity creating the possibility to study microglial cell activation and astroglial reactivity as early markers of neurotoxicity. The model is robust and provides large amount of material for multidisciplinary and multiparametric assays [22]. Disadvantages of the re-aggregating culture models are the original tissue anatomic organization is lost and most neurons are post mitotic at culture initiation comparing to organotypic model. The 3D nature of cell aggregates is generally not suitable for studies at the single-cell level and the model is variable between individual aggregates with respect to size, proportion of neurons versus glial cells, and electrical activity [3].

Transformed cell lines and primary cells are commonly used in DNT assays

Neural cell lines used in DNT assays include rat pheochromocytoma: PC12, rat neuroblastoma: B50, mouse neuroblastoma: NB2a, N2a, N1E-115. In addition, human neuroblastoma: SH-SY5Y, SK-N-SH, IMR-32, LA-N-5 and human embryonal carcinoma cell line NT2 are utilized. These cell lines have been developed for neurotoxic evaluation of metals, pesticides and others like cocaine, ethanol, valproic acid [5]. Cell lines differentially express electrical activity, synthesize various neurotransmitters, and activate associated receptors and ion channels [1]. The cell lines also provide large, reproducible, homogeneous populations for DNT assays. However, since cell lines are derived from tumor or transformed with virus, the original cell phenotype is not consistently replicated. Although cell lines are generally characteristic of neurons, accurate representation of any specific neuronal subpopulation is difficult. For example, neurites elaborated by the PC12 cell line do not exhibit the properties of either axons or dendrites [3]. The models typically contain only one cell type and cell–cell interaction is absent. Moreover,

genetic instability increases with the number of passages. As human cell models with the advantages of human origin and self-renewal (such as NSCs and hNP) become widely accessible, they should be considered in place of cell lines [18].

Primary neuronal cell models use cells dissociated from peripheral or central nervous system tissue. These cells represent morphological, neurochemical, and electrophysiological properties of neurons in situ. When maintained under appropriate culture conditions, primary cells acquire the properties of mature neurons and neurites spontaneously emerged from cell body. The primary culture is committed to a specific lineage in the region of origin, thus providing the advantage of axons and dendrites characteristic of the corresponding cells in situ [1]. Single-cell toxicity assay assessment is easy to obtain and maintain in primary neuronal cell models. The disadvantages of primary neuronal cell models are that prepared neurons are often a mixture of different neuronal populations and have a limited lifespan. It is impossible to expand the primary neuronal cells in culture [23]. Also, three-dimensional tissue organization is lost when primary neural cells are dissociated and cultured [1].

Human embryonic stem cells derived progenitors and derivatives are cell sources for DNT assays

Human NSCs also referred to hNP have a potentially unlimited capacity for proliferation. The hNP cells can generate multiple cell types including neurons and astrocytes. One source of uncertainty in toxicity testing is the extrapolation of data derived from animal tissue to humans, and this uncertainty can be partly eliminated by the use of human neural tissue [24]. The hESC is from inner cell mass of 5–6 days old blastocysts and propagated in tissue culture. In vitro differentiation of these hESC to neural lineage is characterized by formation of neural rosette,

reminiscent of transverse-section of a neural tube [25]. hESC derived hNP cells facilitate an unlimited lineage-restricted cell source for generations of neuronal subtypes and supporting glial cells.

There are two protocols for differentiating hESC into hNP, including embryoid body and adherent differentiation [26]. With longer duration of differentiation in growth factors or morphogens, an embryoid body (EB) is capable of forming a multilayered structure that contains a mixed population of cells including neuron cells. However, during neuron induction and differentiation, EB size varied due to different initial cell numbers and it requires a higher concentration of morphogens in culture to enable the morphogens to reach the innermost layers of the EBs. In addition, being an aggregate of many cells EBs present difficulties in monitoring cell morphology during differentiation[26]. Thus, adherent differentiation of hESC through neural tube-like rosettes using defined growth factor was developed. Neural precursors within rosette formations were isolated by selective enzymatic digestion and further purified on the basis of differential adhesion [26, 27]. Human NP cells were differentiated with a stable expression of NSCs marker nestin in almost all cells [28]. During neural induction and differentiation, several growth factors are involved and play important role for neural fate decision. Stromal-derived activity-mediated differentiation provides an efficient way for neural tissue generation. However, this co-culture technique introduces unknown stromal factors of non-human origin in culture and may obscure the exact mechanisms involved during neural differentiation [26].

Growth factors and morphogens play an important role in ESC neural differentiation

Retinoic acid (RA) plays an important role in many aspects of neural development and activity including organization of the posterior hindbrain and anterior spinal cord [29]. RA also mediates neuronal and glial differentiation occurs by activation of different genes that include transcription factors (BRN2, NFkB, SOX1, SOX6, etc.), cell signaling molecules or associated cell structures (ceramide, PSEN1, MAP2, etc.), and extracellular molecules (WNT signaling members) [29]. As RA is a morphogen, varying concentration may be responsible for generating hNP cell populations with different differentiation potentials. Once the hESC differentiate into hNP cells, the newly formed hNP cells maintain expression of SOX2 and begin expressing other neuroepithelial markers, such as nestin, SOX1, SOX3, PSA-NCAM, and Musashi-1. Similarly, in the dorsal-ventral axis of the neural tube RA works synergistically with other molecules such as sonic hedgehog (SHH), fibroblast growth factors 2 (FGF2), and bone morphogenetic protein (BMP), to determine the fates of sensory neurons, inter neurons, and motor neurons [30]. BMP signaling and FGF2 signaling activation are also involved in neural differentiation. During early embryonic neural specification, FGF2 molecules potentially play two different roles: (1) they may induce a ‘‘pro’’ neural state at an early stage, or (2) while acting as antagonist to BMP signaling, they may stabilize neural identity. Following withdrawal of FGF2, hNP cells differentiate into neurons, astrocytes, and oligodendrocytes [27].

Neural progenitor cells can be isolated and expanded as an enriched population

During in vivo development, the neural plate first forms followed by the neural tube when the human embryo is approximately 3 weeks old [31]. Even though neural rosettes start appearing approximately by day 10 of hESC differentiation, the majority are observed about day

18–21 of differentiation [30]. Therefore, it can be argued that in vivo developmental events in terms of spatial and temporal changes are grossly recapitulated during the in vitro formation of neural rosettes. In vitro differentiation and neural rosette dissociation generate a high percent of nestin positive hNP cells.

Several studies indicate many signaling pathways such as EGF, WNT, Hedgehog, TGFβ, leukemia inhibiting factor (LIF) and FGF2 are important for maintenance of hNP cell proliferation [26]. The hNP cells demonstrate increased proliferation rate when LIF and FGF2 individually and in combination are added to growth medium [32]. Removal of FGF2 from the medium enables differentiation of hNP cells into multiple types of neurons and astro-glial cells [32]. In hNP cells, LIF exerts an effect upon binding to its heterodimeric receptor formed by two protein components: leukemia inhibiting factor receptor (LIFR) and gp130 [33]. The activation of gp130 by LIF is accompanied by the recruitment of activated STAT3 and activation of all three (PI3K/Akt, JAK/STAT, and ERK) pathways which are involved in promotion of growth, invasion, migration. WNT proteins plays a role in many cellular and physiological processes, regulating cell proliferation, differentiation, migration and patterning during development and tissue homeostasis. Basal WNT/β-catenin signaling has been shown to repress neuronal differentiation of human NSCs, and its inhibition promotes neural precursor specification [34]. Switch from WNT/β-catenin to WNT/AP-1 signaling takes place during hNP cell differentiation. WNT-5a has been shown to cooperate with WNT-1 to regulate morphogenesis and neurogenesis during the generation of mouse midbrain dopaminergic (DA) neurons [35]. WNT-4 and WNT-11 play distinct roles in neuronal differentiation of NT2 cells [36]. Inhibition of WNT secretion blocks neuronal differentiation, and its restoration by WNT-3a involves activation of JNK/ATF2 [36].

Human NP cells can uniformly differentiate into neurons

At 14 days after the removal of FGF2 from the culture medium, most hNP cells express MAP2 and class III beta-tubulin (TUJ1) (markers characterizing a post-mitotic neuronal phenotype) as well as neural developmental markers Cdh2 and Gbx2 [28]. Cdh2 is involved in regulation of cortical neuron differentiation in the subventricular zone. Gbx2 participates in early regulation of the midbrain-hindbrain boundary and the development of the midbrain and the cerebellum. NeuroD expression is part of a regulatory pathway that controls early neural differentiation and glutamatergic neurogenesis. It is strongly expressed 14 and 35 days after the removal of FGF2. Expression of these genes in hNP cells differentiated in culture may be indicative of early segmentation of the midbrain and hindbrain regions [28].

Further characterization of these hNP cells differentiated neurons at different stages indicate differentiated hNP cells express subunits of glutamatergic, GABAergic, nicotinic, purinergic and transient potential receptors [28]. Removal of FGF2 from hNP cell cultures leads to a post-mitotic state, and has the capability to produce excitable cells that can generate action potentials, a landmark characteristic of a neuronal phenotype. NMDA *(N-methyl-D-aspartate*) receptor subunits are important for the pruning of developing synapses and are also instrumental in the initiation of many forms of synaptic plasticity. Most functional NMDA receptor subunits contain both Grin1 and Grin2 subunits. Grin1 as well as Grin2b and Grin2d subunit expression increased 14 days after initialization of differentiation by removal of FGF2 [28]. AMPA (α-amino-3-hydroxy-5-methyl-4-isoxazolepropionic acid) receptors are responsible for the initial rapid depolarization in the excitatory postsynaptic potential and are expressed at most excitatory synapses. AMPA receptors lacking subunit transcript Gria2 are calcium permeable while those containing Gria2 have low calcium permeability [28]. Gria2 transcript levels increase in older

cultures suggests that these conditions do allow normal AMPA receptor development in hNP cells. Voltage-gated N-type calcium channels α subunits Cacna1b and Cacna1c as well as β subunit Cacb1 had increased expression after removal of FGF2 as well.

The γ-aminobutyric acid type A ($GABA_A$) receptor is one of the three main classes of receptors activated by GABA, the principal inhibitory neurotransmitter in the central nervous system [37]. Gabrb2, Gabrb3 and Gabrg2 subunits are expressed throughout development while Gabrg1 and Gabrg3 expression decreases as brain development ensues. In vitro differentiation indicated a decrease in all $GABA_A$ receptor subunits in hNP cells and differentiated hNP cells relative to hESCs. Human NP cells do not easily differentiate into peripheral nervous system lineages using these minimal conditions of FGF2 removal [28]. Purinergic receptors when bound with ATP induce fast synaptic potentials. Purinergic receptor subunit P2rx5 is expressed in both hNP cells and differentiated hNP cells. Nicotinic receptors mediate fast synaptic excitation at the neuromuscular junction and are found in neurons in the brain. Nicotinic receptor transcripts α1, α3 and β4 were all induced after FGF2 removal [28]. The capability of differentiated hNP cells to generate action potentials in the minimal culture conditions provides a source of cells that can be maintained with the ease of a cell line and without the upkeep of primary neuronal culture. Thus hNP cell derived neurons represent a population of post-mitotic human neurons containing a mixture of glutamatergic, GABAergic and cholinergic neuron cells.

The hNP cells can generate a mixture of neuron phenotypes expressing TuJ1, GABA, and tyrosine hydroxylase when FGF2 was withdrawn from medium. Using RA, FGF2 and SHH, they could be terminally differentiated into HB9 expressing cells with motor neuron phenotype marked by choline acetyltransferase (ChAT) expression [30]. With different combination of morphogens or factors, hNP cells were induced to various functional neural type or glia cells.

The following is a list of different morphogens used for differentiation of hESC-derived hNP cells to regional subtype cells [32]

Table 1.1 Morphogens in hNP cells differentiation to regional subtype cells

Target population	Morphogens/Factors used	References
To continue as neural progenitors	FGF2, ±EGF	[38], [32]
Neural crest cells; peripheral neurons	SDIA co-culture	[39], [40]
GABA neurons	Neurotrophin-4	[41]
Dopamine neurons	FGF8/Shh followed by ascorbic acid and BDNF	[42]
Serotonin neurons	Same condition as for Dopamine neurons except FGF4 instead of FGF8	[41]
Motoneurons	FGF2, RA, SHH	[43], [44]
Astrocytes	CNTF	[41]
Oligodendrocytes	Triiodothyronine/NT-3 CNTF/PDGF	[30], [45], [32]

hNP cells can differentiate into astrocytes

Human NP derived from pluripotent hESC and propagated in adherent serum-free cultures provide a fate restricted renewable source for quick production of neural cells. However, such cells are resistant to astrocytogenesis and show a strong neurogenic bias, similar to hNP from the early embryonic CNS. Considering that although hESC and induced pluripotent stem cells (hiPSC) are potential sources of unlimited quantities of astrocytes, suitable methods for quick and controlled differentiation of astrocytes from these cells are not available [33].

Human NP derived from ESC/iPSC cells provide unlimited cell source for astrocyte differentiation. With proper epigenetic modulation, these cells express prominent astrocytic markers in as little as 5 days of differentiation. In addition, hNP cells generate highly enriched populations of astrocytes, making it possible to create either neurons or astrocytes from the same

progenitor source. Furthermore, derivation and subsequent maintenance in the same basal media as neurons make these cells amenable to co-culture [33].

LIF and BMP are growth factors implicated in astrocyte specification from hNP cells. LIF signals through its heterodimeric receptor complex, which is composed of LIF receptor (LIFR) and gp130 in hNP [46]. The activation of the downstream janus kinase (JAK)-signal transducer and activator of transcription (STAT) pathway has been shown to induce astrocyte differentiation [47]. BMP also contribute to the expression of astrocyte-specific genes via complex formation between the BMP-downstream transcription factor Smad1 and STATs, bridged by the transcription coactivator p300/CREB-binding protein (CBP) [48]. DNA methylation and histone acetylation regulation is a critical cell-intrinsic determinant of astrocyte differentiation during brain development. Several astrocytic genes are hypermethylated in hNP cells. DNA CpG site (5'—C—phosphate—G—3') dinucleotide within the STAT3 recognition sequence in the glial fibrillary acidic protein (GFAP) gene promoter is highly methylated in hNP cells [49]. Inhibition of DNA methylation and histone deacetylation induces astrocytic differentiation of hNP [49]. RA-induced histone acetylation participates in astrocyte differentiation of hNP cells by facilitating STAT3 binding to an astrocyte-specific gene promoter [50].

Neurite outgrowth assays used in DNT studies

During neural tube formation, neuroepithelial cells give rise to three main types of cells. First, they become the ventricular cells that remain components of neural tube lining. Second, they generate the precursors of the neurons that conduct electric potentials and third they give rise to precursor of the glial cells which aid in the construction of the nervous system [51]. Branching extensions from neuron cell body receive electric impulse from other neuron cell

dendrites. Nerve outgrowth is led by tips of the axon in the growth cone [52]. Growth cones move by elongation and contraction of filopodia known as microspikes. And the microspikes contain microfilaments and disruption of actin in microspikes inhibit further advance of the dendrites and axon [53]. Axons in the developing neuron may extend for several feet for synapse formation [53]. Microtubules support the axon structure and axon elongation is mediated by microtubules while the apical shape is changed by microfilaments [54].

Individual neurons extend a set of neurites (axons and dendrites) that follow chemical guide posts toward appropriate target regions. The control of neurite outgrowth involves interactions among plasma membrane, adhesion molecules and their receptors, the cytoskeleton, intracellular Ca^{2+} concentrations and second messenger systems including protein kinase and phosphatases [55] [56]. Different neurotoxicants disturb one or more of these processes which leads to malfunction of neurite outgrowth. Neurite outgrowth in differentiating hNP cells can be a sensitive endpoint at non-cytotoxic exposure which predicts low dose neurotoxicity [57]. Harrell and coworkers (2010) characterized the cellular phenotype of hESC-derived hN2 (14 day differentiated neuron) and used them in automated high-content image analysis to measure neurite outgrowth in vitro [24]. At 24 hours post-plating hN2 cells express a number of protein markers indicative of a neuronal phenotype, including nestin, βIII-tubulin, MAP 2 and phosphorylated neurofilaments. Concentration-dependent decreases in neurite outgrowth and ATP-content were observed following treatment of hN2 cells with bisindolylmaleimide I and other inhibitors [58]. In another study, neurite outgrowth measurements indicated hNP derived hN2 was more sensitive than rat cortical cultures to chemicals previously shown to inhibit neurite outgrowth [59].

Astrocyte and neuron interaction needed for a more representative DNT assay

The human brain consists of more than 10^{11} neurons associated with over 10^{12} glia cells [60] . Glia cells contribute to homeostasis in the brain by providing neurons with energy and substrates for neurotransmission [61]. Among glia cell population, Astrocytes are now considered far more active than was previously thought and are powerful controllers of synapse formation, function, plasticity and elimination, both in health and disease [62]. Molecules secreted by astrocytes can either inhibit or enhance overall levels of neuronal activity implying astrocytes can affect neurite extension and synapse formation when exposed to neurotoxin in environment [61]. Astrocytes exert protective effects on neuron through the secretion of neurotrophic factors like nerve growth factor, brain-derived neurotrophic factor and glial cell line-derived neurotrophic factor [63]. Astrocytes promote neurite growth by providing various diffusible and nondiffusible proteins. Another important function of astrocytes is active detoxification of foreign substrates, as well as toxification due to reactive metabolites generated during these metabolic processes. In brain astrocytes, various cytochrome P450 (CYP) enzymes exist [64]. These enzymes are reported to be expressed at relatively high levels in astroglial cells and may play a critical role in the biotransformation of endogenous or exogenous compounds. Primary cultures of mouse brain astrocytes indicated CYP2c29 immuno-related CYP isoform was expressed in nearly all culturing astrocytes and perform an essential role in the mediation of toxicity in metabolizing anticonvulsant drug phenytoin to reactive major metabolites dihydrodiol, p-HPPH, and m-HPPH [64].

Endocrine-disrupting compounds affect neural development

Endocrine active compounds (EACs) are substances which interact or interfere with normal hormonal action. When adverse effects occur the substance is labeled as endocrine disruptors. Numerous chemicals, both natural and man-made, are defined as endocrine disruptors and may interfere with the endocrine system producing adverse effects in laboratory animals, wildlife, and humans. Animal studies suggest maternal exposure to endocrine-disrupting chemicals (EDC) produce alterations in rearing behavior, locomotion, anxiety, and learning/memory in offspring, as well as neuronal abnormalities [65]. Endocrine disrupters demonstrate neurotoxic effects on neural development [66].

Testosterone and neural cells

Testosterone acts through activation of the intracellular androgen receptor (AR) [67]. Besides regulating gene expression via the AR, testosterone also produces fast, non-transcriptional responses involving membrane-linked signal transduction pathways[67]. In the brain, testosterone is thought to target several regions, a concept consistent with the widespread distribution of AR [68]. Accumulating evidence suggests testosterone may exert neurotrophic actions. For example, testosterone activates androgen pathways in cultured neural cells, promotes neuronal differentiation and increases neurite outgrowth [69]. Testosterone enhances the neurite outgrowth due to increase in cytosolic Ca^{2+} [70]. In male rodents, testosterone is linked to increases in neuron somal size, neurite growth, plasticity and synaptogenesis in motor neurons of the spinal nucleus of the bulbocavernosus [71]. However, high maternal intrauterine levels of testosterone are associated with autism, attention deficit hyperactivity disorder, oppositional defiant disorder and pervasive developmental disorder [72]. Although testosterone plays a crucial

role in neuronal function, elevated concentrations can have deleterious effects. Micromolar level testosterone concentrations increase the response in neural apoptosis. Elevated testosterone alters InsP3R type 1-mediated intracellular Ca^{2+} signaling plus prolonged Ca^{2+} signals lead to apoptotic cell death [21].

Estrogens and estrogen-like compounds impact neural cells

Estrogens regulate the development, maturation, survival, and function of multiple types of neurons in multiple brain regions. β-estradiol (E2) increased rat embryonic NSCs proliferation, and the response is estrogen receptor (ER) dependent in rat embryonic NSCs isolated from brain striatal tissue [20] . ERα and ERβ are encoded by unique genes located on separate chromosomes. They exhibit distinct brain distribution profiles [73]. The brain region-specific distribution for these receptors is linked to functional distinctions between ERα and ERβ for estrogen-induced neuroprotection, neurotrophic and neurogenic activities. Both estrogen complexes have been observed in rat NP cells and human embryonic NP cells [74], but ERβ is expressed at a higher level in hNP cells [75], and the expression is increased by E2 treatment. Human ESC expresses 5-fold higher ERβ than ERα [74]. E2 induced neuroprotection is regulated through a coordinated signaling cascade. The ER protein interaction with the regulatory subunit (p85) of phosphatidylinositol 3-kinase upon activation, serves as the initiation mechanism for downstream cascades, including AKT and phosphorylated ERK (pERK) [76]. The ERK1/2 cascade is predominant in the control of cell proliferation and differentiation. E2 heightens neuronal responses to lesions, as shown in rodent models for the hippocampal deafferentation of Alzheimer's disease [77]. E2 promotes neurogenesis in the rat brain in vivo and proliferation of NP cells in vitro [77]. In the rodent, E2 induced neurite outgrowth and was

among the first reports of a steroidal impact on the CNS using in vitro tissue culture techniques. Neurite outgrowth is enhanced by E2 in ovariectomized (OVX) female rodents [77]. E2 induced specific gene transcripts which direct neurite growth through ER dependent or independent pathway [78]. E2 acts directly with the MAP kinase signaling pathway in developing neurons. The MAP kinase activating effect of E2 is not blocked by the estrogen receptor antagonist tamoxifen suggesting that other receptors or pathways may be activated [79].

Bisphenol A (BPA) is a high production chemical used in polycarbonate plastics and epoxy resins [80]. The plasticizer is utilized in manufacture of CDs and DVDs, tooth fillings, cash receipts, plastic bottles, inner coatings of cans, and relining of water pipes. Food is the main source of exposure in humans because BPA can migrate from cans coated with epoxy as well as other plastics in contact with food or beverages. BPA is a well-known endocrine disruptor with estrogenic potency. BPA has been acknowledged as an estrogenic chemical able to interact with human ER. Several studies suggest BPA impacts endocrine regulation at low doses. All of these low dose effects of BPA are explained as the output effects of steroid hormone receptors [81]. For example, BPA reduces hepatic metallothionein synthesis and increases damage to the liver after cadmium injection. These effects occur via an ER-mediated mechanism [82]. However, BPA binding to ER and correlation to hormonal activity is extremely weak, making the intrinsic significance of low dose effects obscure [83]. In an ovariectomy rat model, treatment with BPA in a concentration-dependent manner inhibited the estrogen-induced formation of dendritic spine synapses on pyramidal neurons in hippocampal indicating the neurotoxicity of BPA [66]. Prenatal exposure to low-doses of BPA affects the morphology and the expression of some genes related to brain development in the mouse fetal neocortex. The activator-type basic helix-loop-helix (bHLH) genes promote the neuronal fate determination in neural development [84]. The

expression of activator-type bHLH genes was significantly upregulated/disrupted at E14.5 by BPA treatment in mice [85]. The study concluded that BPA possibly disrupts normal neocortical development by accelerating neuronal differentiation/migration. In a rat model, rats were orally administered BPA (50 or 500mg·kg^{-1}/day) from gestational day 10 to postnatal day 14 which is a critical and sensitive period for brain development in the offspring. The male offspring demonstrated impaired spatial learning and memory while locomotor activities and emotionality were not affected [86]. At the cellular level, BPA decreased cell viability and differentiation. Specifically, an increase of apoptotic cell death in undifferentiated PC12 cells and cortical neuronal cells isolated from day 18 of gestation in rat embryos was observed. [87]. ER antagonists did not block these effects. Further investigation of the mechanism revealed BPA significantly activated extracellular signal-regulated kinase (ERK) but inhibited anti-apoptotic nuclear factor kappa B (NF-κB) activation. Neurotoxic effect may not be directly mediated through an ER receptor [88].

The synthetic estrogen diethylstilbestrol (DES) is a potent perinatal endocrine disruptor. DES has been known as a strong synthetic estrogen with agonistic function in ER-α and ER-β [89]. Compared to another endocrine disruptor, DES displayed a two to three fold greater affinity than E2 for nuclear ER [90]. DES has published or regulatory data from humans, non-human primates, and laboratory mammals suggestive of adverse neurological outcomes following developmental exposure [91]. DES is a potent mitogen in vivo in both uterine and pituitary tissues, subsequently, the lesion will perpetuate itself through ER mediated biological response [92]. In utero exposure leads to an increase in vaginal adenocarcinoma around the time of puberty. Prenatal DES exposure inhibited the development of ovarian sympathetic nervous system and was associated with the disruption of follicular maturation. In the DES exposed

ovaries, the tyrosine hydroxylase positive nerve innervation was poor and the innervation density was reduced [93]. Prenatal DES exposure elicits long-lasting changes in the hippocampus as well as cortex, adversely affecting learning and memory formation. Prenatal DES exposure led to a drastic increase in hippocampal calcium/calmodulin-dependent protein kinase II (CaMKII) activity. The exposure is also associated with impairment of protease-activated receptor and enhancement of induction of long-term potentiation in male mice [94]. Perinatal exposure to DES improves olfactory discrimination learning in male and female Swiss-Webster mice [86]. In a human induced pluripotent stem cell-derived neurons model, DES exposure inhibited neurite outgrowth and branch point without inducing cytotoxicity [95].

Pesticides effects on neural cells

Organophosphorus pesticides (OPs) are currently the most commonly utilized insecticides worldwide. Low-level OP exposure is linked to behavioral and cognitive problems in infants and school-aged children. Experimental animal data confirms exposure during critical stages of brain development causes persistent neurobehavioral deficits [96]. One of the OPs most extensively studied in the context of DNT is chlorpyrifos (CPF). It is also one of the most widely used OPs in both developing and industrialized countries, including the United States [97]. In the newborn rat model, CPF exposure during development causes learning deficits and altered locomotor activity at doses that do not elicit acute cholinergic toxicity or significant downregulation of cholinergic receptors [96]. Exposure to apparently subtoxic doses of CPF during late stages of brain development affects DNA synthesis and cell proliferation through a mixture of cholinergic and noncholinergic mechanisms [98]. In the undifferentiated state, CPF evoked an immediate concentration-dependent inhibition of DNA synthesis [99]. Continuous

exposure for up to 24 h maintained the same degree of inhibition [99]. Continuous CPF exposure resulted in severe reductions in macromolecule synthesis including DNA, RNA, protein and a deficit in the total number of cells, effects similar to those seen with CPF treatment in vivo [99]. In mouse N2a cell differentiation model, the outgrowth of axon-like processes was impaired following 4 or 8 h exposure to CPF in both during and post-differentiation experiments [100]. In primary cultures of embryonic rat sympathetic neurons derived from superior cervical ganglia (SCG) following in vitro exposure to CPF, axon outgrowth was significantly inhibited at concentrations >0.001 μM [101]. However, acetylcholinesterase was inhibited only by the highest concentrations of CPF (>1 μM). Thus, CPF perturbs neuronal morphogenesis via an inhibition effect on axonal growth, and it is independent of acetylcholinesterase inhibition [101].

Exposure to CPF can be through multiple routes, including oral, dermal and inhalation [102]. Dermal absorption is low, measured at less than 2% of an applied dose in a controlled human study and likely to be low due to a lack of volatility [102]. However, dermal and inhalation routes of exposure may be important for occupational exposure during manufacture, formulation or use by agricultural workers. CPF may cross the BBB and disrupt BBB integrity and function by altering gene expression for tight junction proteins claudin5, scaffold proteins zona occludens (ZO1) and transient receptor potential (canonical) channels (TRPC4) [103, 104]. CPF blood levels in human are relatively high in farmed region. In a study from Salinas Valley in Monterey County, CA, detected blood CPF ranged from nondetect to 1385ng/mL (~ 4mM) in mothers and from nondetect to1726ng/mL (~5mM) in newborns [105]. The concentrations represented potential neurotoxicity in pregnant women and neonates in the high exposure workplace.

CPF metabolism is mediated by CYP mixed-function oxidases, primarily within the liver. CYP1A2, 2B6, 2C9*1, 2C19, and 3A4 are involved in CPF metabolism. Among all subtypes, CYP2B6 has the highest desulfuration activity (CPF to CPF-oxon) whereas dearylation activity is highest for 2C19 (CPF to TCP). And CYP3A4 has high activity for both dearylation and desulfuration [106]. However, supplementary metabolic systems have been reported in other tissues including the brain. Following dermal and inhalation routes, the pharmacokinetic and pharmacodynamic profile of the metabolites are likely to be very different since first pass liver metabolism, which includes both bioactivation and detoxification. CPF is highly metabolized by CYP via detoxification route of trichloropyridinol (TCP) and to the active CPF-oxon [107]. Studies in humans indicated that TCP represents the primary metabolite of CPF [108, 109]. Biomonitoring for CPF exposures generally involves measurement of the stable metabolite TCP or red blood cell cholinesterase inhibition. CPF and CPF-oxon, but not TCP, are relatively potent inhibitors of axonal growth. In contrast, CPF, CPFO, and TCP all enhanced dendritic growth but at higher concentrations [110].

Pyrethroid insecticides, synthetic type I pyrethroid like permethrin, are one of the most commonly used residential and agricultural insecticides. The study in developing zebrafish model found permethrin exposure led to behavioral defects presented as spastic movements, defined as sudden and uncontrolled body movements that were clearly different from normal swimming behaviors [111]. Fetal exposure to permethrin causes curvature of the body axis and spasms which were neuronal in origin. Permethrin alters neurite outgrowth in a dose-dependent manner, at concentrations similar to those that inhibit other physiological parameters such as Ca^{2+}-ATPase [112]. Permethrin also inhibited neurite initiation and elongation in chick embryo brain neurons [112]. Permethrin may affect neurite outgrowth by altering intracellular calcium

either indirectly, through effects on voltage-sensitive sodium channels, or directly, through effects on calcium dependent processes [112]. Permethrin may act by increasing intracellular calcium to a level greater than optimum for neurite growth [112, 113].

Retinoic acid is an essential factor derived from vitamin A and has a variety of functions including roles as an antioxidant and in cellular differentiation [114]. Retinoids are stored in liver and in several extrahepatic sites and released to target cells. Once bound retinol-binding protein 1, cellular (RBP1) metabolizes in a two-step process to all-trans RA [115]. In embryos, retinol dehydrogenase 10 (RDH10) metabolizes retinol to retinaldehyde (Ral), followed by metabolism to RA by retinaldehyde dehydrogenases (RALDHs) [115]. Retinol-binding proteins assist RA translocation in the nucleus, RA binds to RA receptors (RARs) and retinoid X receptors (RXRs), which heterodimerize and bind to a sequence of DNA known as the retinoic acid-response element (RARE) [29]. This binding activates the transcription of target genes. RA is catabolized in the cytoplasm by CYP26 of CTP family [116].

Retinoic acid is known as morphogen and is involved in neuronal patterning, neural differentiation and axon outgrowth [115, 117]. RA contributes to both the anteroposterior and dorsoventral patterning of the neural plate and neural tube. In the anteroposterior axis of the neural plate, RA, along with WNTs and FGFs, is specifically responsible for the organization of the posterior hindbrain and the anterior spinal cord [115]. In the dorsoventral axis of the developing neural tube, RA is generated by the newly formed somites along with sonic hedgehog (SHH), bone morphogenetic proteins (BMPs), and FGFs, which are expressed at the posterior end of the extending neural tube. ESCs, hematopoietic stem cells and NSCs can be diverted down the neural differentiation route using combinations of RA, growth factors or neurotrophins

[118]. The role of RA in differentiation in vivo is best exemplified by two aspects: the regulation of primary neuron number and the regulation of motor-neuron differentiation.

Retinoic acid is also a well-known teratogenic agent. In vivo neural tube formation and closure is a critical step of embryonic development, and neural tube defects (NTDs) are one of the most common birth defects, affecting on average 0.5–2 newborns per 1000 births [119]. There is clear evidence pharmacological treatments with RA during pregnancy can result in NTDs or in altered neural development syndromes [120]. Both deficiency and excess of RA induce developmental related defects. RA exposure inhibits the movement of neural crest cells and disrupts their migratory pattern [121].

In vitro models include the generation of neural rosettes, representing the in vitro counterpart of the developing neural plate and neural tube is disrupted. Neural rosette forming cells respond to RA with clear concentration-dependent morphological alterations [120]. Gene expression changes are remarkably similar to those induced in vivo by RA exposure in the developing neural tube. hESC derived neural rosettes respond to RA exposure with decreased viability and decreased neural rosette formation at a concentration of 2μM [120]. At lower concentrations ranging from 200 to 20nM RA induced the formation of thicker neural rosettes and cell viability was not inhibited [120].

Specific aims

There has been a rise in the number of infants and children identified with some form of neurodevelopmental abnormality [122]. Some environmental chemicals have been clearly shown to result in damage to the developing brain in both humans and animals e.g. lead, methylmercury, polychlorinated biphenyls (PCB), chlorpyrifos and DDT. Routine testing of all

chemicals with potential for human exposure is warranted. In response to the limitations imposed by the use of animal-based testing, there has been a surge in the development of alternative assays based on in vitro and small non-mammalian test systems that are more efficient in terms of throughput and cost. Select chemicals are known to induce DNT in humans, the so called "gold standards". The chemicals selected in this research are those with demonstrated effects in animals based on peer-reviewed literature and U.S. EPA DNT guideline studies. We hypothesize hESC derived neurons and astrocytes will act as multicellular in vitro DNT testing platform. Neuron proliferation, maturation and functional neurite outgrowth are useful in investigating potential toxins during early human neural WOS. To confirm the hypothesis, we set three specific aims.

Aim 1: Characterize the continuum of neuron maturation and neurite outgrowth based on immunostaining and high content analysis.

Aim 2: Determine developmental neurotoxicity of endocrine active compounds and pesticides in a novel neurite outgrowth model.

Aim 3: Determine astrocyte and neuron interactions in co-culture system and quantify astrocyte effect on DNT during exposure to neurotoxins.

References

1. Coecke, S., et al., *Workgroup report: incorporating in vitro alternative methods for developmental neurotoxicity into international hazard and risk assessment strategies.* Environ Health Perspect, 2007. **115**(6): p. 924-31.
2. Sanders, T., et al., *Neurotoxic effects and biomarkers of lead exposure: a review.* Rev Environ Health, 2009. **24**(1): p. 15-45.
3. Coecke, S., et al., *Workgroup report: Incorporating in vitro alternative methods for developmental neurotoxicity into international hazard and risk assessment strategies.* Environmental Health Perspectives, 2007. **115**(6): p. 924-931.
4. Smirnova, L., et al., *Developmental Neurotoxicity - Challenges in the 21st Century and In Vitro Opportunities.* Altex-Alternatives to Animal Experimentation, 2014. **31**(2): p. 129-156.
5. Radio, N.M. and W.R. Mundy, *Developmental neurotoxicity testing in vitro: models for assessing chemical effects on neurite outgrowth.* Neurotoxicology, 2008. **29**(3): p. 361-76.
6. Hogberg, H.T., et al., *Toward a 3D model of human brain development for studying gene/environment interactions.* Stem Cell Res Ther, 2013. **4 Suppl 1**: p. S4.
7. Andersen, H.R., J.B. Nielsen, and P. Grandjean, *Toxicologic evidence of developmental neurotoxicity of environmental chemicals.* Toxicology, 2000. **144**(1-3): p. 121-127.
8. Andersen, H.R., J.B. Nielsen, and P. Grandjean, *Toxicologic evidence of developmental neurotoxicity of environmental chemicals.* Toxicology, 2000. **144**(1-3): p. 121-7.
9. Ton, C., Y.X. Lin, and C. Willett, *Zebrafish as a model for developmental neurotoxicity testing.* Birth Defects Research Part a-Clinical and Molecular Teratology, 2006. **76**(7): p. 553-567.
10. Nishimura, Y., et al., *Zebrafish as a systems toxicology model for developmental neurotoxicity testing.* Congenital Anomalies, 2015. **55**(1): p. 1-16.
11. Ankley, G.T., et al., *Adverse outcome pathways: a conceptual framework to support ecotoxicology research and risk assessment.* Environ Toxicol Chem, 2010. **29**(3): p. 730-41.
12. Volz, D.C., et al., *Adverse outcome pathways during early fish development: a conceptual framework for identification of chemical screening and prioritization strategies.* Toxicol Sci, 2011. **123**(2): p. 349-58.
13. Yozzo, K.L., S.P. McGee, and D.C. Volz, *Adverse outcome pathways during zebrafish embryogenesis: a case study with paraoxon.* Aquat Toxicol, 2013. **126**: p. 346-54.
14. Yozzo, K.L., S.P. McGee, and D.C. Volz, *Adverse outcome pathways during zebrafish embryogenesis: A case study with paraoxon.* Aquatic Toxicology, 2013. **126**: p. 346-354.
15. Schultz, T.W., *Adverse Outcome Pathways: A Way of Linking Chemical Structure to In Vivo Toxicological Hazards.* In Silico Toxicology: Principles and Applications, 2010. **7**: p. 346-371.
16. Theveneau, E. and R. Mayor, *Neural crest migration: interplay between chemorepellents, chemoattractants, contact inhibition, epithelial-mesenchymal transition, and collective cell migration.* Wiley Interdisciplinary Reviews-Developmental Biology, 2012. **1**(3): p. 435-445.

17. Tonk, E.C., J.L. Pennings, and A.H. Piersma, *An adverse outcome pathway framework for neural tube and axial defects mediated by modulation of retinoic acid homeostasis.* Reprod Toxicol, 2015. **55**: p. 104-13.
18. Radio, N.M. and W.R. Mundy, *Developmental neurotoxicity testing in vitro: Models for assessing chemical effects on neurite outgrowth.* Neurotoxicology, 2008. **29**(3): p. 361-376.
19. Braun, H., et al., *Preparation of a tissue-like cortical primary culture from embryonic rats using Matrigel and serum free Start V Medium.* Journal of Neuroscience Methods, 2006. **157**(1): p. 32-38.
20. Brannvall, K., L. Korhonen, and D. Lindholm, *Estrogen-receptor-dependent regulation of neural stem cell proliferation and differentiation.* Molecular and Cellular Neuroscience, 2002. **21**(3): p. 512-520.
21. Estrada, M., A. Varshney, and B.E. Ehrlich, *Elevated testosterone induces apoptosis in neuronal cells.* J Biol Chem, 2006. **281**(35): p. 25492-501.
22. Braissant, O., et al., *Ammonium-induced impairment of axonal growth is prevented through glial creatine.* Journal of Neuroscience, 2002. **22**(22): p. 9810-9820.
23. Banker, G. and K. Goslin, *Developments in Neuronal Cell-Culture.* Nature, 1988. **336**(6195): p. 185-186.
24. Harrill, J.A., et al., *Quantitative assessment of neurite outgrowth in human embryonic stem cell-derived hN2 (TM) cells using automated high-content image analysis.* Neurotoxicology, 2010. **31**(3): p. 277-290.
25. Wilson, P.G. and S.S. Stice, *Development and differentiation of neural rosettes derived from human embryonic stem cells.* Stem Cell Reviews, 2006. **2**(1): p. 67-77.
26. Dhara, S.K. and S.L. Stice, *Neural differentiation of human embryonic stem cells.* J Cell Biochem, 2008. **105**(3): p. 633-40.
27. Zhang, S.C., et al., *In vitro differentiation of transplantable neural precursors from human embryonic stem cells.* Nat Biotechnol, 2001. **19**(12): p. 1129-33.
28. Young, A., et al., *Ion Channels and Ionotropic Receptors in Human Embryonic Stem Cell Derived Neural Progenitors.* Neuroscience, 2011. **192**: p. 793-805.
29. Maden, M., *Retinoic acid in the development, regeneration and maintenance of the nervous system.* Nat Rev Neurosci, 2007. **8**(10): p. 755-65.
30. Dhara, S.K. and S.L. Stice, *Neural Differentiation of Human Embryonic Stem Cells.* Journal of Cellular Biochemistry, 2008. **105**(3): p. 633-640.
31. Orahilly, R. and F. Muller, *Neurulation in the Normal Human Embryo.* Neural Tube Effects, 1994. **181**: p. 70-82.
32. Shin, S.J., et al., *Long-term proliferation of human embryonic stem cell-derived neuroepithelial cells using defined adherent culture conditions.* Stem Cells, 2006. **24**(1): p. 125-138.
33. Majumder, A., et al., *Neurotrophic Effects of Leukemia Inhibitory Factor on Neural Cells Derived from Human Embryonic Stem Cells.* Stem Cells, 2012. **30**(11): p. 2387-2399.
34. Wexler, E.M., et al., *Endogenous Wnt Signaling Maintains Neural Progenitor Cell Potency.* Stem Cells, 2009. **27**(5): p. 1130-1141.
35. Andersson, E.R., et al., *Wnt5a cooperates with canonical Wnts to generate midbrain dopaminergic neurons in vivo and in stem cells.* Proc Natl Acad Sci U S A, 2013. **110**(7): p. E602-10.

36. Elizalde, C., et al., *Distinct roles for Wnt-4 and Wnt-11 during retinoic acid-induced neuronal differentiation.* Stem Cells, 2011. **29**(1): p. 141-53.
37. Srivastava, S., et al., *A Novel Variant in GABRB2 Associated with Intellectual Disability and Epilepsy.* American Journal of Medical Genetics Part A, 2014. **164**(11): p. 2914-2921.
38. Elkabetz, Y., et al., *Human ES cell-derived neural rosettes reveal a functionally distinct early neural stem cell stage (vol 22, pg 152, 2008).* Genes & Development, 2008. **22**(9): p. 1257-1257.
39. Lee, G., et al., *Isolation and directed differentiation of neural crest stem cells derived from human embryonic stem cells.* Nature Biotechnology, 2007. **25**(12): p. 1468-1475.
40. Pomp, O., et al., *Generation of peripheral sensory and sympathetic neurons and neural crest cells from human embryonic stem cells.* Stem Cells, 2005. **23**(7): p. 923-930.
41. Barberi, T., et al., *Neural subtype specification of fertilization and nuclear transfer embryonic stem cells and application in parkinsonian mice.* Nature Biotechnology, 2003. **21**(10): p. 1200-1207.
42. Perrier, A.L., et al., *Derivation of midbrain dopamine neurons from human embryonic stem cells.* Proceedings of the National Academy of Sciences of the United States of America, 2004. **101**(34): p. 12543-12548.
43. Li, X.J., et al., *Specification of motoneurons from human embryonic stem cells.* Nature Biotechnology, 2005. **23**(2): p. 215-221.
44. Shin, S., S. Dalton, and S.L. Stice, *Human motor neuron differentiation from human embryonic stem cells.* Stem Cells and Development, 2005. **14**(3): p. 266-269.
45. Keirstead, H.S., et al., *Human embryonic stem cell-derived oligodendrocyte progenitor cell transplants remyelinate and restore locomotion after spinal cord injury.* Journal of Neuroscience, 2005. **25**(19): p. 4694-4705.
46. Nakamura, T., et al., *A selective switch-on system for self-renewal of embryonic stem cells using chimeric cytokine receptors.* Biochemical and Biophysical Research Communications, 1998. **248**(1): p. 22-27.
47. Shaltouki, A., et al., *Efficient Generation of Astrocytes from Human Pluripotent Stem Cells in Defined Conditions.* Stem Cells, 2013. **31**(5): p. 941-952.
48. Shaltouki, A., et al., *Efficient generation of astrocytes from human pluripotent stem cells in defined conditions.* Stem Cells, 2013. **31**(5): p. 941-52.
49. Majumder, A., et al., *Inhibition of DNA methyltransferases and histone deacetylases induces astrocytic differentiation of neural progenitors.* Stem Cell Res, 2013. **11**(1): p. 574-86.
50. Asano, H., et al., *Astrocyte Differentiation of Neural Precursor Cells is Enhanced by Retinoic Acid Through a Change in Epigenetic Modification.* Stem Cells, 2009. **27**(11): p. 2744-2752.
51. Yamashita, M., *From neuroepithelial cells to neurons: changes in the physiological properties of neuroepithelial stem cells.* Arch Biochem Biophys, 2013. **534**(1-2): p. 64-70.
52. Letourneau, P.C., *Cell-substratum adhesion of neurite growth cones, and its role in neurite elongation.* Exp Cell Res, 1979. **124**(1): p. 127-38.
53. Bray, D. and K. Chapman, *Analysis of microspike movements on the neuronal growth cone.* J Neurosci, 1985. **5**(12): p. 3204-13.

54. Maeder, C.I., K. Shen, and C.C. Hoogenraad, *Axon and dendritic trafficking.* Curr Opin Neurobiol, 2014. **27**: p. 165-70.
55. Anglister, L., et al., *Localization of voltage-sensitive calcium channels along developing neurites: their possible role in regulating neurite elongation.* Dev Biol, 1982. **94**(2): p. 351-65.
56. Maness, P.F. and W.T. Matten, *Tyrosine phosphorylation of membrane-associated tubulin in nerve growth cones enriched in pp60c-src.* Ciba Found Symp, 1990. **150**: p. 57-69; discussion 69-78.
57. Jeerage, K.M., T.L. Oreskovic, and S.L. Hume, *Neurite outgrowth and differentiation of rat cortex progenitor cells are sensitive to lithium chloride at non-cytotoxic exposures.* Neurotoxicology, 2012. **33**(5): p. 1170-9.
58. Harrill, J.A., et al., *Quantitative assessment of neurite outgrowth in human embryonic stem cell-derived hN2 cells using automated high-content image analysis.* Neurotoxicology, 2010. **31**(3): p. 277-90.
59. Harrill, J.A., et al., *Comparative sensitivity of human and rat neural cultures to chemical-induced inhibition of neurite outgrowth.* Toxicol Appl Pharmacol, 2011. **256**(3): p. 268-80.
60. Bass, N.H., et al., *Quantitative cytoarchitectonic distribution of neurons, glia, and DNA in rat cerebral cortex.* J Comp Neurol, 1971. **143**(4): p. 481-90.
61. Allen, N.J. and B.A. Barres, *NEUROSCIENCE Glia - more than just brain glue.* Nature, 2009. **457**(7230): p. 675-677.
62. Eroglu, C. and B.A. Barres, *Regulation of synaptic connectivity by glia.* Nature, 2010. **468**(7321): p. 223-231.
63. Hansebout, C.R., et al., *Enteric glia mediate neuronal outgrowth through release of neurotrophic factors.* Neural Regeneration Research, 2012. **7**(28): p. 2165-2175.
64. Meyer, R.P., et al., *Possible function of astrocyte cytochrome P450 in control of xenobiotic phenytoin in the brain: in vitro studies on murine astrocyte primary cultures.* Exp Neurol, 2001. **167**(2): p. 376-84.
65. Masuo, Y. and M. Ishido, *Neurotoxicity of endocrine disruptors: possible involvement in brain development and neurodegeneration.* J Toxicol Environ Health B Crit Rev, 2011. **14**(5-7): p. 346-69.
66. MacLusky, N.J., T. Hajszan, and C. Leranth, *The environmental estrogen bisphenol a inhibits estradiol-induced hippocampal synaptogenesis.* Environ Health Perspect, 2005. **113**(6): p. 675-9.
67. Kadi, F., *Cellular and molecular mechanisms responsible for the action of testosterone on human skeletal muscle. A basis for illegal performance enhancement.* Br J Pharmacol, 2008. **154**(3): p. 522-8.
68. Simerly, R.B., et al., *Distribution of androgen and estrogen receptor mRNA-containing cells in the rat brain: an in situ hybridization study.* J Comp Neurol, 1990. **294**(1): p. 76-95.
69. Lustig, R.H., et al., *An in vitro model for the effects of androgen on neurons employing androgen receptor-transfected PC12 cells.* Mol Cell Neurosci, 1994. **5**(6): p. 587-96.
70. Estrada, M., P. Uhlen, and B.E. Ehrlich, *Ca2+ oscillations induced by testosterone enhance neurite outgrowth.* J Cell Sci, 2006. **119**(Pt 4): p. 733-43.
71. Bialek, M., et al., *Neuroprotective role of testosterone in the nervous system.* Pol J Pharmacol, 2004. **56**(5): p. 509-18.

72. James, W.H., *Further evidence that some male-based neurodevelopmental disorders are associated with high intrauterine testosterone concentrations.* Dev Med Child Neurol, 2008. **50**(1): p. 15-8.
73. Matthews, J. and J.A. Gustafsson, *Estrogen signaling: a subtle balance between ER alpha and ER beta.* Mol Interv, 2003. **3**(5): p. 281-92.
74. Hong, S.H., et al., *Expression of estrogen receptor-alpha and -beta, glucocorticoid receptor, and progesterone receptor genes in human embryonic stem cells and embryoid bodies.* Mol Cells, 2004. **18**(3): p. 320-5.
75. Brannvall, K., L. Korhonen, and D. Lindholm, *Estrogen-receptor-dependent regulation of neural stem cell proliferation and differentiation.* Mol Cell Neurosci, 2002. **21**(3): p. 512-20.
76. Mannella, P. and R.D. Brinton, *Estrogen receptor protein interaction with phosphatidylinositol 3-kinase leads to activation of phosphorylated Akt and extracellular signal-regulated kinase 1/2 in the same population of cortical neurons: a unified mechanism of estrogen action.* J Neurosci, 2006. **26**(37): p. 9439-47.
77. Rozovsky, I., et al., *Estradiol (E2) enhances neurite outgrowth by repressing glial fibrillary acidic protein expression and reorganizing laminin.* Endocrinology, 2002. **143**(2): p. 636-646.
78. Heldring, N., et al., *Estrogen receptors: How do they signal and what are their targets.* Physiological Reviews, 2007. **87**(3): p. 905-931.
79. Mccarthy, M.M., *Estradiol and the developing brain.* Physiological Reviews, 2008. **88**(1): p. 91-124.
80. Tamschick, S., et al., *The plasticizer bisphenol A affects somatic and sexual development, but differently in pipid, hylid and bufonid anurans.* Environ Pollut, 2016. **216**: p. 282-291.
81. Welshons, W.V., et al., *Large effects from small exposures. I. Mechanisms for endocrine-disrupting chemicals with estrogenic activity.* Environ Health Perspect, 2003. **111**(8): p. 994-1006.
82. Sogawa, N., et al., *Bisphenol A enhances cadmium toxicity through estrogen receptor.* Methods and Findings in Experimental and Clinical Pharmacology, 2001. **23**(7): p. 395-399.
83. Takayanagi, S., et al., *Endocrine disruptor bisphenol A strongly binds to human estrogen-related receptor gamma (ERRgamma) with high constitutive activity.* Toxicol Lett, 2006. **167**(2): p. 95-105.
84. Kageyama, R., et al., *Roles of bHLH genes in neural stem cell differentiation.* Experimental Cell Research, 2005. **306**(2): p. 343-348.
85. Nakamura, K., et al., *Murine neocortical histogenesis is perturbed by prenatal exposure to low doses of bisphenol A.* Journal of Neuroscience Research, 2006. **84**(6): p. 1197-1205.
86. Kuwahara, R., et al., *Perinatal Exposure to Low-Dose Bisphenol A Impairs Spatial Learning and Memory in Male Rats.* Journal of Pharmacological Sciences, 2013. **123**(2): p. 132-139.
87. Lee, Y.M., et al., *Estrogen receptor independent neurotoxic mechanism of bisphenol A, an environmental estrogen.* Journal of Veterinary Science, 2007. **8**(1): p. 27-38.

88. Seki, S., et al., *Bisphenol-A suppresses neurite extension due to inhibition of phosphorylation of mitogen-activated protein kinase in PC12 cells.* Chem Biol Interact, 2011. **194**(1): p. 23-30.
89. Nam, K., et al., *Simulation of the different biological activities of diethylstilbestrol (DES) on estrogen receptor alpha and estrogen-related receptor gamma.* Biopolymers, 2003. **68**(1): p. 130-8.
90. Okulicz, W.C. and L.D. Johnson, *The relative binding affinity of diethylstilbestrol to uterine nuclear estrogen receptor: effect of serum and serum albumin.* Proc Soc Exp Biol Med, 1987. **185**(4): p. 478-83.
91. Smirnova, L., et al., *Developmental neurotoxicity - challenges in the 21st century and in vitro opportunities.* ALTEX, 2014. **31**(2): p. 129-56.
92. Korach, K.S. and J.A. McLachlan, *The role of the estrogen receptor in diethylstilbestrol toxicity.* Arch Toxicol Suppl, 1985. **8**: p. 33-42.
93. Shinohara, Y., A. Matsumoto, and T. Mori, *Effects of prenatal exposure to diethylstilbestrol on the sympathetic nervous system in the rat ovary.* Neuroscience Letters, 1998. **255**(3): p. 123-126.
94. Kaitsuka, T., et al., *Changes in Ca2+/calmodulin-dependent protein kinase II activity and its relation to performance in passive avoidance response and long-term potentiation formation in mice prenatally exposed to diethylstilbestrol.* Neuroscience, 2007. **144**(4): p. 1415-1424.
95. Ryan, K.R., et al., *Neurite outgrowth in human induced pluripotent stem cell-derived neurons as a high-throughput screen for developmental neurotoxicity or neurotoxicity.* Neurotoxicology, 2016. **53**: p. 271-281.
96. Yang, D., et al., *Chlorpyrifos-oxon disrupts zebrafish axonal growth and motor behavior.* Toxicol Sci, 2011. **121**(1): p. 146-59.
97. Yang, D.R., et al., *Chlorpyrifos-Oxon Disrupts Zebrafish Axonal Growth and Motor Behavior.* Toxicological Sciences, 2011. **121**(1): p. 146-159.
98. Song, X., et al., *Modeling the developmental neurotoxicity of chlorpyrifos in vitro: Macromolecule synthesis in PC12 cells.* Toxicology and Applied Pharmacology, 1998. **151**(1): p. 182-191.
99. Song, X., et al., *Modeling the developmental neurotoxicity of chlorpyrifos in vitro: macromolecule synthesis in PC12 cells.* Toxicol Appl Pharmacol, 1998. **151**(1): p. 182-91.
100. Sachana, M., et al., *The toxicity of chlorpyrifos towards differentiating mouse N2a neuroblastoma cells.* Toxicol In Vitro, 2001. **15**(4-5): p. 369-72.
101. Howard, A.S., et al., *Chlorpyrifos exerts opposing effects on axonal and dendritic growth in primary neuronal cultures.* Toxicol Appl Pharmacol, 2005. **207**(2): p. 112-24.
102. Poet, T.S., et al., *Chlorpyrifos PBPK/PD model for multiple routes of exposure.* Xenobiotica, 2014. **44**(10): p. 868-881.
103. Parran, D.K., et al., *Chlorpyrifos alters functional integrity and structure of an in vitro BBB model: Co-cultures of bovine endothelial cells and neonatal rat astrocytes.* Neurotoxicology, 2005. **26**(1): p. 77-88.
104. Li, W. and M. Ehrich, *Transient alterations of the blood-brain barrier tight junction and receptor potential channel gene expression by chlorpyrifos.* Journal of Applied Toxicology, 2013. **33**(10): p. 1187-1191.

105. Huen, K., et al., *Organophosphate pesticide levels in blood and urine of women and newborns living in an agricultural community.* Environmental Research, 2012. **117**: p. 8-16.
106. Foxenberg, R.J., et al., *Human hepatic cytochrome P450-specific metabolism of parathion and chlorpyrifos.* Drug Metabolism and Disposition, 2007. **35**(2): p. 189-193.
107. Lee, S., et al., *Effects of nicotine exposure on in vitro metabolism of chlorpyrifos in male Sprague-Dawley rats.* J Toxicol Environ Health A, 2009. **72**(2): p. 74-82.
108. Bakke, J.E. and C.E. Price, *Metabolism of O,O-Dimethyl-O-(3,5,6-Trichloro-2-Pyridyl) Phosphorothioate in Sheep and Rats and of 3,5,6-Trichloro-2-Pyridinol in Sheep.* Journal of Environmental Science and Health Part B-Pesticides Food Contaminants and Agricultural Wastes, 1976. **11**(1): p. 9-22.
109. Nolan, R.J., et al., *Chlorpyrifos - Pharmacokinetics in Human Volunteers.* Toxicology and Applied Pharmacology, 1984. **73**(1): p. 8-15.
110. Howard, A.S., et al., *Chlorpyrifos exerts opposing effects on axonal and dendritic growth in primary neuronal cultures.* Toxicology and Applied Pharmacology, 2005. **207**(2): p. 112-124.
111. DeMicco, A., et al., *Developmental neurotoxicity of pyrethroid insecticides in zebrafish embryos.* Toxicol Sci, 2010. **113**(1): p. 177-86.
112. Ferguson, C.A. and G. Audesirk, *Effects of DDT and permethrin on neurite growth in cultured neurons of chick embryo brain and Lymnaea stagnalis.* Toxicol In Vitro, 1990. **4**(1): p. 23-30.
113. Komulainen, H. and S.C. Bondy, *Modulation of Levels of Free Calcium within Synaptosomes by Organochlorine Insecticides.* Journal of Pharmacology and Experimental Therapeutics, 1987. **241**(2): p. 575-581.
114. Lee, H.P., et al., *All-trans retinoic acid as a novel therapeutic strategy for Alzheimer's disease.* Expert Review of Neurotherapeutics, 2009. **9**(11): p. 1615-1621.
115. Maden, M., *Retinoic acid in the development, regeneration and maintenance of the nervous system.* Nature Reviews Neuroscience, 2007. **8**(10): p. 755-765.
116. Thatcher, J.E. and N. Isoherranen, *The role of CYP26 enzymes in retinoic acid clearance.* Expert Opinion on Drug Metabolism & Toxicology, 2009. **5**(8): p. 875-886.
117. Lu, J.F., et al., *All-trans retinoic acid promotes neural lineage entry by pluripotent embryonic stem cells via multiple pathways.* Bmc Cell Biology, 2009. **10**.
118. Levenberg, S., et al., *Neurotrophin-induced differentiation of human embryonic stem cells on three-dimensional polymeric scaffolds.* Tissue Eng, 2005. **11**(3-4): p. 506-12.
119. Greene, N.D. and A.J. Copp, *Development of the vertebrate central nervous system: formation of the neural tube.* Prenat Diagn, 2009. **29**(4): p. 303-11.
120. Colleoni, S., et al., *Development of a neural teratogenicity test based on human embryonic stem cells: response to retinoic acid exposure.* Toxicol Sci, 2011. **124**(2): p. 370-7.
121. Williams, S.S., et al., *Large-scale reprogramming of cranial neural crest gene expression by retinoic acid exposure.* Physiol Genomics, 2004. **19**(2): p. 184-97.
122. Szpir, M., *New thinking on neurodevelopment.* Environ Health Perspect, 2006. **114**(2): p. A100-7.

CHAPTER 2

High content imaging quantification of multiple in vitro human neurogenesis events after neurotoxin exposure[1]

[1]Xian Wu, Anirban Majumder, Robin Webb, Steven L. Stice 2016. High content imaging quantification of multiple in vitro human neurogenesis events after neurotoxin exposure. Submitted to *BMC Pharmacology and Toxicology*, 03/29/2016

Abstract

Background: Our objective was to test neural active compounds in a human developmental neurotoxicity (DNT) model that represents neural tube stages of vulnerability. Previously we showed that 14 days in vitro (DIV 14) was sufficient to generate electrophysiologically active neuronal cells which were used for neurotransmitter potentiating activity and neurite outgrowth assays. However, short exposure and assessment may not detect toxicants that affect the early neurogenesis continuum, from a mitotic neural progenitor (hNP) cell population through post mitotic neurons. Therefore, we attempted to mimic events associated with early human neurogenesis beginning with proliferating radial glia (hNP), progressing through differentiation and polarization of post mitotic neurite extending neurons at DIV 14.

Methods: The Human DNT continuum (DIV 0 to DIV 14) was determined using immunocytochemistry for SOX1+ (proliferating hNP) and HuC/D+ (post mitotic neurons). Five chemicals (Bisindolylmaleimide I, β-estradiol, testosterone, BPA, and acetaminophen) were present during the continuum, starting at DIV 0. At DIV 14 neurite outgrowth (βIII-tubulin+) and neuron density (HuC/D+) were quantified using high content imaging. Further, estrogen receptor expression was analyzed and β-estradiol effect on hNP cell proliferation was quantified. All data were analyzed using a one-way ANOVA with a significance threshold of $p < 0.05$.

Results: We exploited the in vitro developmental continuum to investigate neurotoxicity of select known compounds as this transition occurs. During maturation in vitro, the neural cultures transitioned from uniform hNP cells (DIV 0) to predominantly mature post mitotic neurons (HuC/D+, 65%; DIV14) but also maintained a smaller population of hNP cells (SOX1+). Using this DNT maturation model system, Bis-1, testosterone, and β-estradiol

inhibited neuronal maturation at micromolar levels but were unaffected by acetaminophen. β-estradiol also disrupted neurite extension at 10 µM. Treating cells in this window with Bisphenol A (BPA) significantly inhibited neurite outgrowth and branching in these continuum cultures but only at the highest concentrations tested (10µM).

Conclusions: Neurotoxicant in vitro exposure during a maturation continuum affected human neurogenesis at substantially lower levels than previously known. For example, unlike prior acute studies, β-estradiol was highly toxic from 0.01 to 10 µM when present throughout the continuum and cytotoxicity was manifested starting early in the continuum via a non-estrogen receptor α (ER α) mechanism.

Keywords: Developmental neurotoxicity; Neuron maturation; Neurite outgrowth; Endocrine active compounds; Human neural progenitor

Introduction

There is overwhelming evidence that environmental factors play a role in the development and progression of a host of central nervous system disorders. Neurotoxins can affect radial glia to neuron differentiation, survival, proliferation and cellular functions during neurogenesis (such as neurite outgrowth), resulting in profound functional and behavioral deficits in an exposed developing human *central nervous system* (CNS) [1]. The concept of an embryonic and fetal basis for adult disease has emerged from these findings and has received considerable attention in the scientific community [2, 3]. The extent of damage may be related to not only exposure level, but also exposure duration and developmental stage of exposed neural cells. Several teratogens are thought to mainly affect early stages of neural maturation occurring during and shortly after neural tube formation [4, 5]. In vivo windows of susceptibility (WOS) were observed when valproic acid (an anticonvulsant that increases the risk of spinal neural tube defects by roughly ten times) was taken early in pregnancy. Valproic acid acts as a histone deacetylase inhibitor and disturbs the balance of protein acetylation versus deacetylation, leading to disruption of key signaling pathways in neurulation during neural tube formation [5]. Retinoic acid (RA) has long been studied as a potent teratogen in rodent systems, with neural tube defects among the malformations observed. Any disturbance in the balance between production and turnover of retinoids can adversely affect developmental events including neural tube closure [5]. Using an in vitro model of early neurogenesis events, human pluripotent stem cell (hPSC) derived neural rosettes responded to retinoic acid exposure with decreased viability and decreased neural rosette formation at a concentration of 2μM [6]. Disturbance of any of the sequential events of embryonic neurogenesis produces neural tube defects, with the phenotype

(e.g. anencephaly, spina bifida) varying depending on the region of neural tube that remains open.

hPSC-derived neurons can mimic some of the early human neural maturation events, providing in vitro screening opportunities to identify potential developmental neurotoxins [7, 8]. Human neural progenitor (hNP) cells differentiated from hPSC offer a potential cell source for cell based human DNT assays. Human PSC-derived hNP cells, used in this study, proliferate and maintain a multipotent neural state in presence of leukemia inhibitory factor (LIF) and fibroblast growth factor 2 (FGF2) in neural medium [9, 10]. Removal of FGF2 leads to a significant decrease in proliferation within 48 hours followed by neuronal differentiation. At fourteen days, the differentiated cultures show extensive expression of microtubule-associated protein2 (MAP2) and βIII-tubulin (TUJ1), and have electrophysiologically active membranes characteristic of post-mitotic neurons [11]. These differentiated cultures express subunits of glutamatergic, GABAergic, nicotinic, purinergic, and transient potential receptors, and are responsive to neurotransmitters [7, 11]. Therefore, hPSC-derived cells mimic early neuronal maturation events in vitro, providing the opportunity to experimentally assess the disruption of neural developmental and proliferative processes.

Neurite outgrowth is an established quantitative endpoint for in vitro monitoring of key cellular events in neuronal differentiation and maturation. Human neuronal cells derived from hNP cell cultures 14 days post removal of FGF2 (DIV 14), referred to as hN2 neurons, were used in an in vitro neurite extension/recovery assay for DNT [7]. Compared to a rat primary cortical culture, human hN2 neurons had a lower dynamic range for detecting chemical-induced neurite outgrowth inhibition [7]. Known neurotoxins such as bisindolylmaleimide I (Bis1) and lithium chloride (LiCl) inhibited neurite outgrowth prior to affecting hN2 neuron viability, inducing

cytotoxicity only at higher doses [7, 12]. Past studies, however, only observed effects on mature neurons 2 to 24 hours post thaw following acute neurotoxin exposure, providing information on neurite recovery in a mature cell type during a narrow window of development [7]. More informative DNT studies would ideally identify potential human toxicants applied during a continuum of critical early stages of neurogenesis.

Human exposures to endocrine active compounds (EACs) have been implicated in developmental complications [13, 14]. EAC exposure can perturb developmental programming [15] and potentially transgenerational inheritance via changes in the intracellular pathways leading to neural dysfunction [16]. Despite the need, efforts to identify EACs have been limited to only a small subset of the >100,000 synthetic and naturally occurring plant-derived phytoestrogens [17]. This has left many unanswered questions pertaining to the safety of these chemicals and their effects on developmental processes, including neural development. In vitro assays for these outcomes examine genetic changes in cells and are typically accompanied by tests of cytotoxicity and cell proliferation, but they rarely span developmental processes and have not included the neural maturation process.

Human PSC-based DNT assays may provide a relatively rapid test to prioritize which EACs should undergo expensive and time consuming animal DNT studies while also providing further information on potential susceptibility during the continuum of human neurogenesis. To fill this gap, here we examined the effects of three known EAC compounds: β-estradiol, testosterone and Bisphenol A (BPA), on early neural development using a DNT model spanning a characterized DIV 14 neurogenesis period. β-estradiol affected both early stage hNP cell proliferation and neurite networks, effects likely mediated via an estrogen receptor α (ER α) independent mechanism given the absence of ER α expression during this stage of maturation.

Testosterone affected neuron densities without significantly affecting neurite network morphology. BPA effects were less prevalent and only affected neurite branching at the highest dose tested (10 μM) but did not affect the number of neurons. This study combines both neural maturation and cellular function endpoints in the neurogenesis continuum DNT system and can be used for high content and higher throughput screening of larger compound libraries.

Materials and methods

Cell culture and differentiation. Cryopreserved hNP cells derived from hPSC line WA09 as previously described [9] were obtained from ArunA Biomedical, Inc. hNP cells were subcultured as described by the manufacturer on Matrigel 1:100 (B&D) coated cell culture dishes in proliferation medium comprised of AB2™ basal medium supplemented with ANS™ neural supplement (both from ArunA Biomedical Inc. Athens GA), 2 mM L-glutamine (Gibco), 2 U/ml penicillin (Gibco), 2 μg/ml streptomycin (Gibco), 20ng/ml bFGF (R&D) and 10 ng/ml leukemia inhibitory factor (LIF) (Millipore, Billerica, MA, USA). For neuronal differentiation hNP cells were cultured in differentiation medium (medium above without bFGF). For cellular characterization experiments, hNP cells were cultured overnight in proliferation medium. The next day cells were washed with warm phosphate buffered saline (PBS++) once and then switched to medium lacking bFGF for 1 day before seeding in 96 well cell culture plates. hESC derived germ-like cells, (GLCs), (provided by Franklin D. West, Henderson et al. 2012) and IMR90 fibroblast cells [18] were thawed and plated onto matrigel-coated plates in 20% knockout serum replacement (KSR) medium consisting of Dulbecco's modified Eagle's medium/F12 supplemented with 2mM glutamine, 0.1mM nonessential amino acids, 50 U/ml penicillin, 50 mg/ml streptomycin (Gibco, Grand Island, NY), 0.1mM β-mercaptoethanol (Sigma Aldrich, St

Louis, MO), and 4 ng/ml bFGF (R&D Systems, Minneapolis, MN) and allowed to acclimatize for 24 h. On the day of cell plating, Costar® 96-well cell culture plates were coated with Matrigel 1:100 (B&D) for 20 min (37°C) , rinsed once with warm PBS and hNP cells were plated at 15,000 cells per well in differentiation medium lacking bFGF. A 50% medium change was performed every two days. Cells were fixed at different time points for immunocytochemistry. For experiments to determine effects of test compounds on hNP cell differentiation test compounds were added at every media change until cells were fixed. Cells were maintained in a humidified incubator at 37°C with a 95% air/ 5% CO2 atmosphere.

Chemical treatment. Test compounds Bisindolylmaleimide I (Bis1), BPA, and acetaminophen were purchased from Sigma Aldrich (St Louis, MO), testosterone and β-estradiol were purchased from Steraloids (Newport, RI). All chemicals were prepared as a stock solution (1000X). Bis1 was dissolved in DMSO at concentrations as follows: 0, 0.1, 0.3, 1, 3, 10 mM. BPA and all other chemicals were at concentrations 0, 0.01, 0.1, 1, 10 mM. Selection of concentration ranges was based on previously published work [12, 19-21]. Stock solutions were diluted in AB2 proliferation medium without LIF at a ratio of 1: 500 and 100µl mixed medium was added to cell cultures 6 h after cells were seeded in 96 well culture plates. For second and later medium changes, stock solutions were then diluted in AB2 proliferation medium without LIF 1:1000 and 100µl medium was replaced every two days. Cells were fixed at the end of DIV 14. Final DMSO concentrations were 0.1% for all treatment wells and corresponding vehicle only control wells.

Cell proliferation assay. hNP cell proliferation was analyzed using CellTiter 96AQueous One Solution Cell Proliferation assay kit (Promega, Madison, WI). This kit contains (3-(4, 5-dimethylthiazol-2-yl)-5-(3-carboxymethoxyphenyl)-2-(4-sulfophenyl)-2H-tetrazolium)

(MTS) tetrazolium compound, which is reduced by NADPH produced by dehydrogenase enzymes in metabolically active cells into a colored formazan product. The quantity of formazan product as measured by absorbance at 490nm is directly proportional to live cells and can be used as a measure of proliferation. hNP cells were seeded on Matrigel-coated 96-well plates at 2.5×10^4 cells per well and grown in proliferation medium without LIF. A set of wells on each plate contained medium and no cells and served as 'medium only' background controls. CellTiter 96 AQueous One Solution Reagent was added to each well at end of DIV 3 and DIV14, followed by incubation for 2 h at 37°C in a humidified, 5% CO2 atmosphere. Absorbance at 490 nm was measured for each well using a μQuant Bio-Tek 96-well plate reader. The percentage of cell proliferation was calculated using the following formula: proliferation= 100 × [(experimental − culture medium background)/ (medium only control group − culture medium background)].

Western blotting. Cells were lysed in IP lysis buffer complete with Halt protease and phosphatase inhibitor cocktail (both from Pierce, Rockford, IL), on ice for 5 minutes. Insoluble material was pelleted at 13,000 x g for 10 minutes per the manufacturer's protocol, and supernatant collected. Total protein content was determined by bicinchoninic acid assay (Pierce, Rockford, IL), and 7 μg of protein per cell type was separated by SDS-PAGE using 4-12% bis-tris gels (Biorad, Hercules, CA). Proteins were transferred to 0.45 μM nitrocellulose membranes (Biorad, Hercules, CA), and blocked overnight in Li-Cor's PBS based blocking solution (Li-Cor, Lincoln, NE). Estrogen receptor α was detected using ~ 5 μg of primary (Santa Cruz, Dallas, TX), and Li-Cor's anti-rabbit IRDye 680 LT secondary, while β-actin was detected using β-actin antibody detected using ~ 1 μg of primary antibody and Li-Cor's IRDye 800CW conjugated secondary (Li-Cor, Lincoln, NE). Both secondaries were used at the manufacturer's

recommended dilutions, and membranes were imaged on the Odyssey western blot detection system (Li-Cor, Lincoln, NE).

Immunocytochemistry. For immunocytochemistry cells were fixed with 4% paraformaldehyde - at each time point as described previously [22]. Briefly, 100 µl of a warm (37 °C) solution of 8% paraformaldehyde were added to culture wells containing 100 µl of medium and incubated at room temperature for 20 min [23]. Fixative was then gently aspirated and cells were washed three times with phosphate-buffered saline. Primary antibodies diluted in intracellular blocking solution [24] were then applied as follows: βIII-tubulin 1:300, AB18207 (ABCAM, Cambridge, MA), HuC/D 1:40, A21271 (Invitrogen Corp., Carlsbad, CA), estrogen receptor α 1:50, sc-543 (Santa Cruz, Dallas, TX), SOX1 1:300, AF3369 (R&D, Minneapolis, MN) for 2 h at RT. The entire antibody panel was used to characterize differentiation and phenotype of the hNP and DIV 14 neural cells, while βIII-tubulin was specifically used to label cell bodies and neurites for high-content image analysis. Following incubation in primary antibodies, cells were washed three times with high salt buffer and incubated with a 1:400 dilution of DyLight® 594-conjugated donkey anti-mouse IgG or DyLight® 488-conjugated donkey anti-rabbit IgG secondary antibody in high salt buffer for 1 h at room temperature, protected from light. Cells were then incubated in 0.1% Hoechst 33342 dye in high salt buffer for 20 min, then in PBS washed 3 times with high salt buffer, and stored in phosphate-buffered saline (PBS) at 4 °C prior to image acquisition and analysis [7].

Image acquisition and analysis. Cellomics ArrayScan VTI HCS reader high-content imaging system (ThermoFisher Scientific, Waltham, MA) was used for automated image acquisition and morphometric analyses as previously described for use on hN2 cells [7]. Image analysis was performed using the vHCS Scan software package with a manually optimized

version of the Cellomics Neural Profiling Bioapplication for neurite outgrowth analysis. Target Activation Bioapplication was used for marker protein expression analysis. Image analysis algorithm optimization, including nucleus validation, cell body masking and validation, and neurite tracing parameters, was performed a priori using five representative images from cultures with differentiated neural cells. Output from high content image analysis included total cell count (% viable nuclei per well) and measurements of neurite outgrowth (neurites per neuron, neurite length per neuron, and branch points per neuron). Anti-human neuronal protein HuC/HuD recognizes multiple neuronal proteins of the Elav family; HuC, HuD and Hel-N1and labels neuronal cells at the time that neurons leave the mitotic cycle [25]. HuC/D protein positive expression was analyzed in Target Activation Bioapplication. Briefly, nuclei were first identified in channel 1 as bright objects on a dark background (Fig. 2.2A, 2.2B). Nuclei with size and intensity values outside of the ranges determined a priori for viable cells were identified in the channel 1 image and rejected from further analyses. Spatial coordinates from the channel 1 image were then superimposed on the matching channel 2 image. Protein expression in channel 2 were then cast based on positional data from channel 1 nuclei and a set of user-defined geometric and signal intensity-based parameters (Fig. 2.2C, 2.2D. orange and red traces). Positive objects based on intensity value were then selected (Fig. 2.2C, 2.2D. red traces) and invalid objects rejected (Fig. 2.2C, 2.2D. orange traces). Data were collected on a cell-by-cell basis, and values were averaged to obtain population means within each well. These well level data were treated as the statistical unit for analysis of neurite outgrowth. At x20 magnification, the Cellomics ArrayScan VTI can sample 81 individual fields within each well. In this study, 35 fields were sampled within each well for cell characterization.

Statistics. Cell characterization experiments were performed twice using independent cultures with n = 4–6 wells per condition per culture. For concentration-response experiments, total cell count, HuC/D positive cell number (neuron density), neurite outgrowth data were normalized within experiment to corresponding control wells prior to statistical analysis. For each concentration-response examined, experiments were repeated two to three times using independent cultures as described. In cell proliferation assay, experimental values are a composite of six technical (on same plate) and three biological (different cell vials) replicates. All data analyzed for cell characterization were using a one-way ANOVA with a significance threshold of $p < 0.05$. This was followed by a Tukey's test to determine if different time point means were significantly different from corresponding control means. All concentration-response experiments were analyzed using one-way ANOVA with a significance threshold of $p < 0.05$ followed by a Tukey's test. Mean values ± standard deviations for all measurements are provided throughout the text. Statistical analyses were performed using Graphpad Prism1 v5.

Results

Quantification of neural progenitor cell differentiation using high content analysis. SOX1 is expressed in hNP cells and in vivo radial glial but not in mature cells [26]. SOX1 positive cell were nearly 100% at DIV 0 but only 37.5% at DIV 14; whereas HuC/D+ post mitotic neurons were negligible at DIV 0 and but was 63.5% of the population at DIV14 (Fig 2.2 A-G). Therefore, hNP cells and post mitotic neurons composed nearly 100% of cells during the neurogenesis continuum. To further understand the transition from mitotic hNP cells to post mitotic neurons in the neuronal maturation continuum, expression of neuronal marker HuC/D was determined continuously at regular intervals from DIV 0 to DIV 28 (Fig 2.2 A-F) using a

high content imaging format. HuC/D positive cells increased during the first 14 DIV (Fig. 2.2 G). Only 3.4% ± 0.8% of the hNP cells population (DIV 0) expressed HuC/D compared to 63.5% ± 8.5% at DIV 14 and the percentage of HuC/D positive neuronal cells did not significantly increase further after DIV 14, with 67.3% ± 13.9% expressing HuC/D at DIV 28 (Fig. 2.2 G). Thus, HuC/D expression approached a plateau around DIV 14 and was constant for the additional 14 days of differentiation, presenting DIV 0-14 as a window from a proliferative to a largely post mitotic stage. Distinct hNP and post mitotic neuronal morphologies were evident at DIV 0 and DIV 14 (Fig. 2.1A-B), and co-expression of HuC/D and βIII-tubulin specifically labeled cell bodies and neurites, enabling quantification of neurogenesis at DIV 14. HuC/D was present in the nucleus and βIII-tubulin expression was evident in both axons and dendrites of neural cells providing an accurate measure of neurite outgrowth (Fig. 2.2 H-J).

Effect of test compounds during neurogenesis. The early developmental window described above was used to test a four-point concentration series of one known neurotoxin and protein kinase C (PKC) inhibitor Bis1, an assumed non-neurotoxic drug, acetaminophen, two known endocrine active compounds: testosterone and β-estradiol, and the putative EAC, BPA. Concentration ranges were based on previous research as described in the literature (Table 2.1) [12, 19-21]. All parameters including neuron density and neurite outgrowth were normalized to percentages of non-treated cells. At the end of DIV 14, neurite networks were dramatically developed with neurite length per neuron: 52.8±6.7 μm; neurites per neuron: 1.3±0.1; branch points per neuron: 0.7±0.1 in the untreated group (Fig. 2.2H-J).

Following continuous exposure to test compounds up to DIV 14, Bis1 reduced cell density in culture at all concentrations tested, while only the highest concentration (3 μM; Fig. 2.3A, 2.3B) induced cell death in a differentiated HuC/D+ cell population. In contrast,

concentration dependent decreases in neurite outgrowth parameters were observed following exposure to Bis1 (0.1 to 3 μM). The average number of neurites, neurite total length, and branch points per neuron all decreased in a concentration dependent manner (Fig. 2.3C, 2.3D, 2.3E). These data demonstrated a specific inhibition of neurite outgrowth ranging from 0.1 - 3 μM Bis1. A similar exposure to acetaminophen, the non-toxic control, had no effect on either neuron density or neurite outgrowth at doses ranging from 0.01-10μM (Fig. 2.4A-E). During the continuum, Bis1 was more cytotoxic to hNP cell population than post mitotic neurons but did have a specific effect on neurite outgrowth endpoints (Fig. 2.3A-E).

We then tested increasing doses of three EACs in this DNT continuum. β-estradiol treatment led to a significant reduction in total cell count at 0.01- 10μM as measured in Fig. 2.5A. Additionally significant concentration dependent decreases in HuC/D positive cells (neuron density) were observed following exposure to β-estradiol (Fig. 2.5B) from 0.01-10 μM; a significant decrease in neurite outgrowth was observed only at 10 μM. The number of neurites per neuron decreased by 70.1%. Neurite length per neuron and branch points per neuron were significantly inhibited at 68.3% and 70.3% respectively (Fig. 2.5C, 2.5D, 2.5E).

The β-estradiol low dose cytotoxic effects in the high content assay were investigated further given prior studies suggesting β-estradiol can act via receptor mediated or receptor independent mechanisms (Fig. 2.5A, 2.5B). Estrogen receptor α (ER α) was involved in neural proliferation and differentiation in non-human neural cell lines [27, 28]. The hNP cells were negative for ER expression when compared to known ER positive human PSC-derived cell germ-like cell line (Fig. 2.6A, 2.6B) [18]. Additionally, the absence of ER expression in both hNP cells and DIV 14 neural cells was confirmed by western blot (Fig. 2.6C). Previously β-estradiol has been shown to influence (either increase or decrease) neural progenitor cell

proliferation and neurite extension [27, 29]. β-estradiol decreased hNP cell viability or proliferation early (DIV 3) in neurogenesis (0.1-10 μM dose range); (Fig. 2.6D). At DIV 14 of continuous exposure to β-estradiol during differentiation, this cytotoxicity assay confirmed cumulative effects in the 0.01-10 μM dose range. (Fig. 2.6E). These results suggest the effect of β-estradiol is not mediated via an ER mechanism and confirm the cytotoxicity is not cell type specific given both decreased hNP proliferation and viability (DIV 3) and the number of total of differentiated cells in DIV 14 cell culture.

Exposure to testosterone affected both total cell count and neuron density. At 0.1, 1 and 10 uM, cell numbers were reduced and neuron densities were significantly decreased compared to control group (Fig. 2.7A, 2.7B). There were thus two concentrations, 0.1 and 1 μM, which affected neuron density without concurrent effect on neurite outgrowth (Fig. 2.7C, 2.7D, 2.7E). At 10 μM, neurites per neuron was significantly decreased by 15.0% from control group, while total neurite length nor branch points per neuron were affected over the concentration range tested.

BPA exposure decreased total cell count by 45.2% at the highest dose tested (10μM) while lower concentrations did not induce toxicity. Even though total cell count was substantially reduced, neuron density did not change with BPA treatment at any concentration tested (Fig. 2.8A, 2.8B). Importantly, even though neuron density did not change at any concentration tested, all three neurite outgrowth endpoints were reduced at highest concentration. Following exposure to 10 μM BPA, significant decreases of 29.0%, 13.9%, and 42.8% were observed for neurite length per neuron, neurites per neuron, and branch points per neuron respectively (Fig. 2.8C, 2.8D, 2.8E). Collectively, all data from the chemical exposures indicate that EACs affect neuron maturation

and neurite outgrowth differently, but induce changes within this window, supporting use of the continuum model over single endpoint systems.

Discussion

The current study establishes an in vitro developmental window in a hPSC-based early neurogenesis system that specifically addresses toxin susceptibility during a continuum of early maturation that is observed in vivo. In the neural tube the neuroepithelium proliferates and then post mitotic neurons migrate basally to form the neocortex [30]. Human PSC-based neural development has been shown to recapitulate many aspects of human neural development. While neural rosettes have been used to model the early neural tube [31], polarized post mitotic neurons migrate apically as they do during embryonic development. While hNP cells and post mitotic neurons independently provide opportunities for acute studies on very specific developmental time points, here we describe an early developmental continuum, and test the effects of neurotoxin and EAC exposure throughout a critical developmental period, in a high content analysis amenable model. The wider in vitro developmental window described here spans multiple important developmental processes, beginning with proliferation of radial glia, to the gradual transformation of the cultures to post-mitotic neuronal cells that extend neurites and form neuronal networks [11].

In experiments where we assayed differentiating hNP cells for expression of the neuronal marker HuC/D [32], the observed increase in HuC/D expressing cells through DIV 14, which then plateaued through DIV 28 (the furthest time point tested) suggests we are modeling a population shift, from a proliferating population to a primarily post-mitotic one. Compared to other neural differentiation models [33, 34], this is the first in vitro model measuring both

maturation and neurite outgrowth during neural differentiation based specifically on the HuC/D positive cells, and in turn distinguishing a compound's effect on mature HuC/D+ vs. HuC/D-, SOX1+ hNP cells. For example, previously it was known that Bis1 affected neurite outgrowth in mature neurons [7], but here we show for the first time that Bis1 has a greater neural cytotoxic effect in hNP cells (Fig. 2.3A) than when we just measure the effect in the post mitotic neuron population in these cultures (Fig. 2.3B); potentially indicating that Bis1 is more cytotoxic to proliferating radial glia than post mitotic neurons during this continuum.

At DIV 14 we observed extensive neurite networks, providing a robust assay endpoint after toxin exposure during a developmental continuum, starting with neurite budding and ending with neurite networks. While DIV 14 cryopreserved human neurons have been used previously for acute toxin exposure studies, by extending the window through neuronal maturation, we encompass a true representation of neurite outgrowth. We observed neurite extension starting approximately at DIV 8 and an extensive network was formed by DIV14, which allows toxin treatment to occur concurrently with neurite extension and establishment of neural networks. This is in contrast to the use of cryopreserved DIV 14 neuronal cultures that lose network morphology during cryopreservation and essentially recover and reestablish their neurite networks during toxin treatment post-thaw [7] .

We first tested our model for continuous exposure toxicity using Bis1, which has been studied extensively for effects on neurite recovery in vitro, using rodent and human cells [35]. Bis1 is a competitive inhibitor for the ATP binding site of PKC. PKC can affect neurite outgrowth directly, modulating cytoskeletal protein phosphorylation, or through the MAPK signaling pathway which is active in our differentiating cultures [8, 36]. In a previous study, where cryopreserved hN2^{TM} neurons (14 DIV) where exposed to Bis1 for a short (24 hour)

period post thaw, significant inhibition of neurite outgrowth was observed [7, 37], with a least effective concentration [36] of 10 µM for both neurites per neuron and neurite length per neuron (28.8% and 36.7%), with no cytotoxicity observed at this concentration. In our experiments, a significant reduction in neurites per neuron and neurite length per neuron as well as branch points per neuron was observed with a dose of 0.1 µM, a reduction of 2 logs during the 14 DIV, suggesting significantly more sensitivity in a model where the toxicant exposure occurs during neural differentiation. No effect of Bis1 on neuron density was observed at this concentration, showing endpoint specificity on neurite outgrowth. To ensure that the increased sensitivity is not at the expense of specificity, we also tested acetaminophen, a drug with no reported neurotoxicity in vivo, except with acute overdose. No significant effect was observed at any dose up to 10 µM, the highest tested. The results above suggest a sensitive and accurate DNT continuum assay, although a larger library of compounds must be tested to validate and conclusively describe the sensitivity and accuracy of our DNT model.

We tested the effects of known EACs in this DNT model. EACs are found in many environmental agents including pesticides, industrial chemicals and some plasticizers and surfactants, and are thus of interest to regulatory and public health agencies [38] . Two known EACs: Testosterone and β-estradiol as well as putative EAC, BPA, were tested. Following exposure to β-estradiol, all three neurite outgrowth parameters were affected only at 10mM, the highest dose tested. However, both the number of total cells and neurons were significantly reduced at lower concentrations starting from 0.01 mM. A previous study has indicated that in rat neurons estrogen induced neurite outgrowth in basal forebrain cholinergic neurons in vitro, [39] and another study shows β-estradiol had a neuroprotective effect [40]. Both effects were attributed to estrogen receptor mediated signaling. Given our contrasting results, both neural

progenitors and differentiated neurons that represent the two temporal boundaries for our treatment window were tested for ER protein expression. The absence of ER protein expression in both neural stages suggests that the effects of β-estradiol we observe occurs through ER independent mechanisms. Such ER independent mechanisms can affect cytoplasmic microtubule fibers at interphase, and affect cell growth [41]. Consistent with this we show that β-estradiol, when applied during the first 3 days of our DIV 14 developmental window, significantly increase cytotoxicity in hNP cells.

With long-term exposure to testosterone, the highest dose tested reduced the number of neurites per neuron, but had no effect on other parameters such as neurite length per neuron or branch points per neuron, suggesting non-endpoint specific effects since neurite outgrowth was affected only at 10 μM. However, a significant reduction in both total cells and neurons was observed at lower doses, consistent with previous reports that testosterone in the micromolar range initiates apoptosis and decreases neural cell viability [34].

BPA significantly reduced neurite outgrowth, including neurite length per neuron, neurites per neuron and branch points per neuron at 10 μM, the highest dose tested, without reduction in the number of neurons (Fig. 2.8). This shows endpoint specificity, and suggests higher sensitivity than a cytotoxicity based endpoint for detecting effects of BPA. However, we did observe a reduction in the overall number of cells in cultures exposed at this dose, suggesting a decrease in the proportion of non-neuronal (HuC/D negative or immature) cells by DIV 14 due to continuous BPA exposure. Interestingly, the 10 μM dose point that elicited an effect is significantly higher than the effective dose of 10 ng/ml observed previously with PC12 cells [19] in spite of the long term treatment performed here, suggesting a cell line and /or species specific difference in sensitivity with human cells being less responsive to the effects of BPA.

In summary, we provide evidence that an hPSC-derived neurogenesis continuum DNT model can be used to test EACs and other compounds, providing a multifaceted and potentially more complex understanding of neurotoxin effects during early human neuronal development. Here cell cultures spanning from proliferative hNP cells to post mitotic neurons continuously exposed to β-estradiol resulted in cytotoxic effects early on in the cultures that extended to disruption of neurite formation via a non-ER mechanism later in this continuum. Bis1 was more toxic to hNP cells than post mitotic neurons. BPA had no cytotoxic DNT effects and only at the highest dose affected neurite outgrowth parameters. Based on the data above which show neuron development endpoint specificity, our model could be efficient in large-scale drug and environmental neurotoxicity screening using informative hPSC-derived cultures.

Conclusion

Compared to existing rat cortical neural culture and previously used acute hPSC-derived neural cell differentiation models, our model best describes the chronic exposure of compounds that occur during developmental neurotoxicity and results in screening of compounds throughout neurogenesis in the neural tube, the transition from neural progenitors through primarily post mitotic neurons. In summary, results here clearly suggest that differentiating cells in vitro are affected by known and potential neurotoxicants at substantially lower levels than previously known. Taken together these data suggest this multiplex human neurogenesis model is more sensitive than single cell type endpoint measures, and is a better initial screening model for potential toxicants during very early development of the CNS.

Abbreviations. EACs: endocrine active compounds; DNT: developmental neurotoxicity; hNP: human neural progenitor; DIV 14: 14 days in vitro; BPA: Bisphenol A; ER α: estrogen receptor

α; CNS: central nervous system; WOS: windows of susceptibility; RA: Retinoic acid; hPSC: human pluripotent stem cell; LIF: leukemia inhibitory factor; FGF2: fibroblast growth factor 2; MAP2: microtubule-associated protein2; TUJ1: βIII-tubulin; Bis1: bisindolylmaleimide I; LiCl: lithium chloride; GLCs: germ-like cells; KSR: knockout serum replacement; DMSO: Dimethyl sulfoxide; RT: room temperature; PBS: phosphate-buffered saline; PKC: protein kinase C; ATP: Adenosine triphosphate; MTS: (3-(4, 5-dimethylthiazol-2-yl)-5-(3-carboxymethoxyphenyl)-2-(4-sulfophenyl)-2H-tetrazolium).

Acknowledgements. The authors wish to thank Dr. R. Tripp's Lab for providing Cellomics ArrayScan V^{TI} HCS reader high-content imaging system and funding from an US EPA-G2012-STAR-F1 grant. The germ like cells and IMR90 fibroblast cells were a gift from Dr. Franklin D. West. The authors also wish to thank Dr. William Mundy and Forrest Goodfellow for comments and suggestions on an earlier version of this manuscript.

References

1. Mundy, W.R., et al., *Expanding the test set: Chemicals with potential to disrupt mammalian brain development.* Neurotoxicol Teratol, 2015. **52**(Pt A): p. 25-35.
2. Riley, E.P., M.A. Infante, and K.R. Warren, *Fetal alcohol spectrum disorders: an overview.* Neuropsychol Rev, 2011. **21**(2): p. 73-80.
3. Cui, Z.J., et al., *Prenatal alcohol exposure induces long-term changes in dendritic spines and synapses in the mouse visual cortex.* Alcohol Alcohol, 2010. **45**(4): p. 312-9.
4. Copp, A.J., et al., *The embryonic development of mammalian neural tube defects.* Prog Neurobiol, 1990. **35**(5): p. 363-403.
5. Copp, A.J. and N.D. Greene, *Genetics and development of neural tube defects.* J Pathol, 2010. **220**(2): p. 217-30.
6. Colleoni, S., et al., *Development of a neural teratogenicity test based on human embryonic stem cells: response to retinoic acid exposure.* Toxicol Sci, 2011. **124**(2): p. 370-7.
7. Harrill, J.A., et al., *Quantitative assessment of neurite outgrowth in human embryonic stem cell-derived hN2 (TM) cells using automated high-content image analysis.* Neurotoxicology, 2010. **31**(3): p. 277-290.
8. Radio, N.M. and W.R. Mundy, *Developmental neurotoxicity testing in vitro: Models for assessing chemical effects on neurite outgrowth.* Neurotoxicology, 2008. **29**(3): p. 361-376.
9. Shin, S.J., et al., *Long-term proliferation of human embryonic stem cell-derived neuroepithelial cells using defined adherent culture conditions.* Stem Cells, 2006. **24**(1): p. 125-138.
10. Majumder, A., et al., *Neurotrophic effects of leukemia inhibitory factor on neural cells derived from human embryonic stem cells.* Stem Cells, 2012. **30**(11): p. 2387-99.
11. Young, A., et al., *Ion channels and ionotropic receptors in human embryonic stem cell derived neural progenitors.* Neuroscience, 2011. **192**: p. 793-805.
12. Radio, N.M., et al., *Comparison of PC12 and cerebellar granule cell cultures for evaluating neurite outgrowth using high content analysis.* Neurotoxicol Teratol, 2010. **32**(1): p. 25-35.
13. Colborn, T., F.S.V. Saal, and A.M. Soto, *Developmental Effects of Endocrine-Disrupting Chemicals in Wildlife and Humans.* Environ Health Perspect, 1993. **101**(5): p. 378-384.
14. Fernandez, M.F., et al., *Human Exposure to Endocrine-Disrupting Chemicals and Prenatal Risk Factors for Cryptorchidism and Hypospadias: A Nested Case-Control Study.* Environ Health Perspect, 2007. **115**: p. 8-14.
15. Skinner, M.K., M. Manikkam, and C. Guerrero-Bosagna, *Epigenetic transgenerational actions of endocrine disruptors.* Reproductive Toxicology, 2011. **31**(3): p. 337-343.
16. Novikova, S.I., et al., *Maternal cocaine administration in mice alters DNA methylation and gene expression in hippocampal neurons of neonatal and prepubertal offspring.* PLoS One, 2008. **3**(4): p. e1919.
17. Acerini, C.L. and I.A. Hughes, *Endocrine disrupting chemicals: a new and emerging public health problem?* Archives of Disease in Childhood, 2006. **91**(8): p. 633-638.
18. West, F.D., et al., *Metabolomic response of human embryonic stem cell-derived germ-like cells after exposure to steroid hormones.* Toxicol Sci, 2012. **129**(1): p. 9-20.

19. Seki, S., et al., *Bisphenol-A suppresses neurite extension due to inhibition of phosphorylation of mitogen-activated protein kinase in PC12 cells.* Chem Biol Interact, 2011. **194**(1): p. 23-30.
20. Rozovsky, I., et al., *Estradiol (E2) enhances neurite outgrowth by repressing glial fibrillary acidic protein expression and reorganizing laminin.* Endocrinology, 2002. **143**(2): p. 636-646.
21. Zhang, L., et al., *Testosterone and estrogen affect neuronal differentiation but not proliferation in early embryonic cortex of the rat: the possible roles of androgen and estrogen receptors.* Neurosci Lett, 2000. **281**(1): p. 57-60.
22. Dhara, S.K., et al., *Genetic manipulation of neural progenitors derived from human embryonic stem cells.* Tissue Eng Part A, 2009. **15**(11): p. 3621-34.
23. Doherty, P., G. Williams, and E.J. Williams, *CAMs and axonal growth: a critical evaluation of the role of calcium and the MAPK cascade.* Mol Cell Neurosci, 2000. **16**(4): p. 283-95.
24. Gallegos-Cardenas, A., et al., *Pig Induced Pluripotent Stem Cell-Derived Neural Rosettes Developmentally Mimic Human Pluripotent Stem Cell Neural Differentiation.* Stem Cells Dev, 2015. **24**(16): p. 1901-1911.
25. Marusich, M.F., et al., *Hu neuronal proteins are expressed in proliferating neurogenic cells.* J Neurobiol, 1994. **25**(2): p. 143-55.
26. Venere, M., et al., *Sox1 marks an activated neural stem/progenitor cell in the hippocampus.* Development, 2012. **139**(21): p. 3938-49.
27. Brannvall, K., L. Korhonen, and D. Lindholm, *Estrogen-receptor-dependent regulation of neural stem cell proliferation and differentiation.* Molecular and Cellular Neuroscience, 2002. **21**(3): p. 512-520.
28. Minano, A., et al., *Estradiol facilitates neurite maintenance by a Src/Ras/ERK signalling pathway.* Mol Cell Neurosci, 2008. **39**(2): p. 143-51.
29. Wang, J.M., L.F. Liu, and R.D. Brinton, *Estradiol-17 beta-induced human neural progenitor cell proliferation is mediated by an estrogen receptor beta-phosphorylated extracellularly regulated kinase pathway.* Endocrinology, 2008. **149**(1): p. 208-218.
30. Banda, E., et al., *Cell polarity and neurogenesis in embryonic stem cell-derived neural rosettes.* Stem Cells Dev, 2015. **24**(8): p. 1022-33.
31. Wilson, P.G. and S.S. Stice, *Development and differentiation of neural rosettes derived from human embryonic stem cells.* Stem Cell Rev, 2006. **2**(1): p. 67-77.
32. Boissart, C., et al., *Differentiation from human pluripotent stem cells of cortical neurons of the superficial layers amenable to psychiatric disease modeling and high-throughput drug screening.* Transl Psychiatry, 2013. **3**: p. e294.
33. Das, K.P., T.M. Freudenrich, and W.R. Mundy, *Assessment of PC12 cell differentiation and neurite growth: a comparison of morphological and neurochemical measures.* Neurotoxicol Teratol, 2004. **26**(3): p. 397-406.
34. Estrada, M., A. Varshney, and B.E. Ehrlich, *Elevated testosterone induces apoptosis in neuronal cells.* Journal of Biological Chemistry, 2006. **281**(35): p. 25492-25501.
35. Harrill, J.A., et al., *Comparative sensitivity of human and rat neural cultures to chemical-induced inhibition of neurite outgrowth.* Toxicol Appl Pharmacol, 2011. **256**(3): p. 268-80.
36. Toullec, D., et al., *The bisindolylmaleimide GF 109203X is a potent and selective inhibitor of protein kinase C.* J Biol Chem, 1991. **266**(24): p. 15771-81.

37. Harrill, J.A., et al., *Quantitative assessment of neurite outgrowth in human embryonic stem cell-derived hN2 cells using automated high-content image analysis.* Neurotoxicology, 2010. **31**(3): p. 277-90.
38. Diamanti-Kandarakis, E., et al., *Endocrine-disrupting chemicals: an Endocrine Society scientific statement.* Endocr Rev, 2009. **30**(4): p. 293-342.
39. Dominguez, R., C. Jalali, and S. de Lacalle, *Morphological effects of estrogen on cholinergic neurons in vitro involves activation of extracellular signal-regulated kinases.* Journal of Neuroscience, 2004. **24**(4): p. 982-990.
40. Okada, M., et al., *Estrogen Stimulates Proliferation and Differentiation of Neural Stem/Progenitor Cells through Different Signal Transduction Pathways.* International Journal of Molecular Sciences, 2010. **11**(10): p. 4114-4123.
41. Aizuyokota, E., K. Ichinoseki, and Y. Sato, *Microtubule Disruption Induced by Estradiol in Estrogen Receptor-Positive and Receptor-Negative Human Breast-Cancer Cell-Lines.* Carcinogenesis, 1994. **15**(9): p. 1875-1879.

Table 2.1 Chemicals with evidence of neurite outgrowth inhibition or enhancement.

Compound	Study	Cell type	Effect
Bis 1	Radio et al.	CGC	↓ in neurite outgrowth
β-Estradiol	Rozovsky et al.	cortical neuron	↑ in neurite outgrowth
BPA	Seki et al.	PC 12	↓ in neurite extension
Testosterone	Zhang et al.	Cerebral cortex neuron	↓ Neurite length Neuronal differentiation
Acetaminophen	Radio et al.	PC12, CGC	Not reported in literature

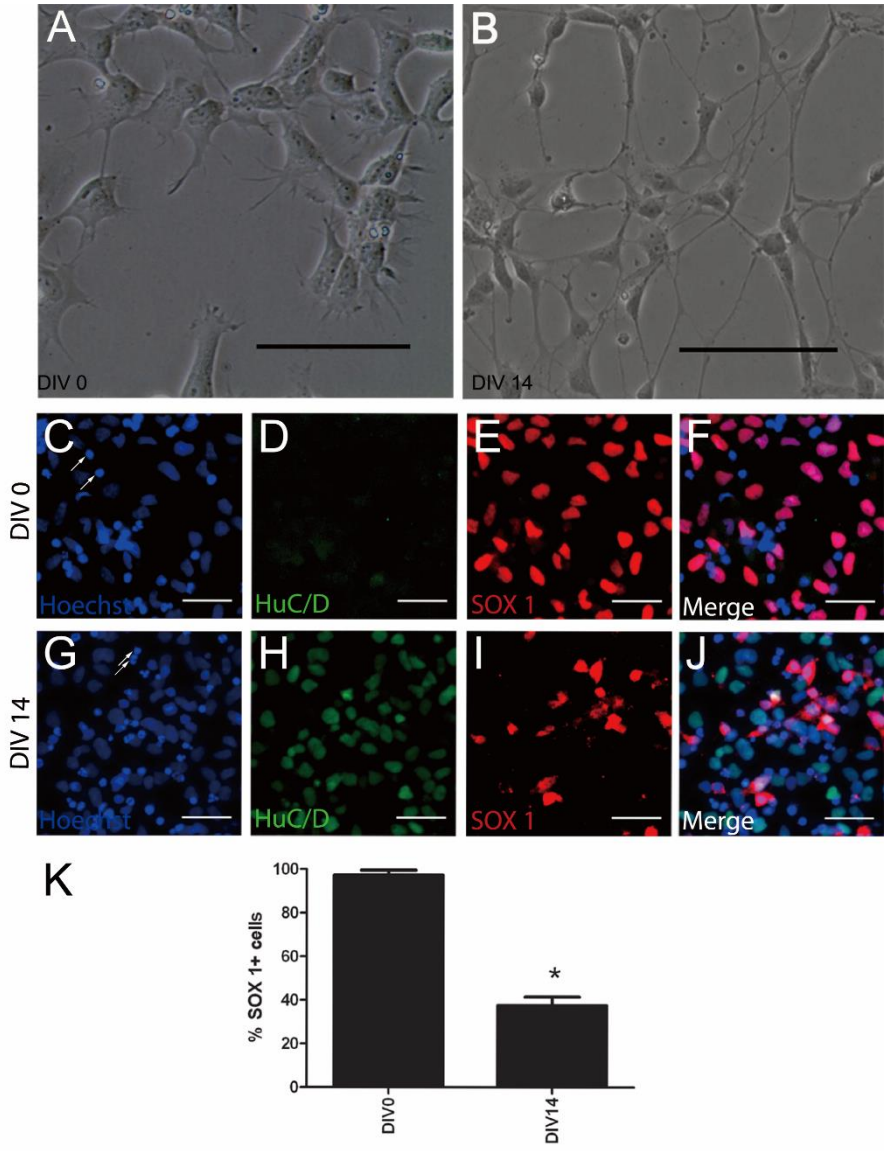

Fig 2.1 DIV 0 and DIV 14 neural cell morphology and SOX 1 expression quantification. hNP cells were seeded onto 96 well plates at a density of 15,000 cells/well, differentiating hNP cultures were fixed at end of DIV 14 for analysis following immunocytochemistry for HuC/D, SOX 1 and nuclear staining. SOX 1+ cells were then imaged and quantified by Cellomics ArrayScan VTI HCS reader high-content imaging system. A, B: Phase contrast images of neural progenitor (DIV 0) and neuron (DIV 14). Scale bars = 100 µm. C, G: DIV 0 and DIV 14 cells hoechst 33342 staining. D, H: DIV 0 and DIV 14 cells HuC/D staining. E, I: DIV 0 and DIV 14 cells SOX 1 staining. F, J: DIV 0 and DIV 14 cells Pseudo colored images. Arrows indicate invalid cells and excluded from quantification. Scale bars = 50 µm. K: The quantification of SOX 1 in DIV0 and DIV14 differentiation. Values are the means ± SD. *significantly difference between group ($P < 0.05$)

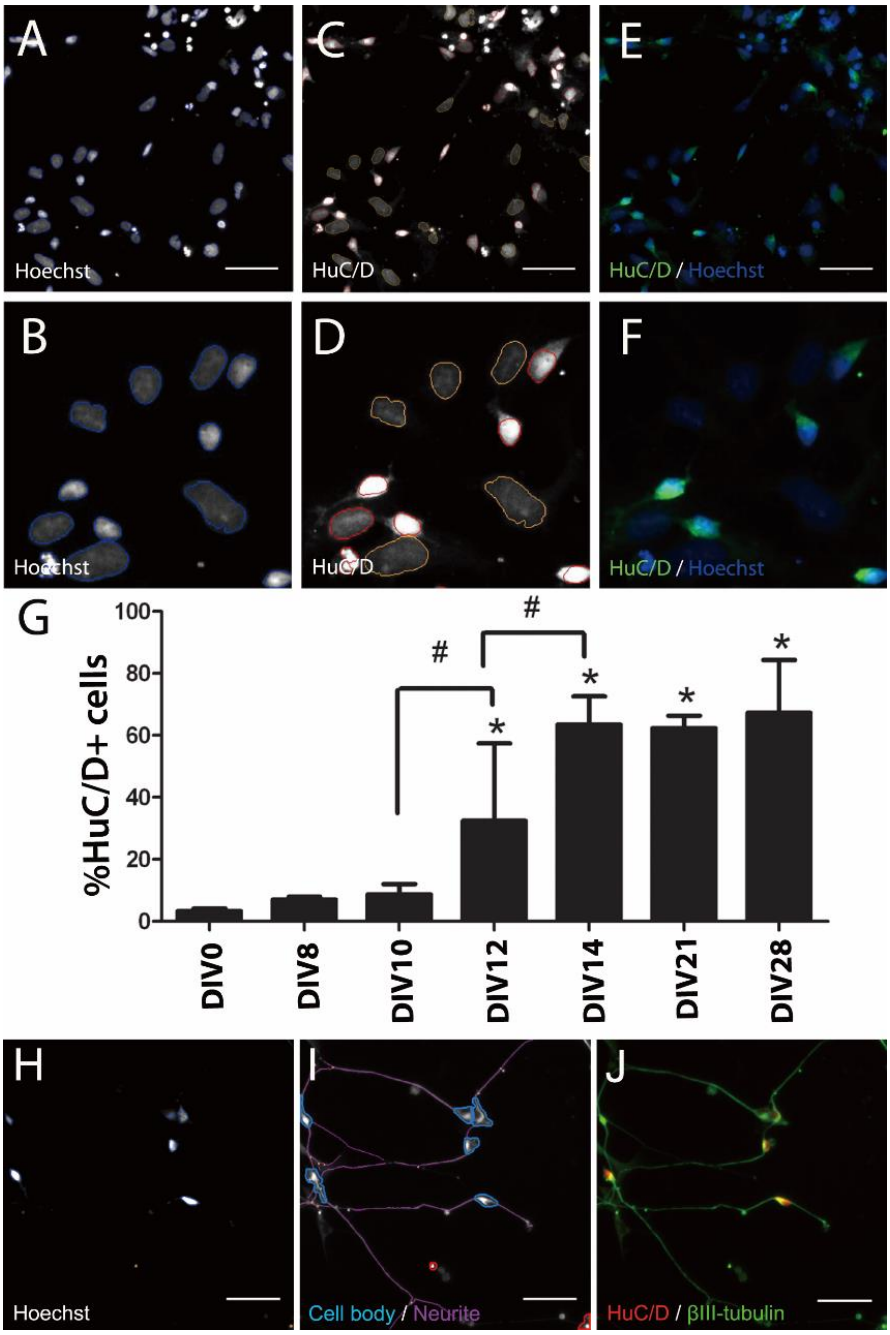

Fig 2.2. Automated measurement of HuC/D expression and quantification of neurite outgrowth during neural differentiation. hNP cells were seeded onto 96 well plates at a density of 15,000 cells/well, differentiating hNP cultures were fixed at different time points for analysis following immunocytochemistry for HuC/D, βIII-tubulin antibody and nuclear staining. Cells were then imaged and quantified by Cellomics ArrayScan V^{TI} HCS reader high-content imaging system. A, B (channel 1): Nuclei stained with Hoechst 33342, live cell nuclei (blue trace). C, D (channel 2): HuC/D+ cells stained (red trace), rejected cells stained (yellow trace). E, F: Pseudocolored composite image combining channels 1 and 2. B, D, F are magnified images to illustrate tracing in panel A-C. Scale bars = 50 µm. G: HuC/D+ expression throughout

differentiation of neuronal cells. * HuC/D expression is significantly different from control group ($P < 0.05$, one-way ANOVA), # HuC/D expression is significantly different between groups ($P < 0.05$, one-way ANOVA). H (Channel 1): Nuclei identification. Blue trace = accepted, Yellow trace = rejected. I (Channel 2): Cell body masks based on β_{III}-tubulin and HuC/D expression; Blue trace = accepted cell, Red trace = rejected cell, Purple line = neurite, Yellow dot = branch point. Cells marked as rejected are not included calculating neurites per neuron or neurite length per neuron. Neurites emerging from accepted cell bodies are traced (purple lines) and quantified. J: Pseudo colored images from C and D merged. Scale bars = 50 μm.

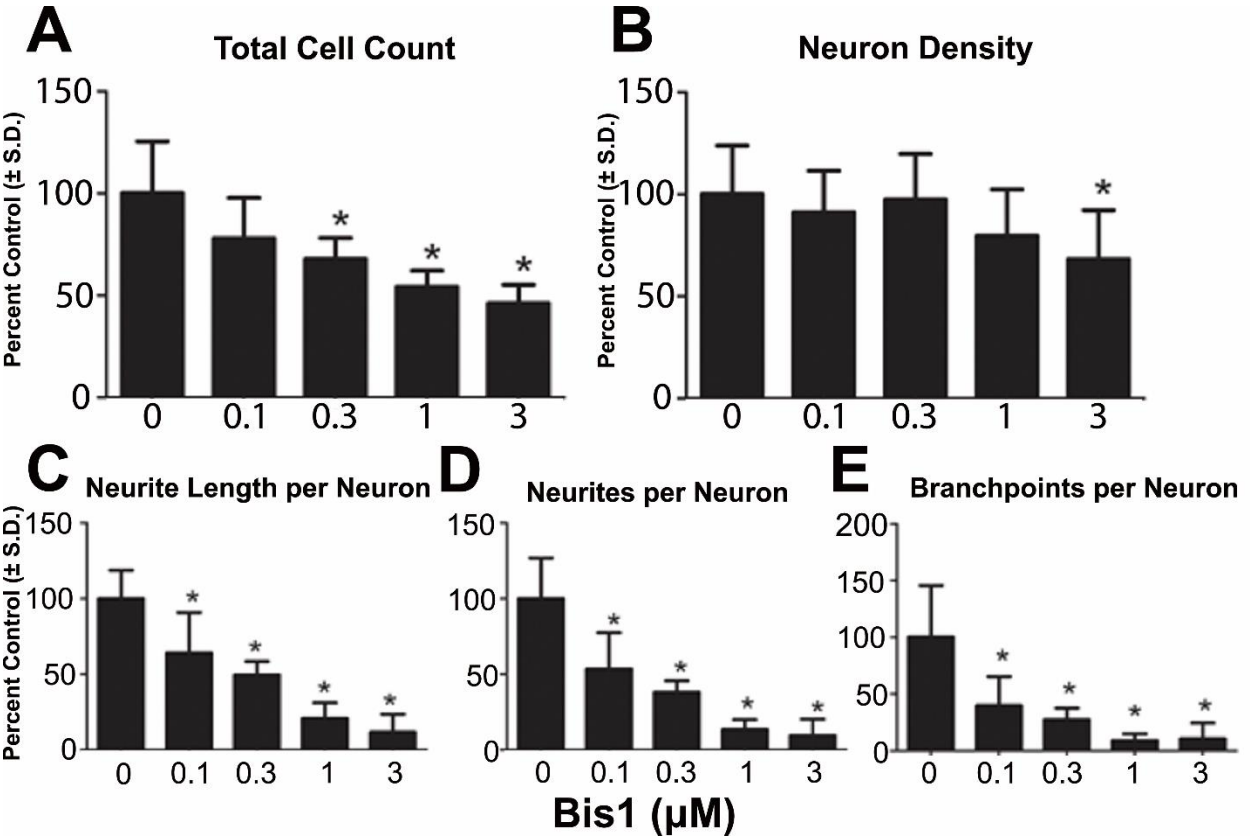

Fig 2.3. Effects of long term Bis1 exposure on neural differentiation and neurite extension. Cells were cultured on 96 well plates and continuously exposed to a range of doses of Bis1 through DIV 14. Cultures were then analyzed by immunocytochemistry staining for HuC/D along with β_{III}-tubulin followed by automated image acquisition and processing. A: Quantification of total live cells using Hoechst 33342 positive nuclei. B: Quantification of neurons (HuC/D+). Neuron density was measured as an indicator of cell health. C, D, E: Neurites per neuron, neurite length per neuron, branch points per neuron were also measured. All data are presented as % change from untreated control wells. Total live cell count, neuron density and neurite outgrowth data are from 2 biological replicates using independent cultures (n = 11 wells total). *Concentration is significant different from control group ($P < 0.05$, one-way ANOVA).

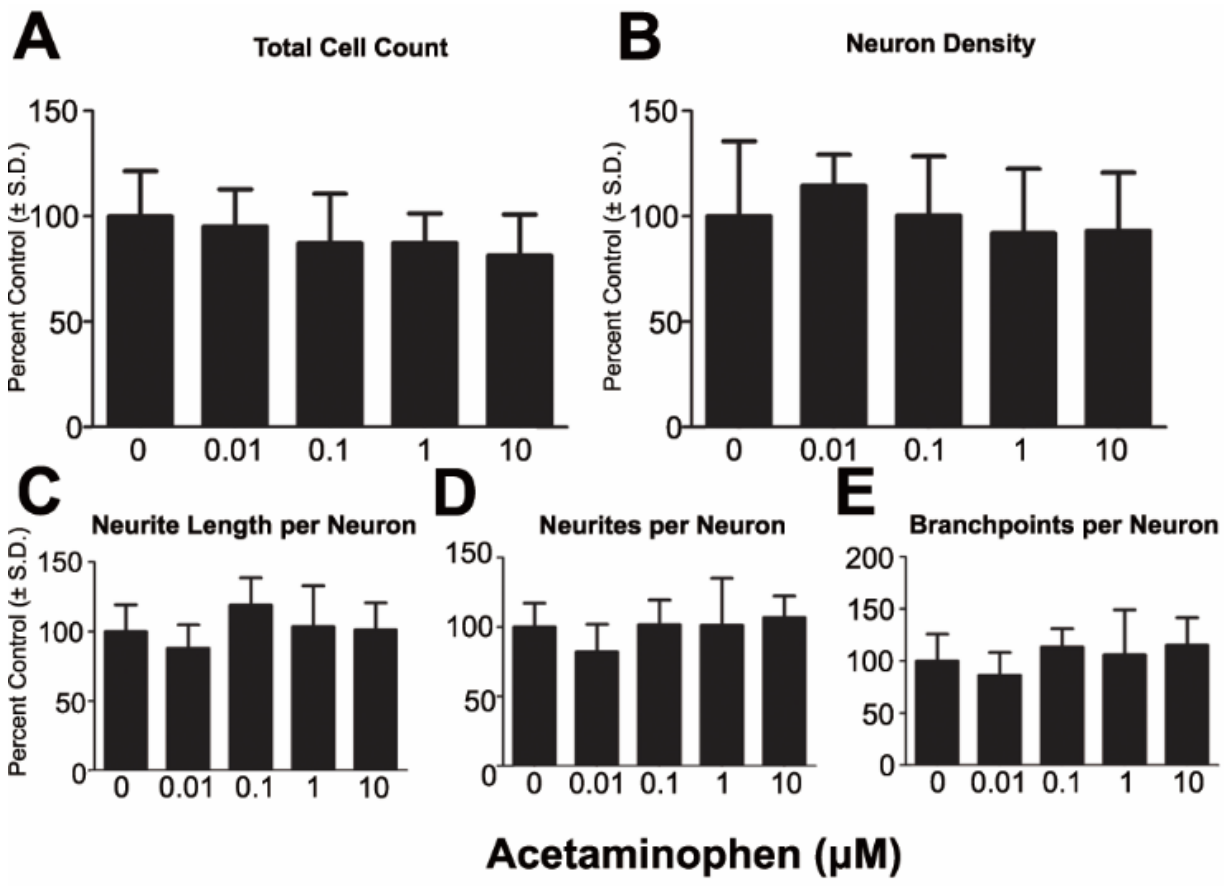

Fig 2.4. Effects of long-term acetaminophen exposure on neural differentiation and neurite extension. A: Quantification of total live cells using Hoechst 33342 positive nuclei. B: Quantification of neurons (HuC/D+). Neuron density was measured as an indicator of cell health. C, D, E: Neurites per neuron, neurite length per neuron, branch points per neuron were also measured. All data are presented as % change from untreated control wells. Total live cell count, neuron density and neurite outgrowth data are from 2 separate experiments using independent cultures (n = 12 wells total). *Concentration is significant different from control group ($P < 0.05$, one-way ANOVA).

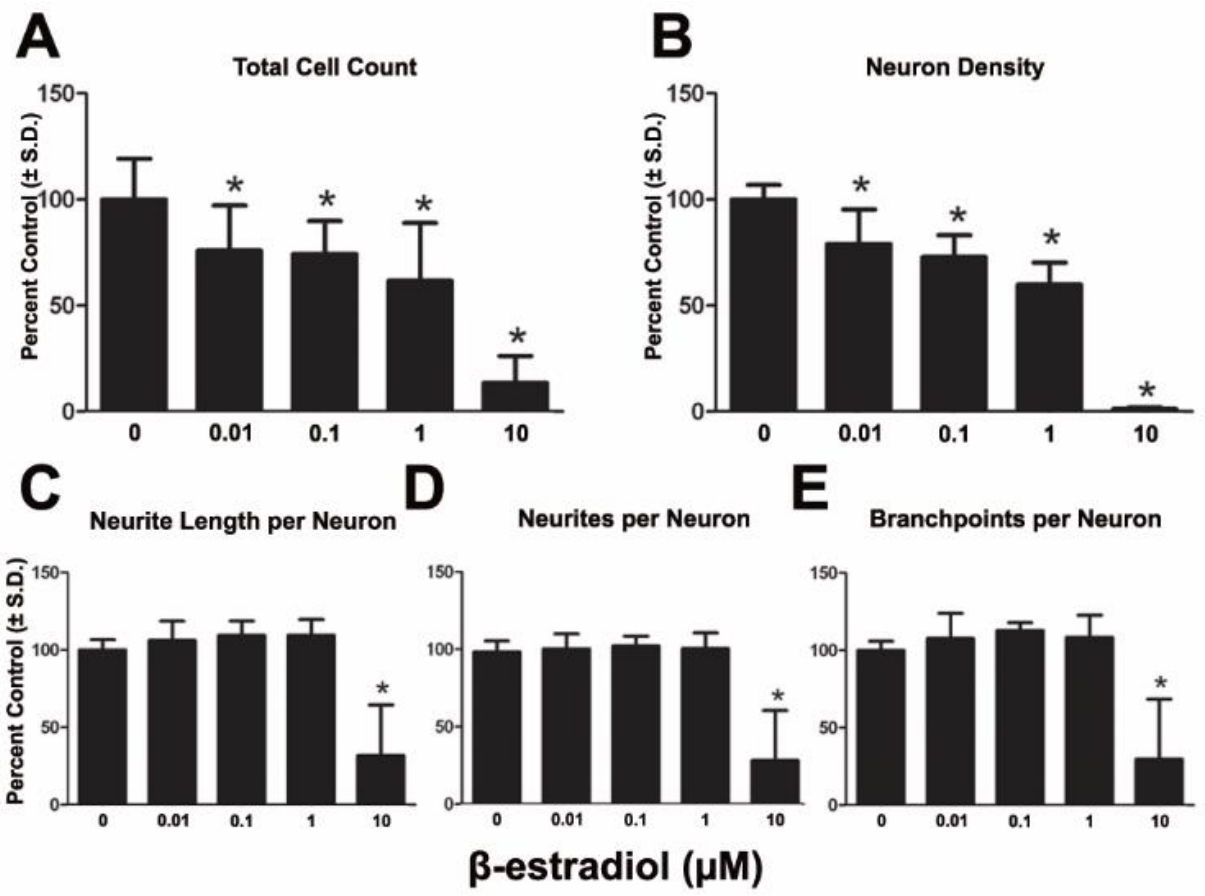

Fig 2.5. Effects of long-term β-estradiol exposure on neural differentiation and neurite extension. A: Quantification of total live cells using Hoechst 33342 positive nuclei. B: Quantification of neurons (HuC/D+). Neuron density was measured as an indicator of cell health. C, D, E: Neurites per neuron, neurite length per neuron, branch points per neuron were also measured. All data are presented as % change from untreated control wells. Total live cell count, neuron density and neurite outgrowth data are from 2 separate experiments using independent cultures (n = 11-12 wells total). *Concentration is significant different from control group ($P < 0.05$, one-way ANOVA).

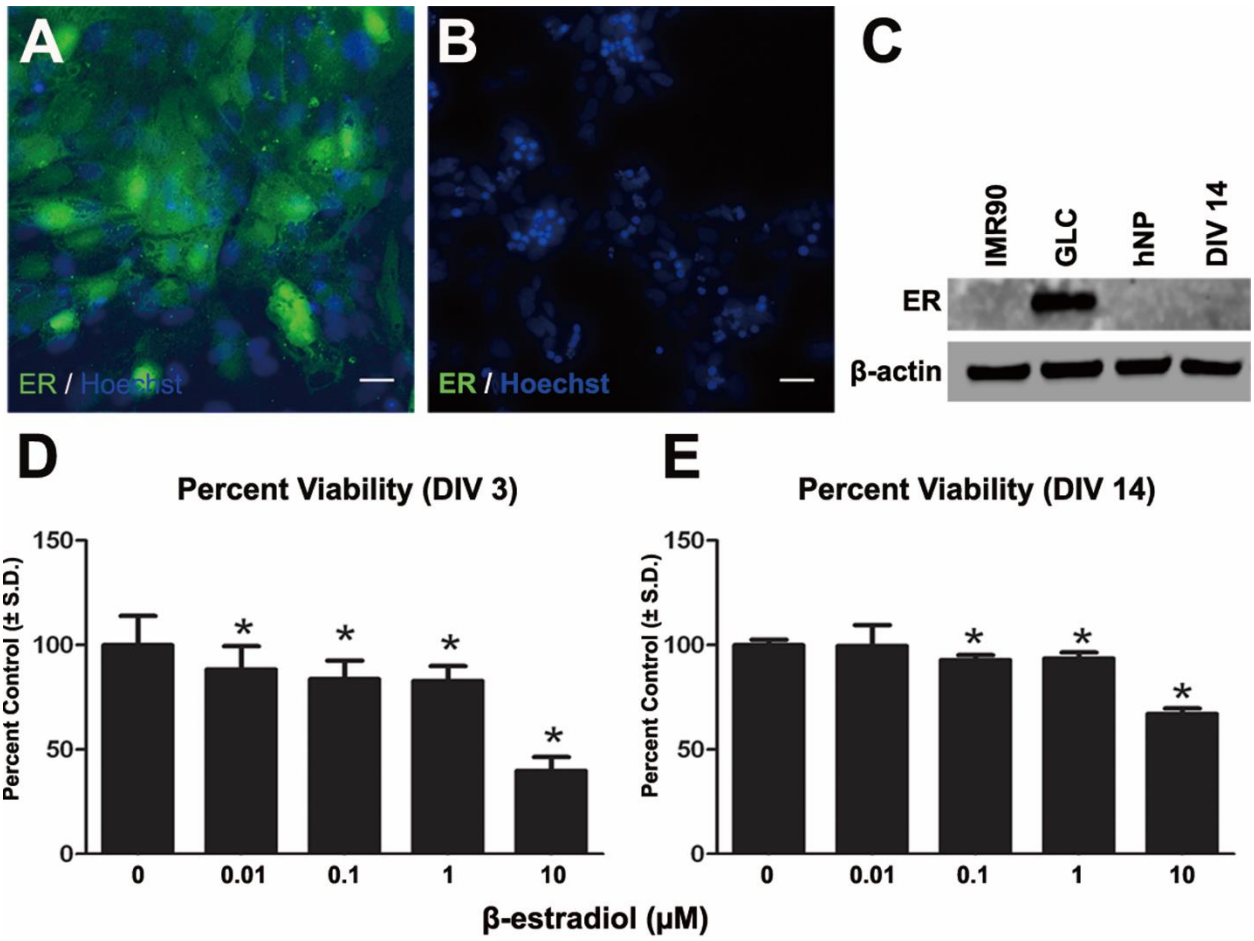

Fig 2.6. Estrogen receptor α protein expression and effect of β-estradiol on neural progenitor cells proliferation. Germ like cells, hNP cells, DIV 14 neuronal cells were seeded in 8 well slide for 24h at density of 30,000 cells per well and fixed for estrogen receptor α protein immunostaining. Germ like cells, hNP cells and DIV 14 neuronal cells were also seeded in 60mm dish and collected at 90% confluent density for western blot experiment. In proliferation assay, hNP cells were seeded onto 96 well plates at a density of 25,000 cells/well, medium was changed with β-estradiol every other day until end of DIV 3 and DIV 14. All data are from 3 separate experiments using independent cultures (n = 18 wells total). *Concentration is significantly different from control group ($P < 0.05$, one-way ANOVA). A: Germ like cell estrogen receptor α staining; B: hNP cell estrogen receptor α staining C: Western blot analysis of IMR90, GLCs, hNP and DIV 14 neuron estrogen receptor α expression. β-actin was used for normalizing the loading of samples. D: DIV 3 cell proliferation assy. D: DIV 14 cell proliferation assy. Scale bars = 50 μm.

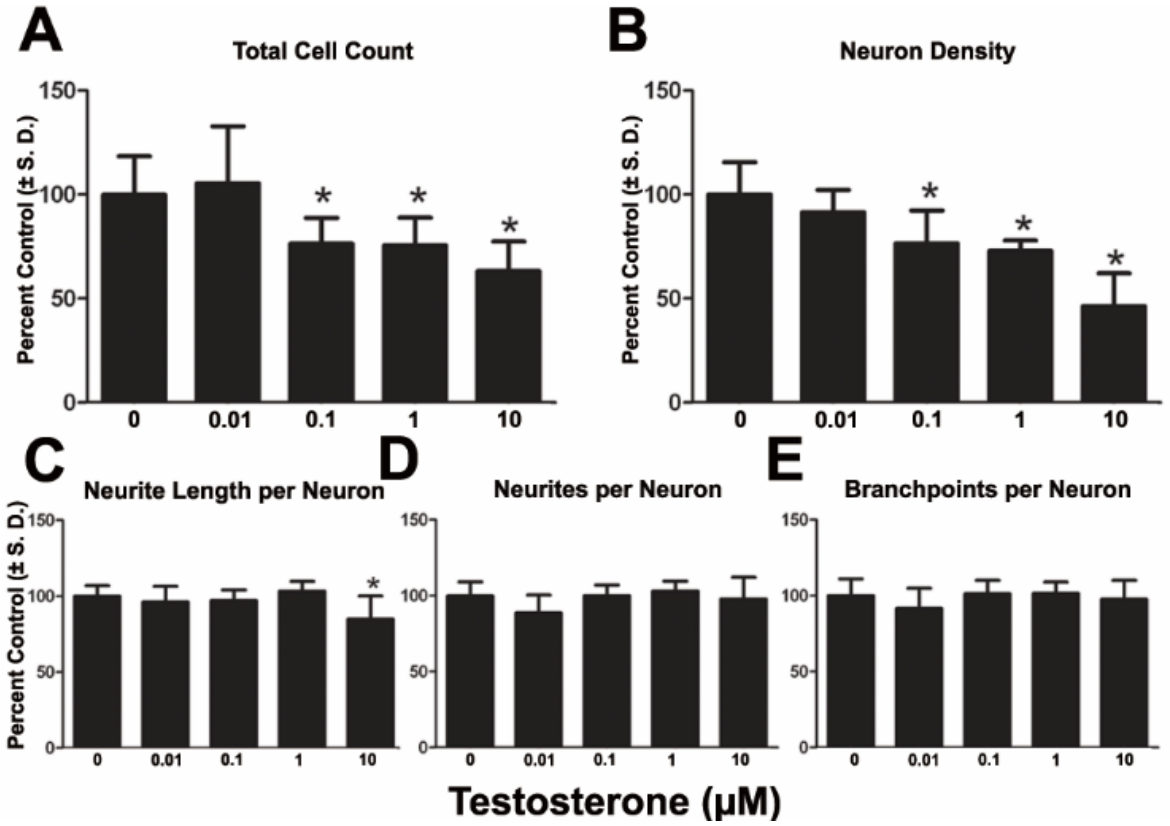

Fig 2.7. Effects of long-term testosterone exposure on neural differentiation and neurite extension. A: Quantification of total live cells using Hoechst 33342 positive nuclei. B: Quantification of neurons (HuC/D+). Neuron density was measured as an indicator of cell health. C, D, E: Neurites per neuron, neurite length per neuron, branch points per neuron were also measured. All data are presented as % change from untreated control wells. Total live cell count, neuron density and neurite outgrowth data are from 2 separate experiments using independent cultures (n = 12 wells total). *Concentration is significant different from control group ($P < 0.05$, one-way ANOVA).

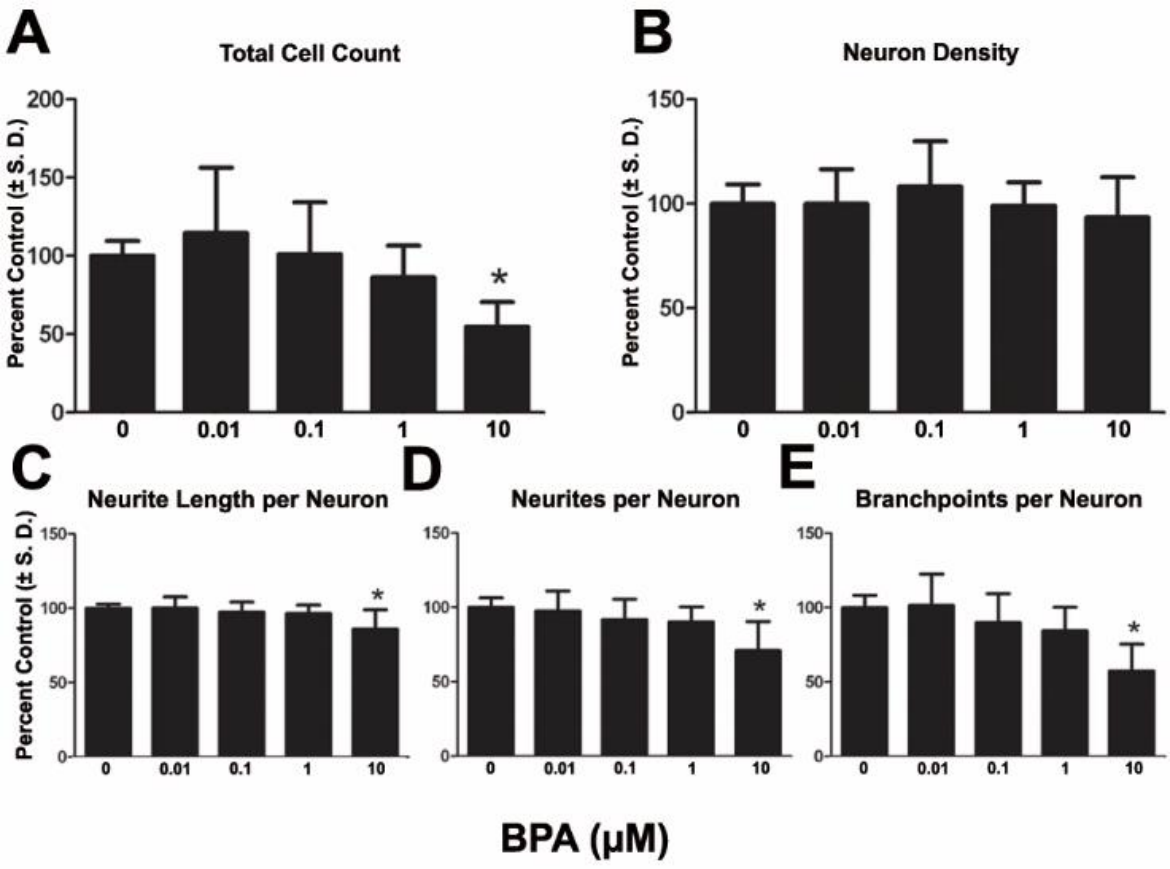

Fig 2.8. Effects of long-term BPA exposure on neural differentiation and neurite extension. A: Quantification of total live cells using Hoechst 33342 positive nuclei. B: Quantification of neurons (HuC/D+). Neuron density was measured as an indicator of cell health. C, D, E: Neurites per neuron, neurite length per neuron, branch points per neuron were also measured. All data are presented as % change from untreated control wells. Total live cell count, neuron density and neurite outgrowth data are from 3 separate experiments using independent cultures (n = 18 wells total). *Concentration is significant different from control group ($P < 0.05$, one-way ANOVA).

CHAPTER 3

Quantitative assessment of endocrine disruptors, pesticides, and retinoic acid neurite outgrowth toxicity in embryonic stem cell derived neurons[1]

[1]Xian Wu, Anirban Majumder, Forrest Goodfellow, Steven L. Stice 2016. Quantitative assessment of endocrine disruptors, pesticides, and retinoic acid neurite outgrowth toxicity in embryonic stem cell derived neurons. Submitted to *Journal of Stem Cells Research, Reviews & reports*, 10/27/2016

Abstract

Human embryonic stem cell (hESC) based developmental neural toxicity (DNT) assays have become an alternative to expensive and time consuming animal DNT models. Previously using hESC derived neuronal cells has been employed as a DNT assay for neurite extension/recovery. However, in these previous studies the cell population contained both human neural progenitor (hNP) cells and neurons. Our objective was to assess the commercially available hESC derived NeuroNet™, here referred to as DIV 28 neurons, in a high content image screening system using a training set of chemicals, previously shown to alter brain development. Results showed that expression of neuronal cell marker microtubule-associated protein 2 (MAP2), which is involved in neuron cell microtubule assembly, was 96.5% in DIV 28 neurons. In the neurite outgrowth toxicity screening, retinoic acid (RA), chlorpyrifos (CPF) and diethylstilbestrol (DES) inhibited neurite outgrowth at 10 µM and did not decrease cell density. β-estradiol inhibited neurite outgrowth at 30µM while this occurred at 10µM for testosterone. Bisphenol A (BPA) did not affect cell density nor neurite outgrowth at any concentration tested. We have tested uniform DIV 28 neurons in high content assay using a training set of neurotoxicants, including BPA. Here, BPA did not induce cellular neurotoxicity in mature human neurons.

Introduction

Developmental neurotoxicity resulting from chemical exposure is of increasing concern regarding recent increases in the prevalence of neurological disorders such as attention deficit hyperactivity disorder and autism [1]. The developing central nervous system (CNS) is often more vulnerable to injury than the adult CNS [2]. Of over 80,000 chemicals commercially available, only about 200 have undergone developmental neurotoxicity testing according the established guidelines [3]. Numerous in vitro cell models had been developed for neurotoxicity endpoint high throughput screening. Neurite outgrowth in differentiating hNP cell cultures is a sensitive endpoint at non-cytotoxic exposure that indicates neurotoxicity at lower doses [4]. The cell source in neurite outgrowth assays range from transformed cell lines, primary cells to hESC sources. Cell lines include the following: rat pheochromocytoma: PC12, rat neuroblastoma: B50, mouse neuroblastoma: NB2a, N2a, N1E-115, human neuroblastoma: SH-SY5Y, SK-N-SH, IMR-32, LA-N-5 and human embryonal carcinoma cell line NT2 [5, 6]. Since these cells are derived from tumor or transformed with virus, they do not necessarily exhibit the same phenotype as the original primary cell [5, 7]. Primary neuronal cell models acquire the properties of mature neurons with neurites, but usually they are a mixture of different neuronal populations and have limited lifespan in culture.

Human PSC, which includes both embryonic and induced sources, are being developed as in vitro model systems for drug and chemical testing. These in vitro model systems have the potential to predict or anticipate toxicity in humans [8]. In an induced pluripotent stem cell (iPSC) derived neuron study, these neuron cells identified 6 neurotoxic compounds specifically inhibiting neurite outgrowth out of a library of 80 compounds. The data demonstrates the potential of human iPSCs in identifying, prioritizing compounds with DNT potential for further

in vivo testing [9]. But uniformity of neural cell population for screening is still of concern since no appropriate neural cell marker quantification was performed in the study [10]. Compared to hESC, iPSCs have significantly reduced efficiency and increased variability [11]. Different iPSC colonies have various gene expression signatures that contributed to viability of iPSC, and consequently could have increased variability among different iPSC cell lines in a DNT assay [12].

The derivation of human neural progenitor (hNP) cells from hESC cells facilitates the interrogation of human embryonic development through the generation of neuronal subtypes and supporting glial cells [13]. Previously in our lab we differentiated hESC cells to proliferating a hNP cell stage. hESC were induced into adherent neural tube-like rosettes over 18–21 days of differentiation and were nestin and Musashi 1 positive [14]. Dissociated neural rosettes cells were proliferated as a uniform hNP cell population and for the sake of this chapter represents 0 DIV. The hNP cells were the initial population for differentiated neuron cultures. At DIV 14 after withdrawal of bFGF, hNP cells differentiated into βIII-tubulin and MAP2 positive neuron cells and generated a population of post-mitotic human neurons containing a mixture of glutamatergic, GABAergic and cholinergic neuron cells [15]. DIV 28 neurons were derived from hNP cells using a proprietary process under defined feeder-free and serum-free conditions. These DIV 28 neurons are cryopreserved and ready to use differentiated neurons for high throughput developmental neurotoxicity screening without contaminating hNP cells.

In an in vitro study using DIV 14 cells, mostly neurons but containing some residual hNP cells, neurite outgrowth was assessed using automated high-content image analysis [16]. In the study, concentration-dependent decreases in neurite outgrowth were observed following treatment of DIV 14 neuron cells with five known chemicals which inhibited neurite outgrowth

in primary rodent neural cultures: bisindolylmaleimide I, U0126, lithium chloride, sodium orthovanadate and brefeldin A [16].

In this study, we utilize MAP2 expression to quantify neuron cell body and neurite outgrowth in DIV 28 neurons. MAP2 belongs to the microtubule associated protein family and is thought to be involved in microtubule assembly, which is an essential step in neurogenesis [17]. MAP2 is restricted to the dendritic compartment while the presence of a number of phosphorylated neurofilaments (detected by the SMI-312 antibody) is specific to axon [18]. Therefore, MAP2 is ideal for labeling all DIV 28 neuron neurite extensions in culture.

To evaluate the predictive ability of the uniform mature DIV 28 neurons, a training set of chemicals that have been shown to alter brain development after in vivo exposure was used. A training set of chemicals is often used to evaluate the relevance of alternative test methods with in vivo developmental neurotoxicity [19]. From the list of chemicals with demonstrating effects on neurodevelopment, our training set consisted of eight chemicals from the literature including two pesticides: CPF and permethrin, a morphogen RA, two endocrine disruptors: BPA and DES, two hormones: β-estradiol, testosterone, and amoxicillin as a negative control. The 48 hours chemical exposure in DIV 28 neurons resulted in neurotoxicity at cellular level. β-estradiol affected neurite outgrowth and the effects likely mediated via an estrogen receptor α (ER α) independent mechanism given the absence of ER α expression in the neural cells. Testosterone significantly affected neurite network morphology without affecting neuron cell viability. Superb performance with this testing set of chemicals suggest that the DIV 28 neurons high purity cell model should now be used for high content and higher throughput screening of larger compound libraries.

Materials and methods

Cell culture. DIV 28 neurons are obtained in cryopreserved state, but originally derived from hNP1™ cells (ArunA Biomedical, Athens GA). Cryopreserved DIV 28 neurons were thawed and live cell were counted by trypan blue cell viability test. DIV 28 neurons (10,000 live cells/well) were subcultured on matrigel 1:100 (B&D) coated costar® 96-well cell culture plate in AB2™ basal medium supplemented with ANS™ neural supplement (both from ArunA Biomedical Inc., Athens, GA), 2 mM L-glutamine (Gibco), 2 U/ml penicillin (Gibco), 2 µg/ml streptomycin (Gibco) and 10 ng/ml leukemia inhibitory factor (LIF) (Millipore, Billerica, MA, USA). Cells were maintained in a humidified incubator at 37°C with a 95% air/ 5% CO2 atmosphere.

Chemical treatment. Test compounds amoxicillin, RA, CPF, permethrin, β-estradiol, testosterone, DES, BPA were all prepared as stock solution: 0.15, 0.5, 1.5, 5, 15 mM. Stock solution in DMSO except amoxicillin in water were then diluted in differentiation medium 50X and a final 10X dilution in culturing differentiation medium to make final concentration to 0.3, 1, 3, 10, 30µM. Test compounds were added to cell cultures 2 hours after cells were seeded in 96 well culture plates. Cells were fixed at the end of 48 hours incubation for immunofluorescent staining.

Immunocytochemistry. Immunofluorescent staining was performed using Eppendorf epMotion system for automated fixing and staining. Briefly, cells were fixed with 4% Paraformaldehyde. 100 µl of a warm (37 °C) solution of 8% paraformaldehyde were added to culture wells containing 100 µl of medium and incubated at room temperature for 20 min. Fixative was then gently aspirated and cells were washed three times with phosphate-buffered saline (PBS). Primary antibody MAP2 (EMD Millipore, Billerica, MA) was diluted in

intracellular blocking solution [20] and was then applied for 2 hours at RT. Following incubation in primary antibodies, cells were washed three times with high salt buffer and incubated with a 1:400 dilution of DyLight® 594-conjugated donkey anti-mouse IgG secondary antibody in high salt buffer for 1 h at room temperature, protected from light. Finally, cells were incubated in 0.1% Hoechst 33342 dye in high salt buffer for 20 min, then in PBS washed 3 times with high salt buffer, and stored in PBS at 4 °C prior to image acquisition and analysis [16].

Image acquisition and analysis. MAP2 labeled DIV 28 neurons were allowed to warm to room temperature. Cellomics ArrayScan VTI HCS reader high-content imaging system (ThermoFisher Scientific, Waltham, MA) was used for automated image acquisition and morphometric analyses as previously described for use on DIV 14 neuron cells [16]. Briefly, optimization of nucleus and cell body selection criteria, as well as cell body masking and neurite tracing parameters, were determined a priori by using representative images from untreated cultures. Nuclei were first identified in channel 1 as bright objects on a dark background (Fig. 3.1A, 3.1B). Nuclei with size and intensity values outside of the ranges determined a priori for viable cells were identified in the channel 1 image and rejected from further analyses. Spatial coordinates from the channel 1 image were then superimposed on the matching channel 2 image. Protein expression in channel 2 were then cast based on positional data from channel 1 nuclei and a set of user-defined geometric and signal intensity-based parameters (Fig. 3.1C). Positive objects based on intensity value were then selected (Fig. 3.1D) and invalid objects rejected. Neurite outgrowth measurements were collected on a cell-by-cell basis, and values were averaged to obtain population means within each well. Population means of each well were treated as the statistical unit for analysis of neurite outgrowth. Output from high content image analysis included total cell count (% viable nuclei per well) and measurements of neurite

outgrowth (neurites per neuron, neurite length per neuron, and branch points per neuron). At 20X magnification, the Cellomics ArrayScan VTI can sample 81 individual fields within each well. In this study, 35 fields were sampled within each well for cell characterization.

Statistics. Neurite outgrowth experiments were performed three times using independent cultures with n = 6 wells per condition per culture. For concentration-response experiments, total cell count, neurite outgrowth data were normalized within experiment to corresponding control wells prior to statistical analysis. For each concentration-response examined, experiments were repeated three times using independent cultures as described. All data analyzed for cell characterization and concentration-response experiments were using a one-way ANOVA with a significance threshold of $p < 0.05$. This was followed by a Tukey's test to determine if different time points means were significantly different from corresponding control means. Mean values ± standard deviations for all measurements are provided throughout the text. Statistical analysis was performed using Graphpad Prism1 v5.

Results

Quantification of DIV 28 neurons using high content analysis. To determine the purity of DIV 28 neurons, the percentage of cells that were MAP2 positive were observed and compared to earlier DIV 0, 14, and 21. The MAP2 positive population increased steadily DIV 0 to DIV 28. MAP2 expression increased to 77.4 % in DIV14 neural cells and continuously increased from 79.9% on DIV 21 to 96.5% in DIV 28 neurons (Fig. 3.2A). Upon comparing DIV 14 neurons to DIV 28 neurons a drastic changes in neurite outgrowth are observed. Neurites per neuron increased from cell body by 166%, neurite length per neuron increased by 465 %, and

branch points per neuron by 251 % (Fig 3.2B, 3.2C, 3.2D). These results indicate increases in neuronal maturity of DIV 28 neurons.

ER α is not expressed in DIV 28 neurons. ER α was involved in neural proliferation and differentiation in non-human neural cell lines [21, 22]. Therefore, we examined expression of ER α in both hNP cells and DIV 28 neurons. The hNP cells were negative for ER α expression when compared to known ER α positive hESC derived cell germ-like cell line (Fig. 3.3). Additionally, the absence of ER α expression in both DIV 0 cells and DIV 28 neurons were confirmed by western blot (Fig. 3.3).

All neurotoxicants, except BPA, affected DIV 28 neurons density or neurite outgrowth. The training set included eight compounds. Seven have well-defined molecular mechanisms of action from the literature as having effects on neurite outgrowth in primary rodent neural cultures [19, 23]. Acetaminophen is an assumed non-neurotoxic drug [24]. All parameters including total cell count and neurite outgrowth were normalized to percentages of non-treated cells. For each compound a five-point concentration-response curve was examined.

Following a 48 hour exposure, concentration-dependent decreases in neurite outgrowth was observed following exposure to RA (Fig. 3.4C, 3.4D). At 30 μM, total cell count was significantly decreased by 37.8% (Fig. 3.4C). Significant decreases in neurite outgrowth were accompanied by concurrent decreases in total cell count also at 30μM compared to untreated controls. Significant (35.1%) decrease in neurites per neuron and a significant (45.1%) decrease in neurite length per neuron were observed at 10 μM. Significant decreases in neurite outgrowth were not observed at concentrations of RA below 10 μM, but significant decreases in branch points per neuron were observed at 3 μM (Fig. 3.4D).

Similarly, chlopyrifos significantly decreased total cell count at 30 μM, but neurite outgrowth was significantly decreased at 10 and 30 μM while branch points were only inhibited at 30 μM (Fig. 3.4E, 3.4F). Permethrin, a pesticide and neurotoxin, inhibited total cell density at 30 μM by 28.8%, and also significantly inhibited branch points per neuron by 20.5%. However, permethrin did not inhibited neurites per neuron and neurite length per neuron independent of cell density in this study (Fig. 3.4G, 3.4H).

We tested increasing doses of four known EACs in this human neuron model. β-estradiol had no significant effects on total cell count at any of the concentrations examined (Fig. 3.5A). In contrast, at 30 μM, there was a significant (16.53%) decrease in neurites per neuron as well as a significant (37.91%) decrease in neurite length per neuron (Fig. 3.5B). Significant decreases in branch points per neuron were also observed at 30 μM and no inhibition effect were observed below 3 μM on all three parameters. These data demonstrate a specific inhibition of neurite outgrowth by 30 μM β-estradiol, a concentration that does not significantly inhibited cell density.

Testosterone significantly decreased neurite outgrowth but did not reduced cell density at any concentration (Fig. 3.5C). Significant decreases in branchpoints per neuron were first observed at 3 μM testosterone. Neurites per neuron, neurite length per neuron, and branchpoints per neuron were inhibited by 10 μM testosterone incubation separately at 17.36%, 17.4%, 22.8% comparing to untreated DIV 28 group. At 30 μM, neurites per neuron, neurite length per neuron, and branchpoints per neuron were inhibited at 19.02%, 34.27%, 35.35% respectively compared to untreated DIV28 neuron (Fig. 3.5D).

DES (30 μM) exposure induced significant decreases in neurite outgrowth and total cell count following exposure. At 3, 10 μM DES, total cell count was not inhibited however branch points per neuron was inhibited by 24.91% and 58.63%, respectively. At 10 μM all neurite

endpoints decreased: neurites per neuron 40.54% neurite length per neuron 58.35%. Total cell number was significantly decreased only at 30μM by 38.56% (Fig. 3.5E, 3.5F).

The effects of BPA were unique among the neurotoxicant compounds examined in that all concentration treatment from 0.3 to 30 μM did not affect total cell density or neurite measurements including neurites per neuron, neurite length per neuron, and branch points per neuron (Fig 3.5G, 3.5H). These data demonstrate that BPA effect on neurite outgrowth was less compared to other EACs at the same concentration.

Discussion

Traditionally, toxicity testing relied heavily on data generated from laboratory animal species. Tens of thousands of chemicals are now in commerce, but very limited toxicology data has been generated for the chemicals [25]. Also there are both quantitative and qualitative differences between laboratory animal and human and the use of animal data generated for pharmaceutical or other chemical toxicity prediction for human is still of concern [26]. Consequently, it is extremely important to employ high throughput methods to provide the toxicology information for the chemicals. Prior methods using DIV 14 neuron cells screening provided a novel method using hESC in neurotoxicity screening [16, 27]. However, here we showed that MAP2 expression was present in only 77.4% of the cells at DIV 14 and expressed at significantly greater level in DIV 28 neurons. This results suggests that less mature or other cell cells were present at DIV 14 but not at DIV 28.

Retinoic acid induced neurite outgrowth in embryonic chick sympathetic neurons (5×10^{-9} M) and in neonatal mouse dorsal root ganglia neurons (10^{-8} M) [28]. In dissociated sympathetic neurons taken from the superior cervical ganglia of rat embryos, RA inhibited initial dendritic

growth, suggesting RA may regulate neuron cells in different ways depending upon type of neuron, and possibly species [29]. In DIV 28 neurons, increasing concentration of RA inhibited neurite outgrowth, but did not alter cell density indicating a specific effect of RA on neurite outgrowth. As a morphogen, RA plays important roles in many aspects of neural development and activity but RA is also a well-known teratogenic agent [30]. In mature DIV 28 neuron population, 3-30 μM RA exposure led to branch point and neurite outgrowth inhibition. Previously, hESC when exposed to 2μM RA and undergoing neural induction formed fewer neural rosettes [31]. Together, our finding of neurite outgrowth inhibition combined with previous teratogenic effect on neural rosettes, indicates RA is neurotoxic through both neural tube formation and neurite elongation windows of susceptibility.

Chlorpyrifos levels in blood ranged from non-detectable to 1385ng/ml (~ 4mM) in mothers and from non-detectable to1726ng/ml (~5mM) in newborns in an intensively farmed region with approximately 200,000 kg of organophosphates applied annually [32]. The concentrations used in this research represent the concentration pregnant women and neonates would encounter in the high exposure workplace. Covalent binding of CPF to tubulin and to tubulin-associated proteins is a potential mechanism of neurotoxicity [33]. Using DIV 28 neurons, chorpyrifos inhibited neurite outgrowth at 10 and 30 μM and inhibited neuron density at 30 μM. Thus there was a neurite outgrowth specific inhibition at 10 μM of CPF. And10 μM is below detected CPF blood concentration indicating the potential human neurotoxicty [32]. CPF inhibited neurite outgrowth at approximate 50 μM in iPSC derived neurons which was higher than observed in the mother and newborn study [32]. The difference could result from uncharacterized MAP2 negative population in iPSC culture comparing to high purity MAP2 positive (96.5%) populations in this study.

In rats primary postmitotic sympathetic neurons cells CPF inhibited axonal neurite outgrowth as low as 0.001 μM [34] and in mouse N2a neuroblastoma cells axon outgrowth was inhibited by 3 μM CPF [35]. Different sensitivity of CPF among DIV 28 neurons, primary cell and cell lines and also between species should be taken in consideration for CPF human risk assessment. Further mechanism study on CPF is needed and could provide information for CPF sensitivity in different cells and species.

Exposure to permethrin showed dose-dependent cytotoxicity evaluated with the ATP assay in a SH-SY5Y neuroblastoma cell model [36]. Permethrin reduced DIV 28 neurons cell viability at highest concentration (30μM) and also branch point at 30μM. The inhibition of cell density detected in our model confirm its toxicity in hESC derived human neuron cells for the first time. Permethrin inhibited neurite extension in chicken isolated primary neuron cells through regulation of Ca^{2+}-ATPase activity [37]. However, we did not observe an inhibition on neurite outgrowth in DIV 28 neurons. Further higher dose exposure and mechanism studies on Ca^{2+}-ATPase activity in the DIV 28 neurons may be necessary to explore permethrin developmental neurotoxicity.

We also tested four known endocrine disruptor chemicals and previously presented DNT activity (β-estradiol, testosterone, BPA and DES). β-estradiol regulates the development, maturation, survival, and function of multiple types of neurons in distinct brain regions. Rat embryonic neural stem cells isolated from brain striatal tissue demonstrated that β-estradiol increased rat embryonic neural stem cell proliferation, and this response is estrogen receptor (ER) dependent. A previous study has indicated that in rat neurons, estrogen induced neurite outgrowth in basal forebrain cholinergic neurons in vitro [38] and another study shows β-estradiol had a neuroprotective effect [39]. Both effects were attributed to ER α mediated

signaling. In our human neural model, β-estradiol inhibited neurite length, neurite number and branch point. This effect was observed without reducing cell density. All these effects were likely mediated via an ER α independent mechanism given the absence of ER α expression in DIV 28 neurons. Although we did not attempt to detect the presence of ER β, and involvement of this receptor in cell differentiation cannot be ruled out. ER α independent mechanisms could also occur, including a cytoplasmic microtubule fibers disruption at interphase that affected cell growth [40].

Testosterone specifically inhibited DIV 28 neurons neurite outgrowth without cell density inhibition. In a primary neuron model from the cortex of 14-day-rat embryos (E14), testosterone inhibited neurite outgrowth at 50 and 100 nM and inhibitory effect of testosterone on differentiation may be androgen receptor (AR)-mediated [41]. Further mechanism study on neurite outgrowth inhibition by testosterone in human neural cells should be addressed focusing on AR expression and intracellular Ca^{2+} signaling change.

The synthetic estrogen DES is a potent perinatal endocrine disruptor. DES is an ER α and ER β antagonist [42]. However DES inhibition effect on neurite outgrowth was likely mediated via an ER α independent mechanism, given the absence of ER α expression in DIV 28 neurons. Our results are consistent with results from a human iPSC derived neurons model. DES exposure inhibited neurite outgrowth and branch point without inhibition on cell density [9]. DES was found to have anti-tumor properties and clinical effectiveness in prostate cancer [43]. In patient treated with DES, range between 1 and 32 mg/ml plasma [44]. A high dose of DES could raise neurotoxicity in the CNS to equivalent concentration tested here (10 μM) that altered neurite outgrowth, suggesting neurotoxicity in humans.

BPA was not toxic on cell density nor did it inhibit neurite outgrowth at any concentrations, ranging from 0.3-30μM. In PC12 cell system, BPA inhibited neurite outgrowth through inhibition of phosphorylation of mitogen-activated protein kinase as low as 10 ng/ml BPA [45]. These conflicting results might have been due to species difference and different levels of kinase activity. However, according to the Organization for Economic Cooperation and Development and U.S. Environmental Protection Agency guidelines for the study of developmental neurotoxicity, our data of BPA concurs with recent findings. There was no data to support BPA being a developmental neurotoxicant and there were no neurological or neurobehavioral effects at either high or low doses of BPA [46]. At the same time, the current testing strategy may overlook sensitive effects of BPA, and possibly other potential endocrine disruptors, especially in female offspring [47]. Our neuron cells were derived from WA09 hESC cell line that came from female donor and may be more suitable for female specific DNT study.

Conclusion

Our screening using DIV 28 neurons detected neurotoxicity in a diverse training set and supports recent finding that BPA as a neurotoxicant, may be over stated.

References

1. Grandjean, P. and P.J. Landrigan, *Developmental neurotoxicity of industrial chemicals.* Lancet, 2006. **368**(9553): p. 2167-78.
2. Costa, L.G., et al., *Developmental neuropathology of environmental agents.* Annual Review of Pharmacology and Toxicology, 2004. **44**: p. 87-110.
3. Makris, S.L., et al., *A retrospective performance assessment of the developmental neurotoxicity study in support of OECD test guideline 426.* Environ Health Perspect, 2009. **117**(1): p. 17-25.
4. Jeerage, K.M., T.L. Oreskovic, and S.L. Hume, *Neurite outgrowth and differentiation of rat cortex progenitor cells are sensitive to lithium chloride at non-cytotoxic exposures.* Neurotoxicology, 2012. **33**(5): p. 1170-9.
5. Coecke, S., et al., *Workgroup report: incorporating in vitro alternative methods for developmental neurotoxicity into international hazard and risk assessment strategies.* Environ Health Perspect, 2007. **115**(6): p. 924-31.
6. Radio, N.M. and W.R. Mundy, *Developmental neurotoxicity testing in vitro: Models for assessing chemical effects on neurite outgrowth.* Neurotoxicology, 2008. **29**(3): p. 361-376.
7. Radio, N.M. and W.R. Mundy, *Developmental neurotoxicity testing in vitro: models for assessing chemical effects on neurite outgrowth.* Neurotoxicology, 2008. **29**(3): p. 361-76.
8. Harrill, J.A., et al., *Comparative sensitivity of human and rat neural cultures to chemical-induced inhibition of neurite outgrowth.* Toxicol Appl Pharmacol, 2011. **256**(3): p. 268-80.
9. Ryan, K.R., et al., *Neurite outgrowth in human induced pluripotent stem cell-derived neurons as a high-throughput screen for developmental neurotoxicity or neurotoxicity.* Neurotoxicology, 2016. **53**: p. 271-281.
10. Druwe, I., et al., *Sensitivity of neuroprogenitor cells to chemical-induced apoptosis using a multiplexed assay suitable for high-throughput screening.* Toxicology, 2015. **333**: p. 14-24.
11. Hu, B.Y., et al., *Neural differentiation of human induced pluripotent stem cells follows developmental principles but with variable potency.* Proceedings of the National Academy of Sciences of the United States of America, 2010. **107**(9): p. 4335-4340.
12. Chin, M.H., et al., *Induced pluripotent stem cells and embryonic stem cells are distinguished by gene expression signatures.* Cell Stem Cell, 2009. **5**(1): p. 111-23.
13. Dhara, S.K. and S.L. Stice, *Neural Differentiation of Human Embryonic Stem Cells.* Journal of Cellular Biochemistry, 2008. **105**(3): p. 633-640.
14. Shin, S.J., et al., *Long-term proliferation of human embryonic stem cell-derived neuroepithelial cells using defined adherent culture conditions.* Stem Cells, 2006. **24**(1): p. 125-138.
15. Young, A., et al., *Ion Channels and Ionotropic Receptors in Human Embryonic Stem Cell Derived Neural Progenitors.* Neuroscience, 2011. **192**: p. 793-805.
16. Harrill, J.A., et al., *Quantitative assessment of neurite outgrowth in human embryonic stem cell-derived hN2 (TM) cells using automated high-content image analysis.* Neurotoxicology, 2010. **31**(3): p. 277-290.

17. Sirenko, O., et al., *High-content high-throughput assays for characterizing the viability and morphology of human iPSC-derived neuronal cultures.* Assay Drug Dev Technol, 2014. **12**(9-10): p. 536-47.
18. Harrill, J.A., et al., *Quantitative assessment of neurite outgrowth in human embryonic stem cell-derived hN2 cells using automated high-content image analysis.* Neurotoxicology, 2010. **31**(3): p. 277-90.
19. Mundy, W.R., et al., *Expanding the test set: Chemicals with potential to disrupt mammalian brain development.* Neurotoxicol Teratol, 2015. **52**(Pt A): p. 25-35.
20. Gallegos-Cardenas, A., et al., *Pig Induced Pluripotent Stem Cell-Derived Neural Rosettes Developmentally Mimic Human Pluripotent Stem Cell Neural Differentiation.* Stem Cells Dev, 2015. **24**(16): p. 1901-11.
21. Brannvall, K., L. Korhonen, and D. Lindholm, *Estrogen-receptor-dependent regulation of neural stem cell proliferation and differentiation.* Molecular and Cellular Neuroscience, 2002. **21**(3): p. 512-520.
22. Minano, A., et al., *Estradiol facilitates neurite maintenance by a Src/Ras/ERK signalling pathway.* Mol Cell Neurosci, 2008. **39**(2): p. 143-51.
23. O'Connor, J.C., et al., *An ongoing validation of a Tier I screening battery for detecting endocrine-active compounds (EACs).* Toxicological Sciences, 1998. **46**(1): p. 45-60.
24. Radio, N.M., et al., *Comparison of PC12 and cerebellar granule cell cultures for evaluating neurite outgrowth using high content analysis.* Neurotoxicology and Teratology, 2010. **32**(1): p. 25-35.
25. Judson, R., et al., *The toxicity data landscape for environmental chemicals.* Environ Health Perspect, 2009. **117**(5): p. 685-95.
26. Shanks, N., R. Greek, and J. Greek, *Are animal models predictive for humans?* Philos Ethics Humanit Med, 2009. **4**: p. 2.
27. Harrill, J.A., et al., *Comparative sensitivity of human and rat neural cultures to chemical-induced inhibition of neurite outgrowth.* Toxicology and Applied Pharmacology, 2011. **256**(3): p. 268-280.
28. Clagett-Dame, M., E.M. McNeill, and P.D. Muley, *Role of all-Trans retinoic acid in neurite outgrowth and axonal elongation.* Journal of Neurobiology, 2006. **66**(7): p. 739-756.
29. Chandrasekaran, V., et al., *Retinoic acid regulates the morphological development of sympathetic neurons.* Journal of Neurobiology, 2000. **42**(4): p. 383-393.
30. Colleoni, S., et al., *Development of a Neural Teratogenicity Test Based on Human Embryonic Stem Cells: Response to Retinoic Acid Exposure.* Toxicological Sciences, 2011. **124**(2): p. 370-377.
31. Colleoni, S., et al., *Development of a neural teratogenicity test based on human embryonic stem cells: response to retinoic acid exposure.* Toxicol Sci, 2011. **124**(2): p. 370-7.
32. Huen, K., et al., *Organophosphate pesticide levels in blood and urine of women and newborns living in an agricultural community.* Environmental Research, 2012. **117**: p. 8-16.
33. Jiang, W., et al., *Mice treated with chlorpyrifos or chlorpyrifos oxon have organophosphorylated tubulin in the brain and disrupted microtubule structures, suggesting a role for tubulin in neurotoxicity associated with exposure to organophosphorus agents.* Toxicol Sci, 2010. **115**(1): p. 183-93.

34. Sachana, M., et al., *The toxicity of chlorpyrifos towards differentiating mouse N2a neuroblastoma cells.* Toxicol In Vitro, 2001. **15**(4-5): p. 369-72.
35. Howard, A.S., et al., *Chlorpyrifos exerts opposing effects on axonal and dendritic growth in primary neuronal cultures.* Toxicol Appl Pharmacol, 2005. **207**(2): p. 112-24.
36. Kakko, I., T. Toimela, and H. Tahti, *The toxicity of pyrethroid compounds in neural cell cultures studied with total ATP, mitochondrial enzyme activity and microscopic photographing.* Environ Toxicol Pharmacol, 2004. **15**(2-3): p. 95-102.
37. Ferguson, C.A. and G. Audesirk, *Effects of DDT and permethrin on neurite growth in cultured neurons of chick embryo brain and Lymnaea stagnalis.* Toxicol In Vitro, 1990. **4**(1): p. 23-30.
38. Dominguez, R., C. Jalali, and S. de Lacalle, *Morphological effects of estrogen on cholinergic neurons in vitro involves activation of extracellular signal-regulated kinases.* Journal of Neuroscience, 2004. **24**(4): p. 982-990.
39. Okada, M., et al., *Estrogen Stimulates Proliferation and Differentiation of Neural Stem/Progenitor Cells through Different Signal Transduction Pathways.* International Journal of Molecular Sciences, 2010. **11**(10): p. 4114-4123.
40. Aizuyokota, E., K. Ichinoseki, and Y. Sato, *Microtubule Disruption Induced by Estradiol in Estrogen Receptor-Positive and Receptor-Negative Human Breast-Cancer Cell-Lines.* Carcinogenesis, 1994. **15**(9): p. 1875-1879.
41. Zhang, L., et al., *Testosterone and estrogen affect neuronal differentiation but not proliferation in early embryonic cortex of the rat: the possible roles of androgen and estrogen receptors.* Neurosci Lett, 2000. **281**(1): p. 57-60.
42. Nam, K., et al., *Simulation of the different biological activities of diethylstilbestrol (DES) on estrogen receptor alpha and estrogen-related receptor gamma.* Biopolymers, 2003. **68**(1): p. 130-8.
43. Bosset, P.O., et al., *Current role of diethylstilbestrol in the management of advanced prostate cancer.* Bju International, 2012. **110**(11c): p. E826-E829.
44. Oelschlager, H., D. Rothley, and U. Dunzendorfer, *[Plasma concentrations of fosfestrol as well as diethylstilbestrol on their conjugates following intravenous administration on prostatic carcinoma patients]*. Arzneimittelforschung, 1986. **36**(8): p. 1284-9.
45. Seki, S., et al., *Bisphenol-A suppresses neurite extension due to inhibition of phosphorylation of mitogen-activated protein kinase in PC12 cells.* Chemico-Biological Interactions, 2011. **194**(1): p. 23-30.
46. Stump, D.G., et al., *Developmental neurotoxicity study of dietary bisphenol A in Sprague-Dawley rats.* Toxicol Sci, 2010. **115**(1): p. 167-82.
47. Beronius, A., et al., *The influence of study design and sex-differences on results from developmental neurotoxicity studies of bisphenol A: implications for toxicity testing.* Toxicology, 2013. **311**(1-2): p. 13-26.

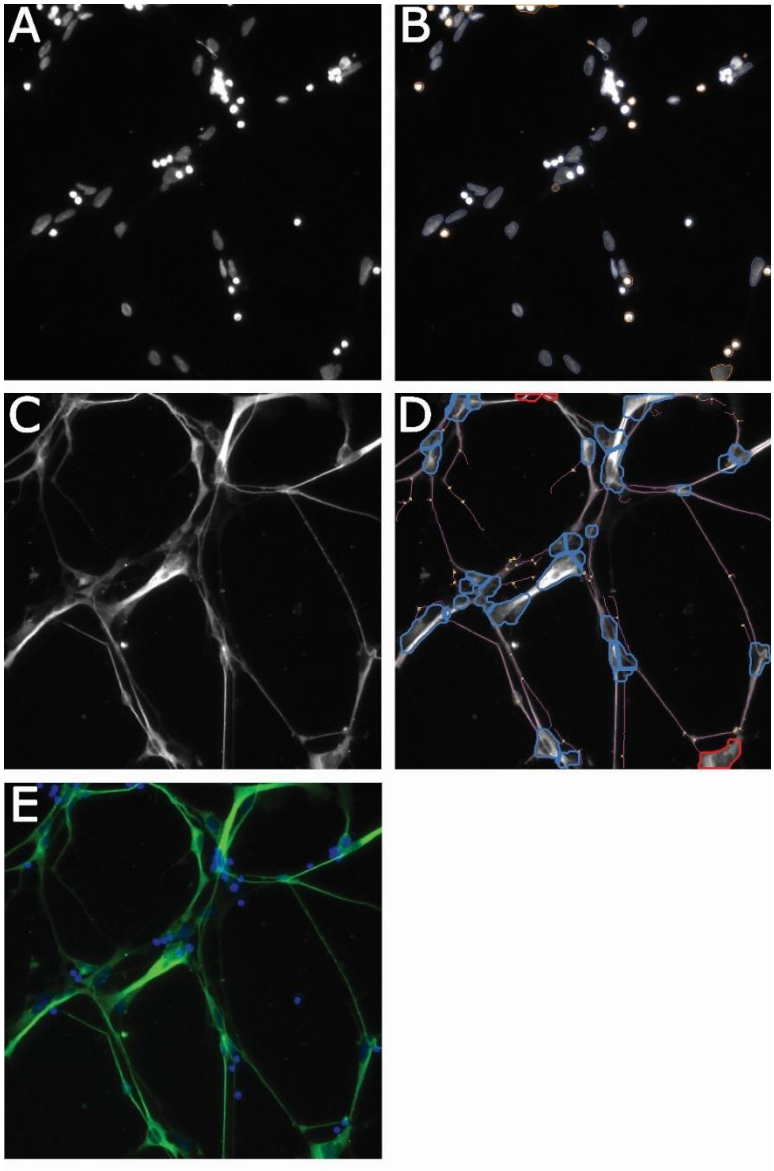

Fig. 3.1. Automated quantification of neurite outgrowth. Human embryonic stem cell derived DIV 28 neurons (10,000 cells/well in 96 well plate) were cultured for 48 hours and fixed for immunofluorescent staining. A) Hoechst nuclear staining. B (Channel 1): Nuclei identification. Blue trace = accepted, Yellow trace = rejected. C) MAP2 staining of neurite outgrowth. D (Channel 2): Cell body masks based on MAP2 expression; Blue trace = accepted cell, Red trace = rejected cell, Purple line = neurite, Yellow dot = branch point. Cells marked as rejected are not included calculating neurites per neuron or neurite length per neuron. Neurites emerging from accepted cell bodies are traced (purple lines) and quantified. E: Pseudo colored images from A and C merged.

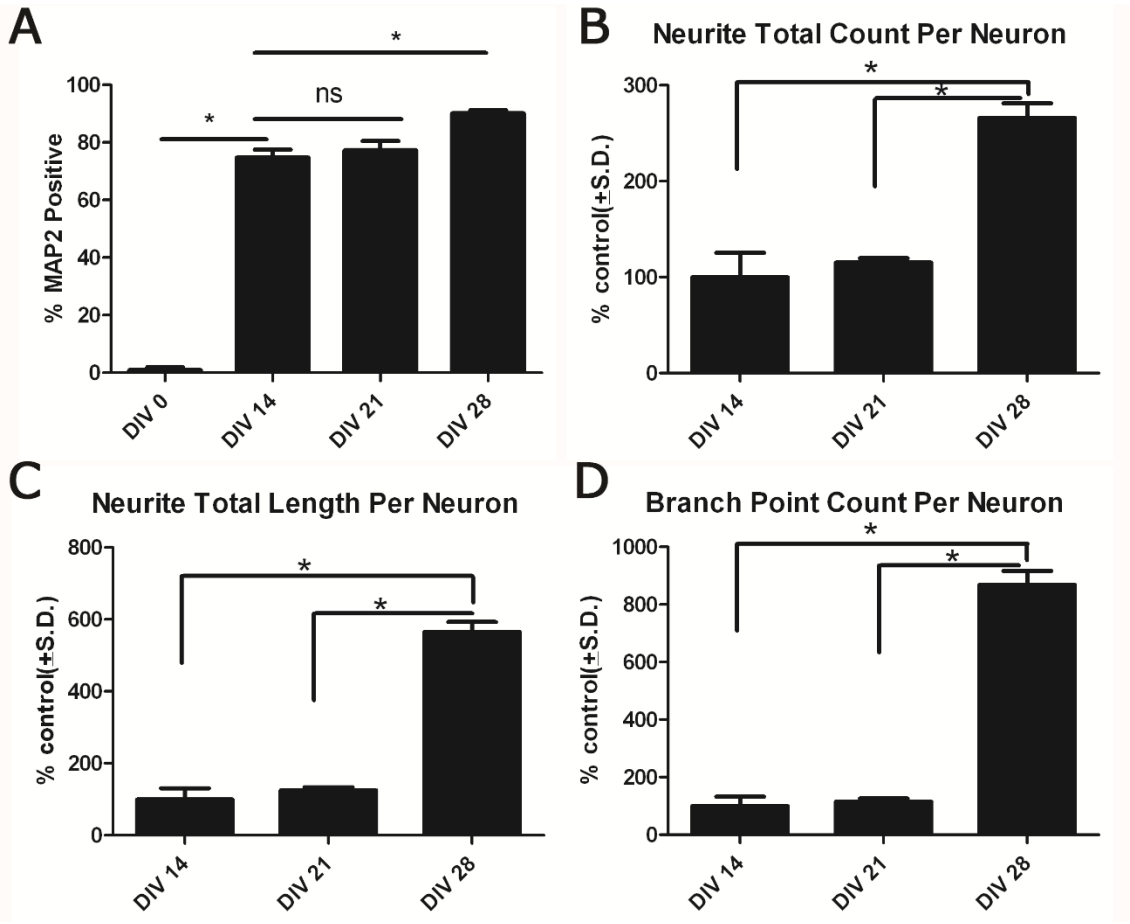

Fig. 3.2. Quantification of neuron purity and neurite outgrowth in neuron (MAP2+). Human embryonic stem cell derived neurons at different days were cultured (10,000 cells/well in 96 well plate) and fixed for MAP2 immunofluorescent staining after 48 hours. A) Total MAP2 positive neuron cells were counted as an indicator of cell viability. B, C, D) neurite outgrowth parameters: neurites per neuron, neurite length per neuron, branch points per neuron were also measured. All data are presented as % from untreated control wells. (*) indicates significant difference between groups ($P < 0.05$).

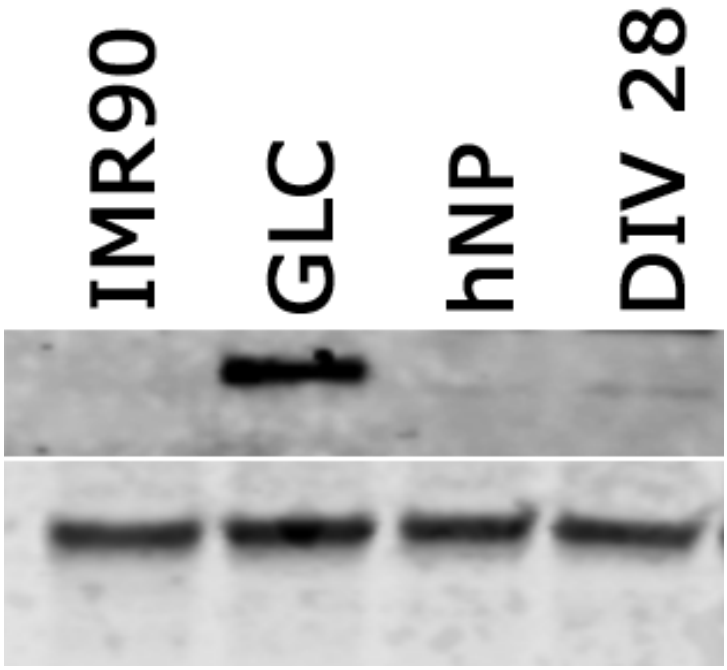

FIG. 3. 3. Estrogen receptor α protein expression. Human fibroblast (IMR90) cell, germ like cells, hNP cells, DIV 28 neurons were seeded in 60mm dish and collected at 90% confluent density for western blot experiment. Western blot analysis of IMR90, GLCs, hNP and DIV 14 neuron estrogen receptor α expression was examined. β-actin was used for normalizing the loading of samples.

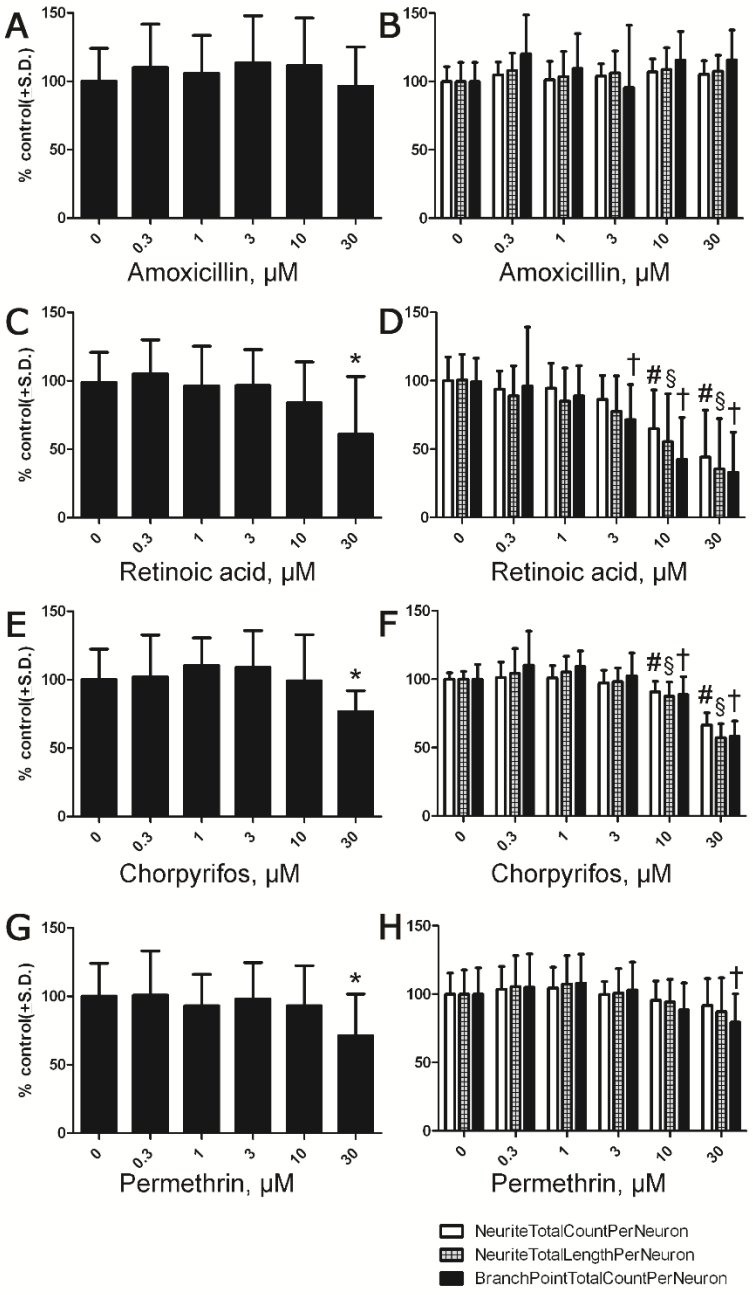

FIG. 3.4. Effects of chemical exposure on neural viability and neurite extension. A, C, E, G: Quantification of total MAP2 positive cells. B, D, F, H: Quantification of neurites per neuron, neurite length per neuron, branch points per neuron. All data are presented as % change from untreated control wells. Total MAP2 positive cells and neurite outgrowth data are from 3 separate experiments using independent cultures (n = 18 wells total). (*) indicates concentration is significant different from control group; #, §, † Concentration is significant different from control neurites per neuron, neurite length per neuron, branch points per neuron group separately ($P < 0.05$, one-way ANOVA).

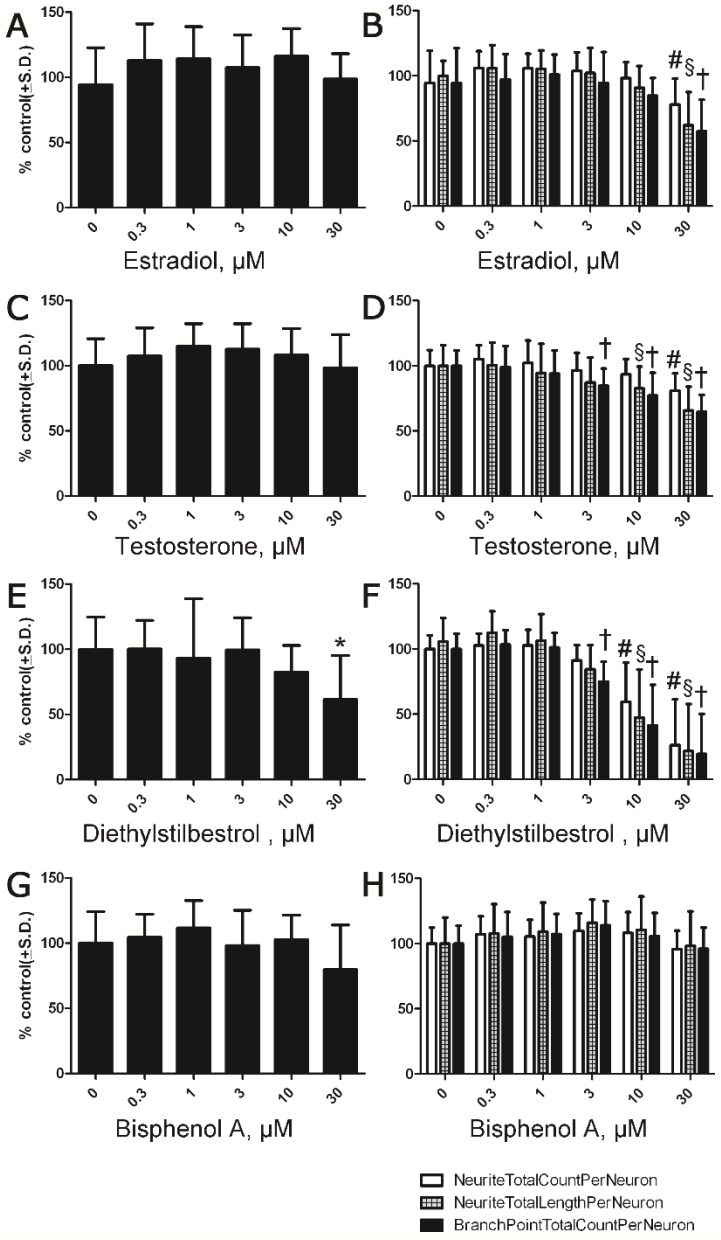

FIG. 3.5. Effects of endocrine disruptor chemicals on neural viability and neurite extension. A, C, E, G: Quantification of total MAP2 positive cells. B, D, F, H: Quantification of neurites per neuron, neurite length per neuron, branch points per neuron. All data are presented as % change from untreated control wells. Total MAP2 positive cells and neurite outgrowth data are from 3 separate experiments using independent cultures (n = 18 wells total). (*) indicates concentration is significant different from control group; #, §, † Concentration is significant different from control neurites per neuron, neurite length per neuron, branch points per neuron group separately ($P < 0.05$, one-way ANOVA).

CHAPTER 4

Human pluripotent stem cell derived astrocytes metabolize chlorpyrifos through Cytochrome P450 and protect neuron neurite outgrowth inhibition[1]

[1]Xian Wu, Xiangkun Yang, Anirban Majumder, Raymond Swetenburg, Forrest Goodfellow, Michael G. Bartlettc, Steven L. Stice 2016. Human pluripotent stem cell derived astrocytes metabolize chlorpyrifos through Cytochrome P450 and protect neuron neurite outgrowth inhibition. Submitted to *Toxicological Sciences*, 11/14/2016

Abstract

Human neural progenitor (hNP) cells are capable of directed independent differentiation into astrocytes, oligodendrocytes and neurons and offer a potential cell source for developmental neurotoxicity (DNT) assays. These hNP cells derived astrocyte and neuron can then be co-cultured at ratios to ideally mimic brain cell composition and interaction. In our recently research, hNP cells derived astrocytes have an integral role in the maintenance of early neuron differentiation and neurite outgrowth, and are also associated with neuroprotection when they are exposed to toxic substances. Chlorpyrifos (CPF) is organophosphate insecticide and affects the nervous system by inhibiting the breakdown of acetylcholine (ACh), a neurotransmitter. Cytochrome P450 enzymes (CYP) metabolizes CPF to CPF-oxon (CPF-oxon) and CPF-oxon is metabolized primarily to 3, 5, 6-trichloropyridinol (TCP) in addition to diethylphosphate and diethylthiophosphate. In the central nervous system (CNS), the levels of various CYP was expressed at relatively high level in astroglial cells and may play a critical role in the biotransformation of endogenous or exogenous compounds. Our objective was to establish days in vitro (DIV) 28 neurons alone and human astrocytes/DIV 28 neurons co-culture models to identify the interactive role of astrocytes and DIV 28 neurons in CPF induced neuron toxicity. In neuronal cell alone cultures CPF inhibited neurite length, neurites and branchpoints per neuron in a dose dependent manner during a 48h exposure starting at 10 μM. However, astrocytes proved neuronal cell protective to CPF at these same concentrations, up to 30μM CPF. When CYP inhibitor propyladiphenin (SKF525A) was added to these co-cultures it negated the protective effect of astrocyte, reducing branchpoints number in the CPF (10μM) plus SKF525A 5μM and 10μM treatment. We for the first time established a scalable and defined cell number hNP cells

to astrocytes (10,000 cells/well)/DIV 28 neurons (10,000 cells/well) co-culture model and potentially identify the role of CYP in astrocyte neuroprotection.

Introduction

The human brain consists of more than 10^{11} neurons associated with over 10^{12} glia cells. Specifically, the human cortex contains 1.4 astrocytes for every neuron [1]. Glia cells contribute to homeostasis in the brain by providing neurons with energy and substrates for neurotransmission [2]. Within the glia cell population, astrocytes are now considered far more active than previously thought and are powerful controllers of synapse formation, function, plasticity and elimination both in health and disease [3]. Astrocytes exert their protective effects on neurons through releasing neurotrophic factors such as nerve growth factor, brain-derived neurotrophic factor and glial cell line-derived neurotrophic factor in immune response against infection, injury, cellular debris, or abnormal protein aggregates [4, 5]. In neural development, astrocytes promote neurite outgrowth by providing various diffusible and nondiffusible proteins [6]. The astrocytes secrete nerve growth factor and display neurite growth-promoting activity for the clonal rat pheochromocytoma (PC-12) cell line through promoting microtubule assembly [7, 8]. Astrocyte derived growth factor S100β is known to promote survival and neurite outgrowth of serotonergic neurons in rat model through interaction with tau protein to stabilize microtubules leading to the formation of axonal processes [9, 10]. Molecules secreted by astrocytes can either inhibit or enhance overall levels of neuronal activity implying astrocytes broad roles in regulating neurite outgrowth and synapse formation [2].

The neuronal support role of astrocytes in CNS extends beyond the molecules they produce and include unique contributions to the exclusion and metabolism of toxins as part of blood-brain barrier (BBB) [11]. The BBB is important in protecting the brain from fluctuations in plasma composition and from circulating agents such as neurotransmitters and xenobiotics capable of disturbing neuronal function [12]. While the brain endothelium is clearly the major

barrier interface, the transport activity of both pericytes and perivascular astrocytic endfeet contributes to barrier function under physiological conditions [13]. Astrocytic detoxification processes includes the tripeptide glutathione (GSH) which serves as electron donor in the GSH peroxidase-catalyzed reduction of peroxides. And GSH is substrate in the detoxification of xenobiotics and endogenous compounds by GSH-S-transferases which generate GSH conjugates that are efficiently exported from the cells by multidrug resistance proteins [14]. Also, astrocyte CYP has an important role in the detoxification of xenobiotics for subsequent body elimination [15]. The CYP isoforms CYP1A1, CYP1A1/2, CYP2B1, CYP2B6, CYP2C11, CYP2C, CYP2D6, CYP2E1, and CYP3A were identified in rat and human astrocytes and considered functionally active [16]. Given their role in the BBB, astrocytes may perform a vital role as protectors to safeguard highly vulnerable neurons from toxicity by xenobiotics [15]. Therefore, astrocytes function both as a second line of defense if the primary barrier is breached or dysfunctional, as well as a link between the BBB and neurons. Thus, to assess the effect of a neurotoxic agent, it is vital to understand the innate ability of neurotoxins to cross the BBB, as well as how astrocytes metabolize them.

CPF is one of the most widely used insecticides in both developing and industrialized countries, including the United States [17]. Acute CPF exposure can lead to neurotoxic effects through inhibition breakdown of neurotransmitter ACh by acetylcholinesterase [18]. The impact of CPF is also evident over a wide neural developmental period, including neural cell proliferation and differentiation, axonogenesis and synaptogenesis [19, 20]. In addition, there is evidence that CPF can also form adducts with other proteins, impairing the functions of more molecular pathways in human [21]. CPF may cross the BBB and disrupts BBB integrity and function by altering gene expression for tight junction proteins claudin5, scaffold proteins zona

occludens (ZO1) and transient receptor potential (canonical) channels (TRPC4) [22]. The alteration on BBB function is reversible upon removal of CPF [22, 23]. CPF is metabolized by CYP in the liver to either CPF-oxon, by replacing the sulfur group with oxygen or other metabolite TCP which is much less toxic on axonal and growth [24]. In the brain, various CYP enzymes were reported to be expressed at relatively high levels in astroglial cells and may play a critical role in the biotransformation of endogenous or exogenous compounds [15]. However, the astrocyte-derived neuroprotective qualities in regard to CPF exposure are understudied and poorly understood.

The hNP cells differentiated from human embryonic stem cell (hESC) can replace costly animal models and offer a potentially unlimited and uniform cell source for DNT assays [25]. The hESC provides cell sources for cellular decision to proliferate or differentiation as well as migration [26]. Stem cell in vitro model fills the gap of chemical exposure with organism disorder or malfunction in adverse outcome pathway (AOP) mapping. The AOP is a conceptual framework that portrays existing knowledge concerning the linkage between a direct molecular initiating event and an adverse outcome at a level of biological organization relevant to risk assessment [27]. For example, in a retinoic acid–neural tube/axial patterning adverse outcome pathway (RA–NTA AOP) framework, RA induced neural differentiation using hESC. It was accompanied by gene down regulation of CYP26a1 and up regulation of Aldh1a2 [28]. All of these patterning related genes are regulated by RA exposure in cell culturing models and potentially used as biomarkers of neural tube developmental effects. The hNP cell has been developed as a sensitive and reproducible cell model for apoptosis assay in high-throughput screening [29]. The hNP cell derived hN2 (DIV 14 differentiated neuron) culture was characterized via automated high-content image analysis to measure neurite outgrowth in vitro

[30]. These cells are non-transformed and provide an alternative to the use of tumor-derived or transfected clonal cell lines. However, the role of astrocytes remains unexplored in these models. In co-culture models, astrocytes have been shown protective role for neurons against xenobiotics neurotoxicity [31]. Recent studies have suggested that the use of astrocytes in an in vitro neurotoxicity test system may prove more relevant to human CNS structure and function than neuronal cells alone [32]. The hNP derived astrocytes and DIV 28 neurons share similar culture conditions, providing an ideal platform to mimic heterotypic cellular interaction in the CNS as in vitro co-culture model. Our objective was to establish an astrocytes/DIV 28 neurons co-culture model in order to identify the mechanism of neuronal toxicity of CPF. The hESC derived astrocytes have an integral role in the maintenance of early neuronal differentiation and neurite outgrowth, and were also associated with neuroprotection when they are exposed to toxic substances [33]. In this study, we showed that CPF inhibited neurite outgrowth in a dose dependent manner during 48 hours exposure. However, the neurotoxic effect of CPF was reduced if astrocytes were co cultured with the DIV 28 neurons. Further, the CYP inhibitor reversed this protective effect. For the first time, we have established an hNP derived astrocytes/DIV 28 neurons co-culture model and identified a role for the CYP enzyme in astrocytic neuroprotection upon exposure to the known neurotoxicant CPF.

Materials and methods

Cell culture. Cryopreserved NeuroNet™ human neurons (DIV 28 neurons) (ArunA Biomedical Inc., Athens, GA) and hAstroPro™ human astrocyte cells (ArunA Biomedical Inc., Athens, GA) were thawed and live cells were counted by a trypan blue cell viability test. In the neuron only group, DIV 28 neurons (10,000 live cells/well) were cultured on growth factor

reduced matrigel basement membrane matrix (R&D, Minneapolis, MN) (diluted in AB2™ basal medium 1:100) coated costar® 96-well cell culture plate(Corning incorporated, Corning, NY) in differentiation medium comprised of AB2™ basal medium supplemented with ANS™ neural supplement (both from ArunA Biomedical Inc., Athens, GA), 2 mM L-glutamine (Gibco), 2 U/ml penicillin (Gibco), 2 µg/ml penicillin and streptomycin (Gibco) and 10 ng/mL leukemia inhibitory factor (LIF) (Millipore, Billerica, MA, USA). In the co-culture group, DIV 28 neurons (10,000 live cells/well) and hAstroPro™ human astrocytes (10,000 live cells/well) were cultured together on matrigel 1:100 coated costar® 96-well cell culture plates in the same differentiation medium as with the DIV 28 neurons only group.

Chemical treatment. Chlorpyrifos (99.5% pure), CPF-oxon (98.5% pure), and 3, 5, 6-trichloro-2-pyridinol (TCP; 99% pure) were all purchased from Chem Service (West Chester, PA). CYP inhibitor SKF525A were from Abcam, Cambridge, MA. Diisopropyl ether, LC-MS grade acetonitrile, methanol, water and formic acid were purchased from Sigma–Aldrich (St. Louis, MO). Test compounds were prepared as stock solution: 0.15, 0.5, 1.5, 5, 15 mM. Stock solution in dimethyl sulfoxide (DMSO) were then diluted in differentiation medium 50X and then final 10X dilution in culturing differentiation medium to make final concentration to 0.3, 1, 3, 10, 30µM. Compounds were added to cell cultures 2 h after cells were seeded in 96 well culture plates. Cells were fixed at the end of 48 hours incubation for immunofluorescent staining.

Immunocytochemistry. Immunofluorescent staining was performed using Eppendorf epMotion system (Eppendorf, Hauppauge, NY) for automated fixing and staining. Cells were stained as described with minor changes [34].Briefly, Cells were first fixed with 4% paraformaldehyde (Electron Microscopy Sciences, Hatfield, PA). 100 µl of a warm (37 °C) solution of 8% paraformaldehyde were added to culture wells containing 100 µl of medium and

incubated at room temperature for 20 min [35]. Fixative was then gently aspirated and cells were washed three times with phosphate-buffered saline (PBS) (GE Healthcare Bio-Sciences, Pittsburgh, PA). Primary antibody MAP2 (microtubule-associated protein 2) (EMD Millipore, Billerica, MA) was diluted at 1:200 and βIII-tubulin (ABCAM, Cambridge, MA) was diluted at 1:1000 in intracellular blocking solution (saponin: 0.96g, PBS: 480ml, bovine serum albumin: 9.6g) and was then applied for 2 hours at room temperature. Following incubation in primary antibodies, cells were washed three times with high salt buffer (sodium chloride:14.6g, 1M Tris base 50ml, distilled water 1L) and incubated with a 1:400 dilution DyLight® 594-conjugated donkey anti-mouse IgG secondary antibody or DyLight® 488-conjugated donkey anti-rabbit IgG secondary antibody in high salt buffer for 1 hour at room temperature, protected from light. Cells were then incubated in 0.1% Hoechst 33342 (Sigma–Aldrich, St. Louis, MO) dye in high salt buffer for 20 min, then in PBS washed 3 times with high salt buffer, and stored in PBS at 4°C prior to image acquisition and analysis [30].

Data acquisition and analysis of metabolites

Sample preparation. Each 100 µL of media was extracted with 1.7 mL isopropyl ether. The sample was vortexed for 10min, centrifuged at 7500 g, 5°C for 10 min. 1.5 mL supernatant was transferred and evaporated at 55 °C for 10 min. The residue was dissolved with 100 µL ACN, sonicated for 5min, vortexed for 5min, centrifuged at 7500 g for 10min, 80 µL supernatant was transferred before analysis.

Instrumentation

An Agilent 1100 binary pump HPLC system (Santa Clara, CA) coupled with a Waters Micromass Quattro Micro triple quadrupole mass spectrometer with an ESI source (Milford, MA) was operated for LC–MS/MS analysis. Masslynx 4.0 software by Waters (Beverly, MA)

was used for data processing. A Labconco CentriVap Complete Vacuum Concentrator (Kansas City, MO) was utilized to evaporate samples.

LC-MS/MS conditions

A Zorbax Eclipse XDB-C8 (2.1×150 mm, 5 μm) column coupled with a Phenomenex SecurityGuard C-8 guard column (4.0 mm×2.0 mm) was used to separate the analytes. The column temperature was controlled at 32 °C. The mobile phase A was 0.025% formic acid in water, mobile phase B was acetonitrile (ACN). The injection volume was 15 μL. Analytes were separated using a gradient method, with a 0.3 mL/min flow rate, (time/minute, % mobile phase B): (0, 60), (2, 80), (2.01, 80), (5, 80), (6, 60), (10, 60). The LC system was interfaced by a six-port divert valve to the mass spectrometer, introducing eluents to the ion source. The autosampler injection needle was washed with methanol after each injection. Samples were analyzed by the mass spectrometer in positive ion ESI mode for CPF and CPF-oxon, and in negative ion mode for TCP. Nitrogen was used as the desolvation gas at a flow rate of 500 L/h. The desolvation temperature was 500 °C and the source temperature was 120 °C. Argon was used as the collision gas, the collision cell pressure was 3.5×10-3 mbar. The capillary voltage was 4 kV, the cone voltage was -22 V for TCP, while 3.5 kV and 28 V for CPF and CPF-oxon. The collision energy for CPF was 22 eV and 15 eV for CPF-oxon. A multiple reaction monitoring (MRM) function was applied for quantification of CPF and CPF-oxon, the ion transitions monitored were 352→200 for CPF and 336→280 for CPF-oxon. A selected ion recording (SIR) of 198 was applied for the quantitation of TCP.

Image acquisition and analysis. A Cellomics ArrayScan VTI HCS reader high-content imaging system (ThermoFisher Scientific, Waltham, MA) was used for automated image acquisition and morphometric analyses as previously described for use on hN2 cells [36]. Cell

body validation was quantified based on MAP2 positive expression in DIV 28 neurons. At 20x magnification, the Cellomics ArrayScan VTI can sample 81 individual fields within each well. In this study, 35 fields were sampled within each well for cell characterization. Image analysis algorithm optimization, including nucleus validation, cell body masking and validation, and neurite tracing parameters, was performed a priori using five representative images from cultures with untreated DIV 28 neurons and co-cultured well. Output from high content image software included total cell count (cell density) (% MAP2 cells per well) and measurements of neurite outgrowth (neurites per neuron, neurite length per neuron, and branchpoints per neuron). Briefly, nuclei were first identified in channel 1 as bright objects on a dark background (Fig. 4.1E, 4.2A). Nuclei with size and intensity values outside of the ranges determined a priori for viable cells were identified in the channel 1 image and rejected from further analyses. Spatial coordinates from the channel 1 image were then superimposed on the matching channel 2 image. MAP2+ protein expression in channel 2 were then cast based on positional data from channel 1 nuclei and a set of user-defined geometric and signal intensity-based parameters (Fig. 4.1H, 4.2B. orange and red traces). Astrocytes were rejected through increased intensity threshold based on fluorescent intensity. MAP2+ DIV 28 neurons based on intensity value were then selected (Fig. 1H, 2B. blue traces) and invalid objects rejected (Fig. 4.2C, 4.2D. red traces). Data were collected on a cell-by-cell basis, and values were averaged to obtain population means within each well. These well level data were treated as the statistical unit for analysis of neurite outgrowth.

Results

MAP2 expression shows hNP differentiate to pure neuronal population. To characterize hNP derived DIV28 neurons, neuronal microtubule protein βIII-tubulin and MAP2 was specially stained to label DIV 28 neurons after 48 hours culture. Co-immunostaining of βIII-tubulin and MAP2 demonstrated that neurite outgrowth in cryopreserved neuronal cells plated for 48 hours progressed rapidly (Fig 4.1A, B, C). Both neural cytoskeleton marker βIII-tubulin and MAP2 were present in DIV28 neurons cell bodies and all neurites of viable cells (Fig 4.1D). Quantification of MAP2+cells compared to viable hoechst staining nuclear ratio in DIV 28 neurons was 96.5% while hNP cells were negative for MAP2 expression (Fig 4.1F).

Chlorpyrifos reduces cell density and inhibites neurite outgrowth. To investigate the effects of CPF, metabolites CPF-oxon and TCP on DIV 28 neurons, cells were incubated with a serial concentration of all three chemicals (CPF, CPF-oxon, TCP) at 0, 0.3, 1, 3, 10, 30μM. Following continuous exposure for 48 hours, cells were immunostained with MAP2 antibody and quantified in high content imaging system (Fig 4.2A, B, C). CPF reduced cell density only at the highest concentration by 23.33% (Fig. 4.2D) while CPF-oxon and TCP had no effect at any concentration treated on cell density (Fig. 4.2D). CPF inhibited neurites per neuron, neurite length per neuron, and branchpoints per neuron at 10 μM (9.14%, 12.38%, 19.25% reductions, respectively) without reducing cell density (Fig. 4.2 E, F, G). CPF-oxon, while not affecting cell density at any concentration, only inhibited neurite length per neuron at 10 μM by 14.06%. But CPF-oxon inhibited neurites per neuron, neurite length per neuron, and branchpoints per neuron at 30 μM by 15.23%, 25.11%, 22.78% (Fig. 4.2 E, F, G). Comparing to CPF and CPF-oxon specific inhibition effect on neurite outgrowth, all concentrations of TCP incubation didn't reduce cell density or inhibit neurite outgrowth parameters (Fig 4.2D, E, F, G).

Astrocytes reduce toxic effect of chlorpyrifos on neurite outgrowth. To study CPF neurotoxicity on DIV 28 neurons in presence of astrocytes, two groups of DIV 28 neurons-only and astrocytes/DIV 28 neurons co-culture were incubated in 96-well plate with CPF at concentrations of 0.3, 1, 3, 10, 30 µM. MAP2+ DIV 28 neurons were then quantified in presence of astrocytes by high content imaging system. Cell density and neurite outgrowth was compared between DIV 28 neurons-only and astrocytes/DIV 28 neurons co-culture groups (Fig 4.1G, H, I). Presence of astrocytes did not significantly change CPF induced toxicity on cell density at any concentration (Fig 4.3A). However, presence of astrocytes changed CPF neurite outgrowth inhibition effect on DIV 28 neurons. Neurites per neuron inhibited by CPF in DIV 28 neurons culturing group were reversely increased in presence of astrocytes by 10.36% at 10 µM and 24.73% at 30 µM (Fig 4.3B). Comparing to DIV 28 neurons group, neurite length per neuron were increased in co-cultured group by 13.46% at 10 µM and 31.34% at 30 µM (Fig 4.3C). Branchpoints per neuron inhibited by CPF in DIV 28 neurons were also increased in co-cultured group by 14.99% at 10 µM and 27.34% at 30 µM (Fig 4.3D).

To investigate role of astrocytes in reducing CPF neurotoxicity, medium from astrocytes, DIV 28 neurons-only and co-cultured groups incubated with CPF 10 µM after 48 hours were collected for metabolite TCP analysis. TCP was detected at retention time 2.35 min using TCP standard. In DIV 28 neurons-only group, TCP peak area was 4489 and increased in astrocytes and co-cultured groups, peak area was 91620 and 110880, respectively. The 10 fold increase of TCP indicated CPF was metabolized to TCP in the presence of astrocytes (Fig 4.3E).

Chlorpyrifos metabolism to TCP in astrocyte is reduced by CYP inhibitor. We then asked whether the increase in TCP peak area in both astrocytes and co-cultured groups was mediated by CYP. A serial concentration of CYP inhibitor SKF525A was added to the

astrocytes, DIV 28 neurons-only and co-cultured groups. Cell density was decreased by 29.31% in the astrocytes group at 30 µM. In the DIV 28 neurons-only group, cell density was decreased at 10 and 30 µM by 35.63% and 48.24%. In the co-cultured group, cell density was decreased with by 20 and 40 µM SKF525A but not at lower concentrations (Fig 4.4 A, B, C). 10 µM SKF525A was chosen for further study the role of CYP in CPF metabolism. SKF525A 10 µM was added along with CPF 10 µM in DIV 28 neurons-only, astrocytes and co-cultured groups. TCP peak area was 4249 in DIV 28 neurons-only, 4657 in astrocyte and 4074 in co-cultured groups in, and after 48 hours incubation with CPF (10 µM) (Fig. 4.4D). TCP concentration in the astrocyte group medium was 1011.14 ng/ml. TCP concentration dramatically decreased to 67.50ng/ml in presence of SKF525A 10 µM. In the co-cultured group, TCP concentration was 1347.31ng/ml in absence of SKF525A 10 µM. However, in presence of SKF525A 10 µM, TCP concentration decreased to 53.56ng/ml. In DIV 28 neurons cultures, TCP concentration were low and wasn't significantly different in both group with and without SKF525A 10 µM (Fig. 4.4E). To investigate SKF525A effects and potential inhibition on CPF metabolism to TCP, co-cultured astrocytes/DIV 28 neurons were incubated with a serial concentration of SKF525A in the presence of an effect dose of CPF (10 µM) and neurite outgrowth was quantified after 48 hours. Branchpoints per neuron were dose dependently decreased to 71.5% and 67.57% with SKF525A incubation at 5 and 10 µM separately comparing to co-cultured group without SKF525A treatment (Fig 4.4F). SKF525A effects and potential inhibition on CPF metabolism to TCP were investigated by using co-cultured astrocytes/DIV 28 neurons. The co-culture was incubated with serial concentrations of SKF525A in the presence of an effect dose of CPF (10 µM). Neurite outgrowth was quantified after 48 hours. Branchpoints per neuron were dose dependently

decreased to 71.5% and 67.57% with SKF525A incubation at 5 and 10 μM respectively, as compared to the co-cultured group without SKF525A treatment (Fig 4.4F)..

In summary, CPF negatively affected neurite outgrowth outcomes, including neuron count (cell density), neurites, length and also branchpoints per neuron (Fig 4.5A). However, in presence of astrocytes, CPF neurotoxicity was significantly reduced (all neurite outgrowth measurement) possibly through metabolism to TCP (Figure 4.5B). And when astrocyte CYP inhibitor SKF525A activity was inhibited, CPF accumulated in co-cultured cells and showed toxicity on DIV 28 neurons (Fig 4.5C).

Discussion

A murine astrocyte-neuron co-culture model has previously demonstrated the impact of secreted astrocytic factors on neurons including neuronal survival, synapse formation, and plasticity [37]. Human astrocytes play an integral role in the maintenance of early neuronal differentiation and neurite outgrowth, and are also associated with neuroprotection when they are exposed to toxic substances [5, 38] . This study presented a first human pluripotent stem cell-derived astrocytes/DIV 28 neurons co-culture model. In contrast to primary cultures, hNP cell derived astrocytes/DIV 28 neurons facilitated an unlimited lineage-restricted cell sources for generation of neuronal subtypes and supporting glial cells for high throughput DNT screening. [39]. One advantage to this model is a reduced uncertainty in toxicity testing caused by extrapolation of data derived from animal tissue to humans [30]. Unlike primary cultures that contain multiple cell types that may vary widely among cell preparation made from tissues [40];

our model can maintain a defined ratio of astrocytes to DIV 28 neurons designed to mimic different cellular composition and interaction in vivo plate to plate on every screening campaign. Defined ratio of human astrocytes/DIV 28 neurons co-culture DNT assays may be more physiologically relevant to human CNS cell composition and function than mixed cultures or predominantly neuronal cell cultures [41].Human induced pluripotent stem cell (iPSC) derived neurons co-cultured with rat astrocyte was developed for neuronal network function assay but also induced uncertainty in toxicity testing caused by animal tissue [40].

In this study, human astrocytes and DIV 28 neurons were co-cultured and DIV 28 neurons were MAP2+ while astrocytes were negative and excluded from quantification. This unique strategy quantified only DIV 28 neurons in co-culture and provided the opportunity for high throughput quantification of chemicals which could alter neurite outgrowth in a multicellular vitro model comparing to existing neuron only models [30]. This astrocytes/DIV 28 neurons co-cultured model could also extend in application for astrocyte neuron interaction study including astrocyte secreting factors effect on neuron function or bidirectional signaling between astrocytes and neurons on regulating neurite outgrowth [42].

CPF decreased neurites per neuron, neurite length per neuron and branchpoints per neuron at 10 and 30 µM. At 10 µM, CPF specifically inhibited neurite outgrowth without decreasing cell density. The results in DIV 28 neurons confirmed CPF neurotoxicity especially on neurite outgrowth in human neurons cells. CPF inhibited neurite outgrowth at approximate 50 µM in iPSC derived neurons which was higher than what we observed and at a level higher than what was observed in a report on humans exposed to CPF (mother and newborns)[43]. The difference could be due to several factors. The MAP2+ population was not characterized in the

iPSC study [29]. Whereas the DIV 28 neurons were highly enriched mature neurons, 96.5% MAP2+.

The CPF metabolite TCP did effect neurite outgrowth or cell density indicating that CPF toxicity when it is metabolized to TCP. These results were consistent with earlier findings that axon outgrowth was significantly inhibited by CPF but not TCP [44]. In human hepatocytes and liver microsomes, CPF is metabolized to CPF-oxon and TCP via a CYP-dependent mechanism [45]. Human liver cell plays an important role in detoxification of CPF through converting CPF-oxon to TCP by A-esterase metabolism [46]. TCP detection was developed as metabolite biomarker for humans exposed to ganophosphorus insecticides including CPF in plasma [47]. In this study, TCP metabolite concentration significantly increased in astrocytes alone and co-cultured astrocytes after 48 hour CPF exposure compared to the DIV 28 neurons-only group. This difference suggests vital role for astrocytic metabolizes CPF to TCP. Next, we investigated the role of CYP activity in astrocytes by adding CYP inhibitor SKF525A to CPF treated co-cultures. Based on the observed decrease branchpoints per neuron when SKF525A was present, we believe the inhibitor decreased astrocytic metabolism of CPF to TCP and thus reversed the astrocytes ability to protect neurons. All data in this study implies presence of CYP in hNP cells derived astrocytes and CYP was active in metabolizing neurotoxic CPF into nontoxic TCP and the metabolism can be interrupted by CYP inhibition. Current xenobiotics or drug metabolism by astrocytes CYP were studied using mouse primary isolated astrocytes [15]. However, it's important to know that humans and mice are different in CYP isoform composition, expression and catalytic activities [48]. CYP1A, -2C, -2D and -3A show appreciable interspecies differences in terms of catalytic activity and some caution should be applied when extrapolating metabolism data from animal models to humans [49]. Also, the active CYPs in hNP cell derived astrocytes

provided unlimited human cell source to study xenobiotics toxification and detoxification through P450 in astrocytes in vitro.

This study for the first time identified CYP as a key modulator in human astrocyte mediated neuroprotection for CPF. In human liver cells, several CYP subtypes including CYP1A2, 2C, 2D6, 3A4/5 were identified in CPF metabolism to CPF-oxon and TCP [45]. CYP2B1/2, CYP2B6 are only active in CPF metabolism toward direction to CPF-oxon and CYP1A2, CYP2C are only involved in CPF metabolism to TCP [45]. It will be important to identify CYP activity and subtypes in hNP cell derived astrocyte for CPF metabolism and predicting other organophosphorus pesticides metabolism. CYP have reduced activities in cultured condition in vitro comparing to CYP hepatocyte activity in liver. CYP transcription was decreased in vitro and it correlates with an alteration in the expression of key transcription factors [50]. Since astrocytes were derived from hNP cells in vitro, CYP activity could also be at low level and should be characterized before being used extensively in high throughput screening for neurotoxicants. In current DNT model to date, chemical neurotoxicity was mainly focused directly on their effect in neurons [30]. However, if compound toxicity mechanisms are cell type or organ specific, new more representative DNT analysis of compounds may be required for AOP studies and both astrocytes and hepatocytes may need to be included in larger DNT compound screening campaigns.

Conclusion

For the first time, we established a scalable, tunable and defined human PSC derived astrocytes/DIV 28 neurons CNS co-culture model and identified the role of CYP in astrocyte

neuroprotection. In the future, the role of astrocytes in metabolizing and altering potential neural toxicants that cross the blood brain barrier should be considered in AOP mapping.

References

1. Bass, N.H., et al., *Quantitative cytoarchitectonic distribution of neurons, glia, and DNA in rat cerebral cortex.* J Comp Neurol, 1971. **143**(4): p. 481-90.
2. Allen, N.J. and B.A. Barres, *NEUROSCIENCE Glia - more than just brain glue.* Nature, 2009. **457**(7230): p. 675-677.
3. Eroglu, C. and B.A. Barres, *Regulation of synaptic connectivity by glia.* Nature, 2010. **468**(7321): p. 223-231.
4. Hansebout, C.R., et al., *Enteric glia mediate neuronal outgrowth through release of neurotrophic factors.* Neural Regeneration Research, 2012. **7**(28): p. 2165-2175.
5. Belanger, M. and P.J. Magistretti, *The role of astroglia in neuroprotection.* Dialogues Clin Neurosci, 2009. **11**(3): p. 281-95.
6. Kanemaru, K., et al., *Regulation of neurite growth by spontaneous Ca2+ oscillations in astrocytes.* J Neurosci, 2007. **27**(33): p. 8957-66.
7. Tarris, R.H., M.E. Weichsel, Jr., and D.A. Fisher, *Synthesis and secretion of a nerve growth-stimulating factor by neonatal mouse astrocyte cells in vitro.* Pediatr Res, 1986. **20**(4): p. 367-72.
8. Drubin, D.G., et al., *Nerve growth factor-induced neurite outgrowth in PC12 cells involves the coordinate induction of microtubule assembly and assembly-promoting factors.* J Cell Biol, 1985. **101**(5 Pt 1): p. 1799-807.
9. Jaw, S.P., D.D. Su, and D.D. Truong, *Astrocyte-derived growth factor (S100 beta) and motor function in rats following cardiac arrest.* Pharmacol Biochem Behav, 1995. **52**(4): p. 667-70.
10. Yu, W.H. and P.E. Fraser, *S100 beta interaction with tau is promoted by zinc and inhibited by hyperphosphorylation in Alzheimer's disease.* Journal of Neuroscience, 2001. **21**(7): p. 2240-2246.
11. Meyer, R.P., et al., *Possible function of astrocyte cytochrome P450 in control of xenobiotic phenytoin in the brain: in vitro studies on murine astrocyte primary cultures.* Exp Neurol, 2001. **167**(2): p. 376-84.
12. Abbott, N.J., L. Ronnback, and E. Hansson, *Astrocyte-endothelial interactions at the blood-brain barrier.* Nature Reviews Neuroscience, 2006. **7**(1): p. 41-53.
13. Banerjee, S. and M.A. Bhat, *Neuron-glial interactions in blood-brain barrier formation.* Annu Rev Neurosci, 2007. **30**: p. 235-58.
14. Dringen, R., et al., *Glutathione-Dependent Detoxification Processes in Astrocytes.* Neurochem Res, 2015. **40**(12): p. 2570-82.
15. Meyer, R.P., et al., *Possible function of astrocyte cytochrome P450 in control of xenobiotic phenytoin in the brain: In vitro studies on murine astrocyte primary cultures.* Experimental Neurology, 2001. **167**(2): p. 376-384.
16. Pitanga, B.P., et al., *The Role of Astrocytes in Metabolism and Neurotoxicity of the Pyrrolizidine Alkaloid Monocrotaline, the Main Toxin of Crotalaria retusa.* Front Pharmacol, 2012. **3**: p. 144.
17. Yang, D.R., et al., *Chlorpyrifos-Oxon Disrupts Zebrafish Axonal Growth and Motor Behavior.* Toxicological Sciences, 2011. **121**(1): p. 146-159.
18. Costa, L.G., et al., *Paraoxonase (PON1) and organophosphate toxicity.* Paraoxnases: Their Role in Disease Development and Xenobiotic Metabolism, 2008. **6**: p. 209-220.
19. Qiao, D., F.J. Seidler, and T.A. Slotkin, *Developmental neurotoxicity of chlorpyrifos modeled in vitro: Comparative effects of metabolites and other cholinesterase inhibitors*

on DNA synthesis in PC12 and C6 cells. Environmental Health Perspectives, 2001. **109**(9): p. 909-913.
20. Qiao, D., et al., *Chlorpyrifos exposure during neurulation: cholinergic synaptic dysfunction and cellular alterations in brain regions at adolescence and adulthood.* Developmental Brain Research, 2004. **148**(1): p. 43-52.
21. Yang, X.K. and M.G. Bartlett, *Identification of protein adduction using mass spectrometry: Protein adducts as biomarkers and predictors of toxicity mechanisms.* Rapid Communications in Mass Spectrometry, 2016. **30**(5): p. 652-664.
22. Li, W. and M. Ehrich, *Transient alterations of the blood-brain barrier tight junction and receptor potential channel gene expression by chlorpyrifos.* Journal of Applied Toxicology, 2013. **33**(10): p. 1187-1191.
23. Parran, D.K., et al., *Chlorpyrifos alters functional integrity and structure of an in vitro BBB model: Co-cultures of bovine endothelial cells and neonatal rat astrocytes.* Neurotoxicology, 2005. **26**(1): p. 77-88.
24. Howard, A.S., et al., *Chlorpyrifos exerts opposing effects on axonal and dendritic growth in primary neuronal cultures.* Toxicology and Applied Pharmacology, 2005. **207**(2): p. 112-124.
25. Radio, N.M. and W.R. Mundy, *Developmental neurotoxicity testing in vitro: models for assessing chemical effects on neurite outgrowth.* Neurotoxicology, 2008. **29**(3): p. 361-76.
26. Theveneau, E. and R. Mayor, *Neural crest migration: interplay between chemorepellents, chemoattractants, contact inhibition, epithelial-mesenchymal transition, and collective cell migration.* Wiley Interdisciplinary Reviews-Developmental Biology, 2012. **1**(3): p. 435-445.
27. Ankley, G.T., et al., *Adverse outcome pathways: a conceptual framework to support ecotoxicology research and risk assessment.* Environ Toxicol Chem, 2010. **29**(3): p. 730-41.
28. Tonk, E.C., J.L. Pennings, and A.H. Piersma, *An adverse outcome pathway framework for neural tube and axial defects mediated by modulation of retinoic acid homeostasis.* Reprod Toxicol, 2015. **55**: p. 104-13.
29. Druwe, I., et al., *Sensitivity of neuroprogenitor cells to chemical-induced apoptosis using a multiplexed assay suitable for high-throughput screening.* Toxicology, 2015. **333**: p. 14-24.
30. Harrill, J.A., et al., *Quantitative assessment of neurite outgrowth in human embryonic stem cell-derived hN2 (TM) cells using automated high-content image analysis.* Neurotoxicology, 2010. **31**(3): p. 277-290.
31. Anderl, J.L., S. Redpath, and A.J. Ball, *A neuronal and astrocyte co-culture assay for high content analysis of neurotoxicity.* J Vis Exp, 2009(27).
32. Wu, Y., et al., *Primary neuronal-astrocytic co-culture platform for neurotoxicity assessment of di-(2-ethylhexyl) phthalate.* Journal of Environmental Sciences, 2014. **26**(5): p. 1145-1153.
33. Gupta, K., et al., *Human embryonic stem cell derived astrocytes mediate non-cell-autonomous neuroprotection through endogenous and drug-induced mechanisms.* Cell Death Differ, 2012. **19**(5): p. 779-87.

34. Gallegos-Cardenas, A., et al., *Pig Induced Pluripotent Stem Cell-Derived Neural Rosettes Developmentally Mimic Human Pluripotent Stem Cell Neural Differentiation.* Stem Cells and Development, 2015. **24**(16): p. 1901-1911.
35. Doherty, P., G. Williams, and E.J. Williams, *CAMs and axonal growth: A critical evaluation of the role of calcium and the MAPK cascade.* Molecular and Cellular Neuroscience, 2000. **16**(4): p. 283-295.
36. Harrill, J.A., et al., *Quantitative assessment of neurite outgrowth in human embryonic stem cell-derived hN2 cells using automated high-content image analysis.* Neurotoxicology, 2010. **31**(3): p. 277-90.
37. Jones, E.V., D. Cook, and K.K. Murai, *A neuron-astrocyte co-culture system to investigate astrocyte-secreted factors in mouse neuronal development.* Methods Mol Biol, 2012. **814**: p. 341-52.
38. Zhu, Y.B., et al., *Astrocyte-derived phosphatidic acid promotes dendritic branching.* Scientific Reports, 2016. **6**.
39. Fukushima, K., et al., *Establishment of a Human Neuronal Network Assessment System by Using a Human Neuron/Astrocyte Co-Culture Derived from Fetal Neural Stem/Progenitor Cells.* J Biomol Screen, 2016. **21**(1): p. 54-64.
40. Kidambi, S., I. Lee, and C. Chan, *Primary Neuron/Astrocyte Co-Culture on Polyelectrolyte Multilayer Films: A Template for Studying Astrocyte-Mediated Oxidative Stress in Neurons.* Adv Funct Mater, 2008. **18**(2): p. 294-301.
41. Odawara, A., et al., *Long-term electrophysiological activity and pharmacological response of a human induced pluripotent stem cell-derived neuron and astrocyte co-culture.* Biochem Biophys Res Commun, 2014. **443**(4): p. 1176-81.
42. Allen, N.J. and B.A. Barres, *Signaling between glia and neurons: focus on synaptic plasticity.* Current Opinion in Neurobiology, 2005. **15**(5): p. 542-548.
43. !!! INVALID CITATION !!! [30].
44. Yang, D., et al., *Chlorpyrifos-oxon disrupts zebrafish axonal growth and motor behavior.* Toxicol Sci, 2011. **121**(1): p. 146-59.
45. Lee, S., et al., *Effects of nicotine exposure on in vitro metabolism of chlorpyrifos in male Sprague-Dawley rats.* J Toxicol Environ Health A, 2009. **72**(2): p. 74-82.
46. Poet, T.S., et al., *In vitro rat hepatic and intestinal metabolism of the organophosphate pesticides chlorpyrifos and diazinon.* Toxicol Sci, 2003. **72**(2): p. 193-200.
47. Wang, L.M., et al., *A novel immunochromatographic electrochemical biosensor for highly sensitive and selective detection of trichloropyridinol, a biomarker of exposure to chlorpyrifos.* Biosensors & Bioelectronics, 2011. **26**(6): p. 2835-2840.
48. Nelson, D.R., et al., *Comparison of cytochrome P450 (CYP) genes from the mouse and human genomes, including nomenclature recommendations for genes, pseudogenes and alternative-splice variants.* Pharmacogenetics, 2004. **14**(1): p. 1-18.
49. Martignoni, M., G.M.M. Groothuis, and R. de Kanter, *Species differences between mouse, rat, dog, monkey and human CYP-mediated drug metabolism, inhibition and induction.* Expert Opinion on Drug Metabolism & Toxicology, 2006. **2**(6): p. 875-894.
50. Rodriguez-Antona, C., et al., *Cytochrome P450 expression in human hepatocytes and hepatoma cell lines: molecular mechanisms that determine lower expression in cultured cells.* Xenobiotica, 2002. **32**(6): p. 505-520.

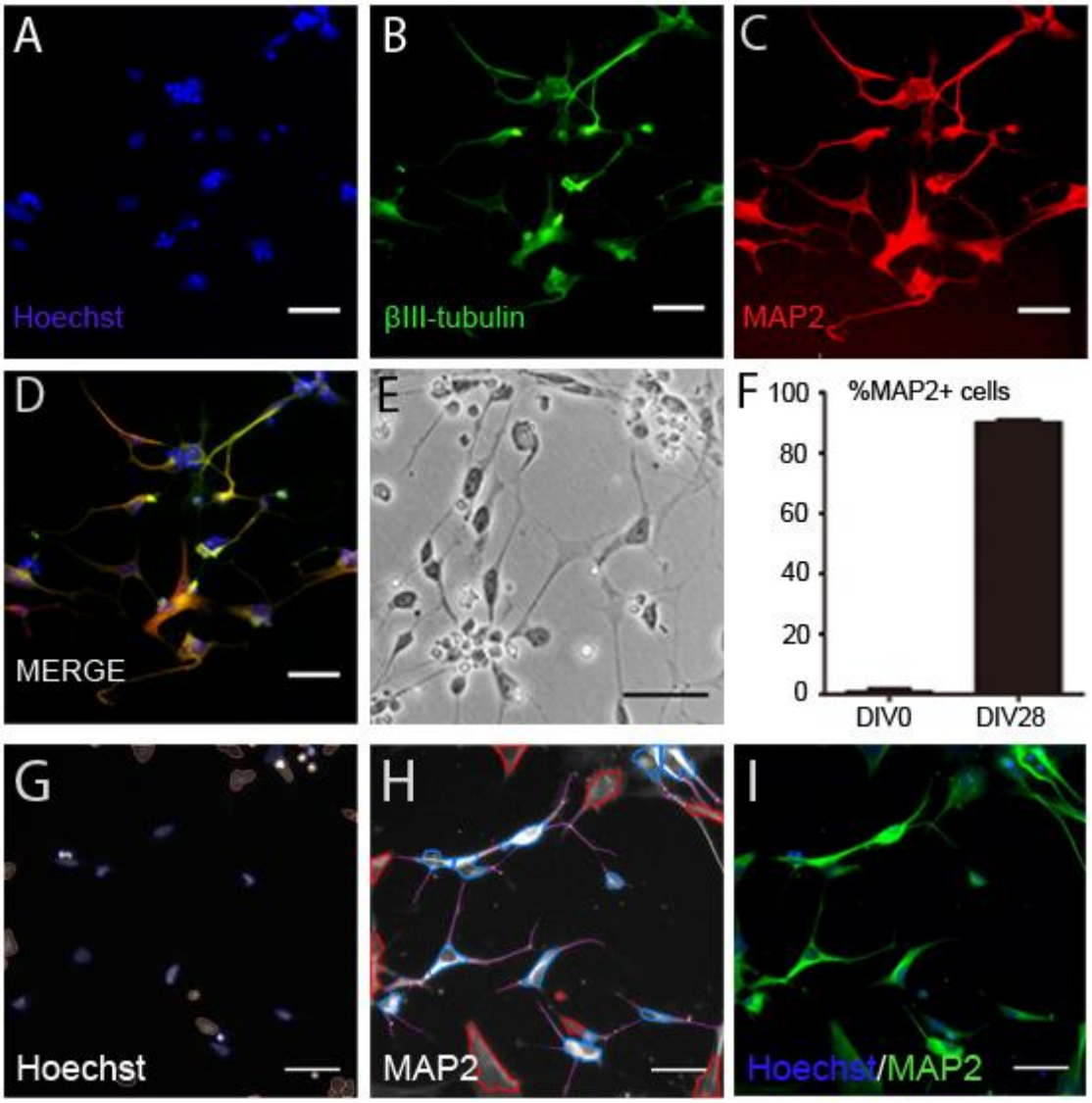

Fig. 4.1 Quantification of neuron purity and neurite outgrowth in DIV 28 neuron and astrocyte co-culture (MAP2+). Human DIV 28 neuron (10,000 cells/well) was separately and co-cultured with astrocyte (10,000 astrocyte & 10,000 neuron) for 48 hours and fixed for immunofluorescent staining. A) Hoechst nuclear staining. B) β-III tubulin staining of neurite outgrowth. C) MAP2 staining of neurite outgrowth. D) Hoechst, β-III tubulin, MAP2 staining merge image. E) Neuron cell phase contrast image. F) Statistical analysis of MAP2 positive cell ratio in DIV0 hNP cells and DIV 28 neuron. G (Channel 1): Nuclei identification. Blue trace = accepted, Yellow trace = rejected. H (Channel 2): Cell body masks based on MAP2 expression; Blue trace = accepted cell, Red trace = rejected cell, Purple line = neurite, Yellow dot = branch point. Cells marked as rejected are not included calculating neurites per neuron or neurite length per neuron. Neurites emerging from accepted cell bodies are traced (purple lines) and quantified. I: Pseudo colored images from G and H merged. Scale bars = 50 µm.

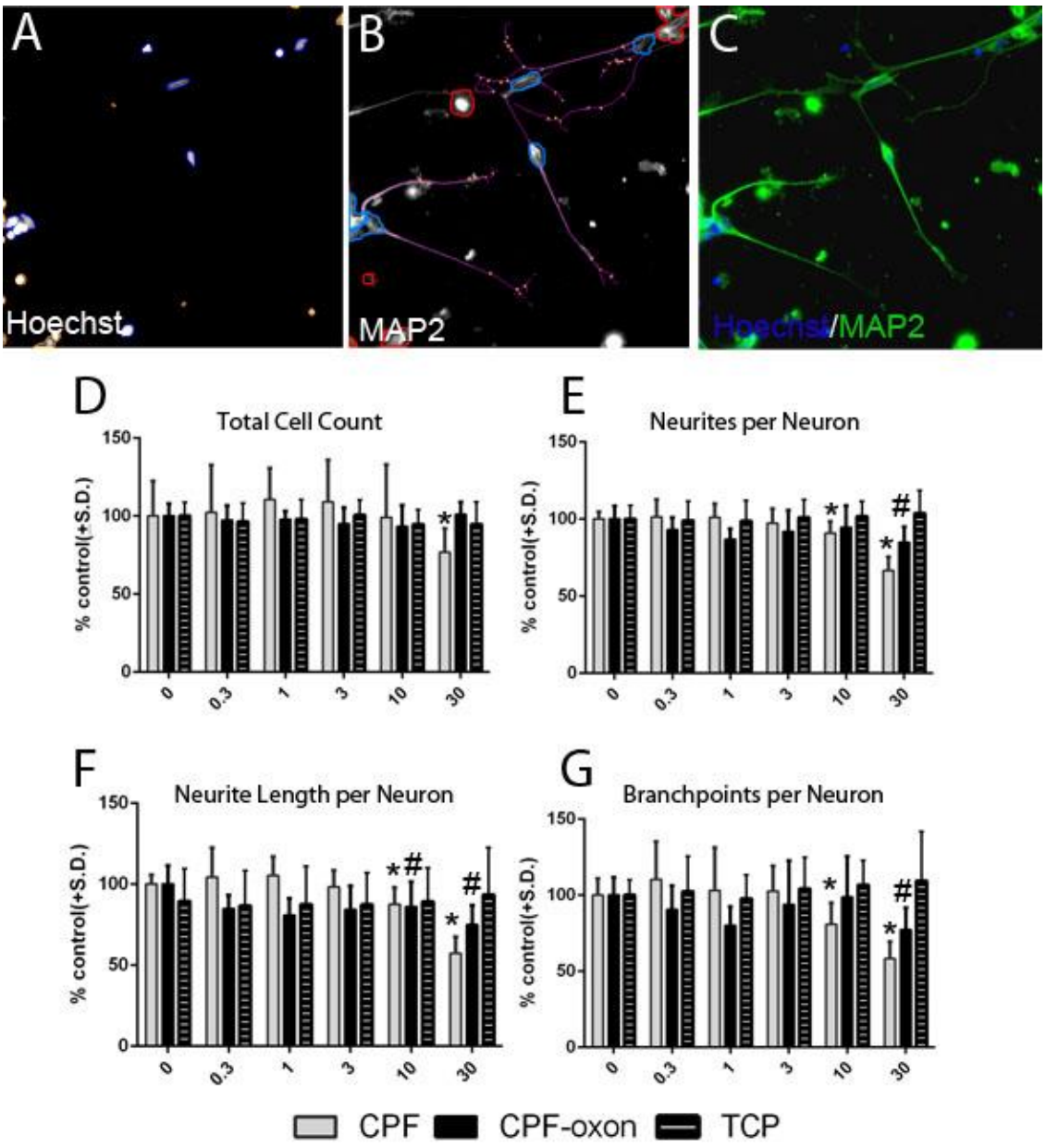

Fig. 4.2 Comparison of CPF, CPF-oxon and TCP toxic effect on neuron density and neurite outgrowth. Human DIV 28 neuron cells (10,000 cells/well) were continuously exposed to a range of doses of CPF, CPF-oxon and TCP for 48 hours. A (Channel 1): Nuclei identification. Blue trace = accepted, Yellow trace = rejected. B (Channel 2): Cell body masks based on MAP2 expression; Blue trace = accepted cell, Red trace = rejected cell, Purple line = neurite, Yellow dot = branch point. Cells marked as rejected are not included calculating neurites per neuron or neurite length per neuron. Neurites emerging from accepted cell bodies are traced (purple lines) and quantified. C: Pseudo colored images from A and B merged. D) Total neuron density (cell density) were measured as an indicator of cell viability. E, F, G) Average number of neurites per neuron, total neurite length per neuron and total branch points per neuron were also measured. All data are presented as % from untreated control wells. (*, #) indicates significant difference from control group ($P < 0.05$).

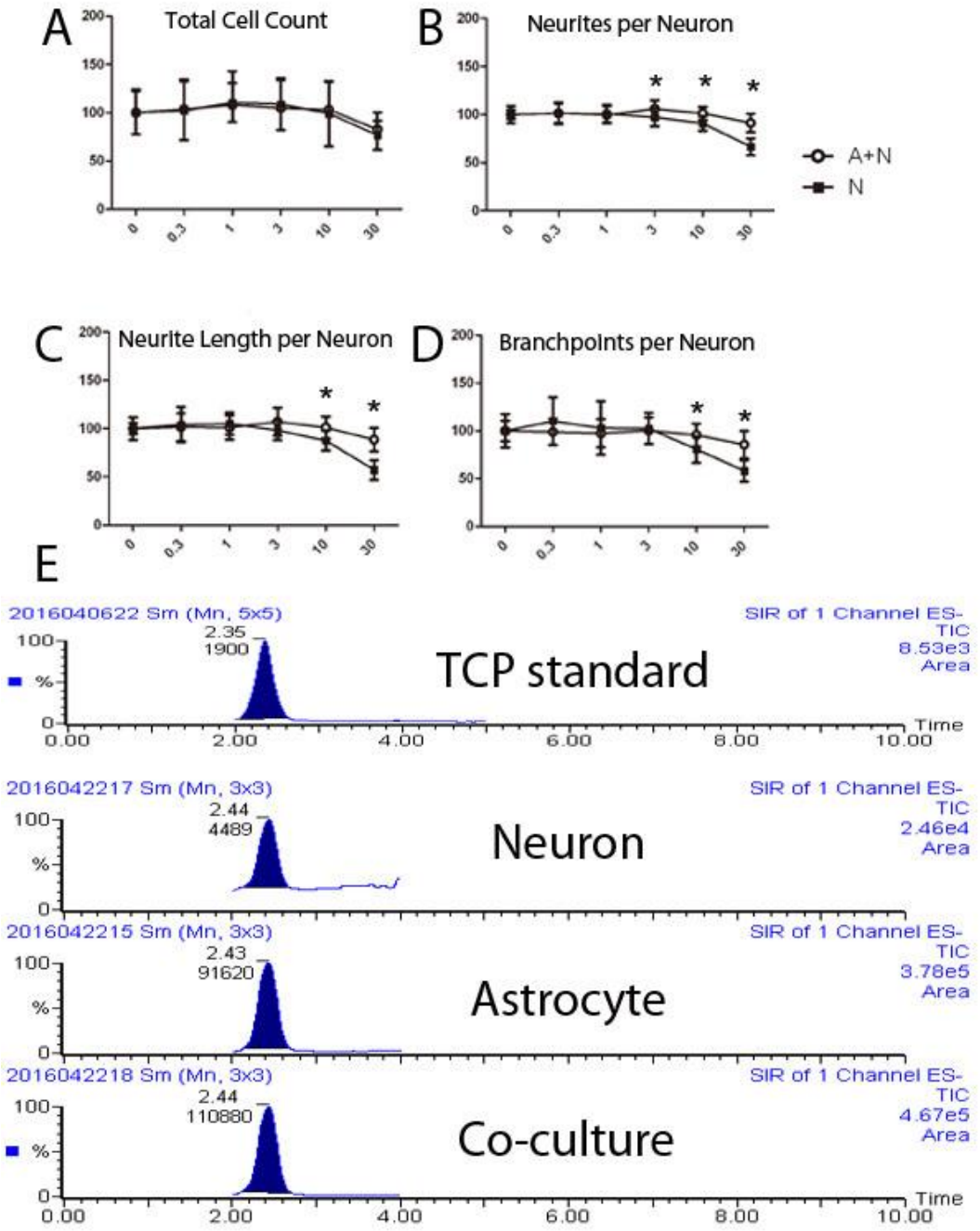

Fig. 4.3 Quantification of chlorpyrifos toxicity in DIV 28 neuron and co-cultured group. Human neuron (10,000 cells/well) was separately and co-cultured with astrocyte (10,000 astrocyte & 10,000 neuron) for 48 hours and fixed for immunofluorescent staining. Cells were seeded at 15,000 cells per well in 6 well plate for metabolite analysis. A) Total neuron density (cell density) was counted as an indicator of cell viability. B, C, D) neurite outgrowth parameters were measured. All data are presented as % from untreated control wells. (*) indicates significant difference between co-culture and neuron group at the same concentration ($P < 0.05$). E) Quantification of chlorpyrifos metabolite TCP in neuron, astrocyte and co-culture medium after 48h exposure to chlorpyrifos(10µM).

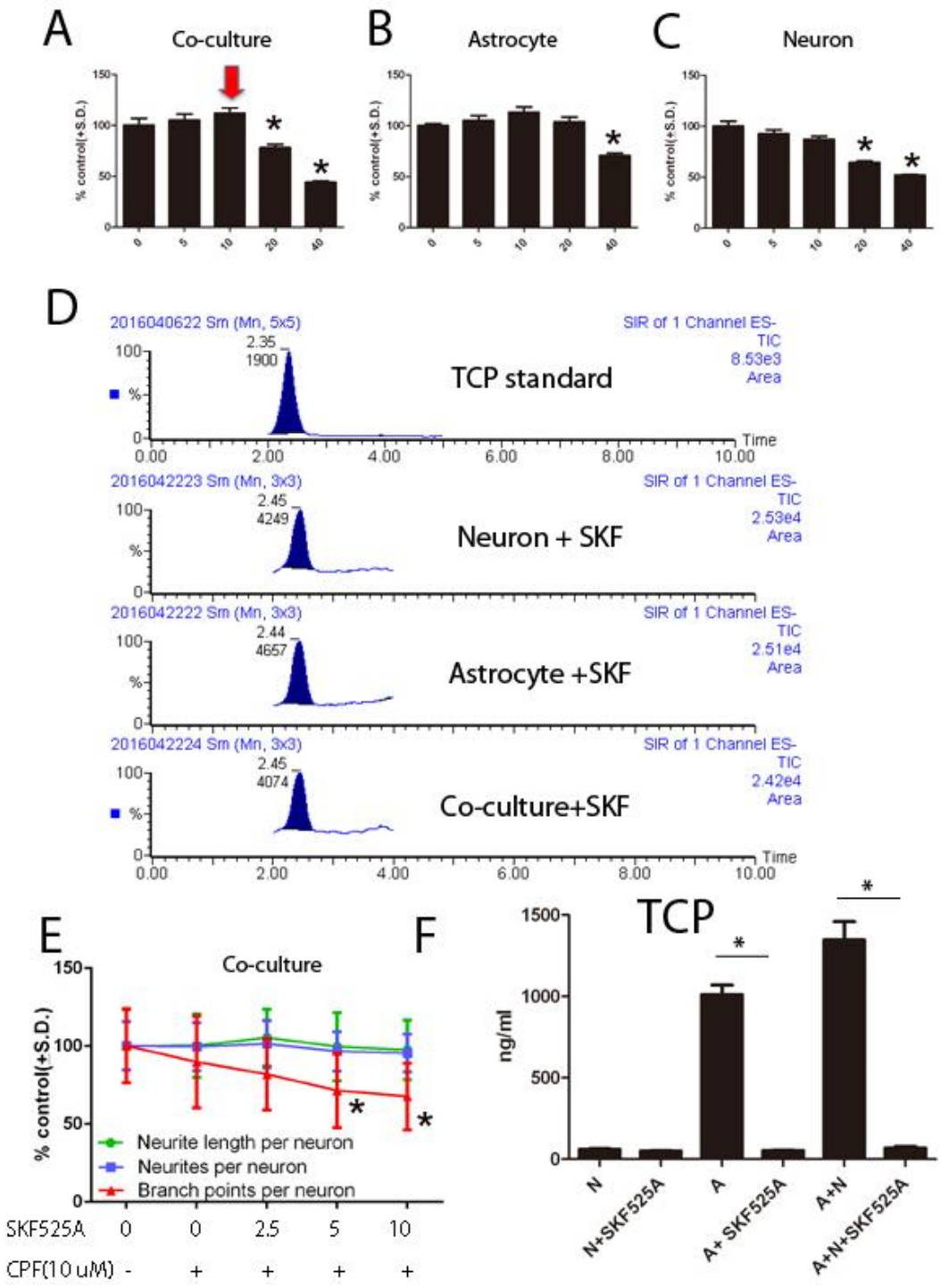

Fig. 4.4 SKF525A inhibited P450 activity and reverses astrocyte decreasing CPF toxicity effect. Human DIV 28 neuron, astrocyte and co-culture cells (10,000 cells/well, 10,000 astrocyte & 10,000 neuron in co-culture) were continuously exposed to CPF (10μM) and a range of doses of SKF525A for 48 hours. A) SKF525A exposure in co-culture medium for 48h. B) SKF525A exposure in astrocyte culture medium for 48h. C) SKF525A exposure in DIV 28 neuron culture medium for 48h. D) Quantification of chlorpyrifos metabolite TCP in DIV 28 neuron, astrocyte

and co-culture medium after 48h exposure to chlorpyrifos (10μM) and SKF525A (10μM). E) Statistical analysis of average number of neurites per neuron, total neurite length per neuron and total branch points per neuron in co-culture exposed to CPF (10μM) and a range of doses of SKF525A for 48 hours. F) Statistical analysis of TCP concentration in medium of neuron, astrocyte and co-culture with or without SKF525A (10 μM).

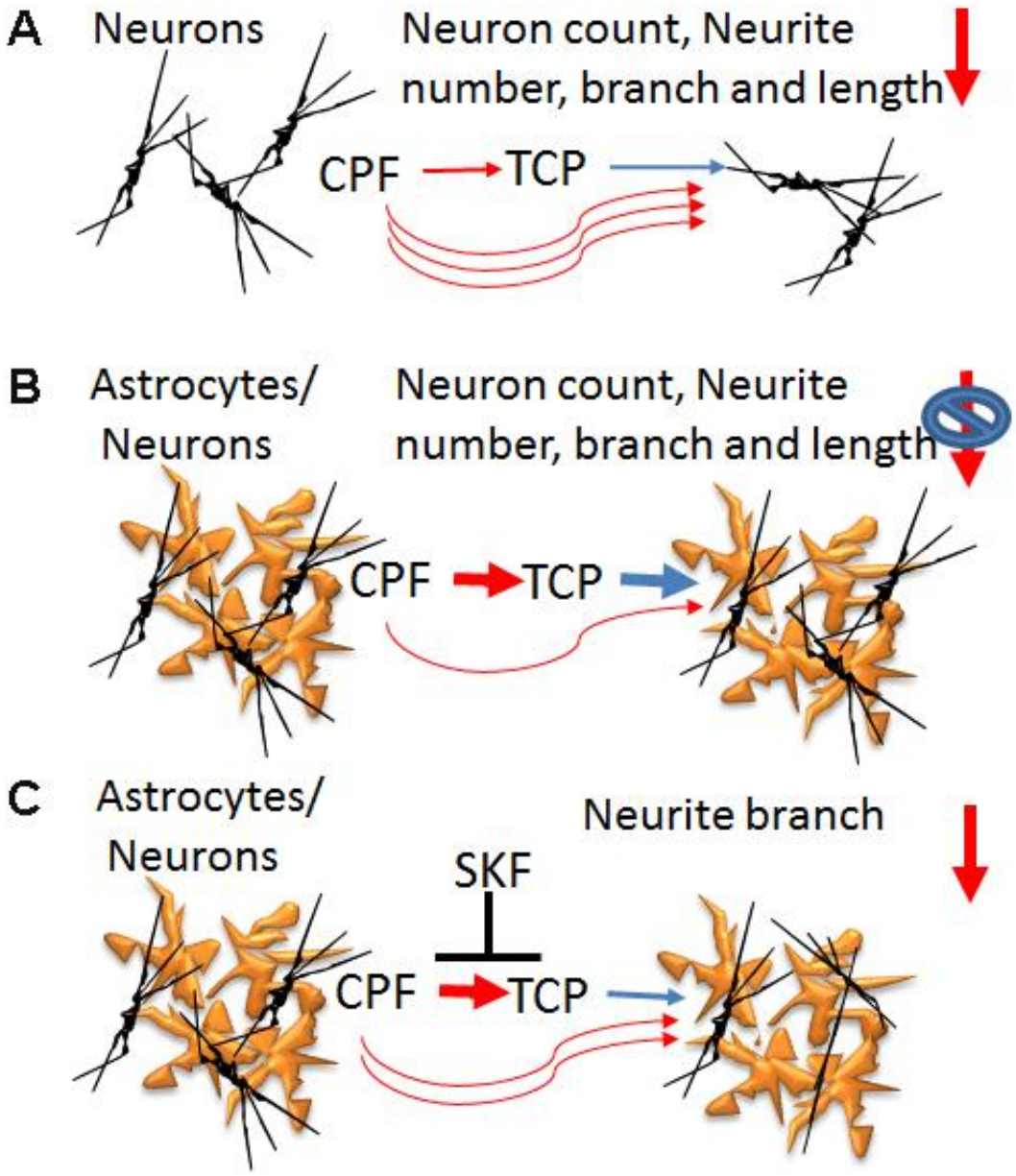

Fig. 4.5 Schematic diagram explaining possible mechanism of astrocyte reducing chlorpyrifos neurotoxicity. Chloypyrifos inhibited average number of neurites per neuron, total neurite length per neuron and total branch points per neuron as well as neuron density when exposed to DIV 28 neural cells. Astrocyte metabolized chloypyrifos to TCP and thus reduced the toxic effect of chlorpyrifos on neurite outgrowth and branching. Inhibition of P450 in astrocyte reduced chlorpyrifos metabolism and leaded to branching inhibition in co-culture.

CHAPTER 5

Conclusion

The goal of this dissertation was to study hESC derived neurons and astrocytes as complex multicellular in vitro developmental neurotoxicity testing platform (neuron proliferation, maturation, functional neurite outgrowth) for investigating potential toxins during early human neural windows of susceptibility.

Previously, different cell lines or primary cells have been used for neurotoxicity screening. Human ESC have been differentiated to neuron cells for neurotoxicity screening. Human ESCs are certain advantages over other cells. Primarily, hESC provide an unlimited source and no species interruption for risk assessment. Cryopreserved human neuronal cells from hESC had been developed for acute neurite outgrowth assay and successfully demonstrate the neurotoxicity events. However, development of reliable high purity neuron cells and human in vitro differentiation model of neurite formation from neurite initiation to elongation is still a challenge.

To solve the problem and achieve the goal of this dissertation, we have differentiated neurons from hNP cells at different stages and characterized the cells with different neural marker (HuC/D, beta III tubulin, MAP2) for three different in vitro neurotoxicity high through screening systems. The model we developed has potential for developmental neurotoxcity (DNT) screening and also to study astrocyte effect on neuron protection when exposed to neurotoxins.

Study 1: High content imaging quantification of multiple in vitro human neurogenesis events after neurotoxin exposure

To develop in vitro neural differentiation model, we started with hNP cells from hESC and differentiated them with leukemia inhibitory factor. Quantification result with post-mitotic neural marker HuC/D indicated that hNP cells gradually ceased proliferation and started differentiation to neuron cells with neurite extension. Comparing to previous neurite recovery model, the exposure with the same chemical bisindolylmaleimide I from hNP cell to neural cells at DIV14 indicated higher sensitivity in this model, neurites were inhibited at 0.1 μM comparing to 10 μM in acute neurite recovery model. The model also characterized endocrine disruptor chemicals estradiol, testosterone and BPA neurotoxicity on neurite outgrowth and branching. Analysis of estrogen receptor indicated estradiol inhibition effect on neurite outgrowth was independent of estrogen receptor α. The DIV0- DIV14 in vitro neural differentiation model demonstrated neurotoxicity of endocrine disruptors during neuron development from hNP cells which was multipotent stage to neural cells at DIV14 which was postmitotic neuron cells.
In this neural differentiation model, we quantified neural proliferation and neurite extension and chose DIV 14 as endpoint for long term exposure. Our next step was to quantify the differentiation process from DIV0 to DIV14 with additional cellular marker like KI67 and then define endpoints of proliferation, neurite initiation and elongation stage in DIV0 to DIV14. Additionally, expose of more chemicals at beginning of each endpoint for acute or subacute risk assessment would help define different windows of susceptibility (WOS) and explain of uniquely sensitive WOS for each chemical.

Study 2: Quantitative assessment of endocrine disruptors, pesticides, and retinoic acid neurite outgrowth toxicity in embryonic stem cell derived neurons

After characterization of neural differentiation with post-mitotic marker HuC/D and found cells proliferation ceased at DIV 14, we further characterize cells with neuron marker MAP2. MAP2 is a neuron specific and restricted to the dendritic compartment of neural cells. MAP2 and neurite outgrowth both increased at DIV28 vs DIV14 despite minimal increase in HuC/D expression after DIV14. A training set of eight chemicals with known neurotoxicity was applied to this high throughput system screening model to determine the utility of DIV 28 neurons in neurite outgrowth assay for DNT. Surprisingly, we found that BPA had no effect at any dose exposed, which was in contrast to previous literature which indicate BPA neurotoxicity in animal model and cells [1-3]. However, Organization for Economic Cooperation and Development and U.S. Environmental Protection Agency guidelines for the study of developmental neurotoxicity states that there was no data to support BPA being a developmental neurotoxicant and there were no neurological or neurobehavioral effects at either high or low doses of BPA. Our BPA data concurs with recent findings.

In summary, the current model used a uniform MAP2 positive hESC derived neuron cells for neurotoxicity screening and proved to be sensitive for known neurotoxins. However, characterization of this novel cell type with functional neuron biomarker is still necessary to identify the corresponding location in brain and the receptor for glutamatergic, GABAergic, nicotinic, purinergic neurons. Since human neuron cells can be isolated from human brain or differentiated from pluripotent stem cells (either hESCs or iPSCs), another important question is to compare the sensitivity of each model in identifying existing known chemicals neurotoxicity.

Study 3: Human pluripotent stem cell derived astrocytes metabolize chlorpyrifos through cytochrome p450 and protect neuron neurite outgrowth inhibition

As shown with the previous studies, hNP cells differentiated from hESC offer a unique cell source for DNT assays. Astrocyte and neuron derived from hNP cells share the similar culturing condition and mimic CNS cell interaction when used as in vitro co-culture model. Recent studies have indicated that in vitro co-culture neurotoxicity test system may prove more relevant to human CNS structure and function than neuronal cells alone when astrocytes exist [5]. In our recently research, hESC derived astrocytes play an integral role in the maintenance of early neuron differentiation and neurite extension, and are also associated with neuroprotection when they are exposed to toxic substances.

Chlorpyrifos is organophosphate insecticide and affects the nervous system by inhibiting the breakdown of acetylcholine (ACh), a neurotransmitter. Cytochrome P450 enzymes (CYP) metabolizes chlorpyrifos to chlorpyrifos-oxon by replacing the sulfur group with oxygen. Chlorpyrifos-oxon is metabolized primarily to 3,5,6-trichloropyridinol along with diethylphosphate and diethylthiophosphate [6]. In the CNS, the levels of various cytochromes P450 enzymes were reported to be expressed at relatively high levels in astroglial cells and may play a critical role in the biotransformation of endogenous or exogenous compounds [7, 8]. This study established an astrocyte and neuron co-culture system and identified a role for astrocytes in reducing chlorpyrifos DNT activity.

Chorpyrifos inhibited neurite outgrowth in a dose dependent manner during 48 hours' exposure. However, the chlorpyrifos neurotoxic effect was inhibited in astrocyte and neuron co-culture system. CYP inhibitor SKF525A partially reversed the protective effect of astrocytes by inhibiting branchpoint per neuron of chlorpyrifos (10μM) treatment. Metabolites analysis also

indicated that astrocyte metalized chlorpyrifos to TCP which was much less neurotoxic, while neuron cells did not significantly metabolize chlorpyrifos to TCP. For the first time, we have established human hESC derived astrocyte and neuron co-culture model and potentially identified a key role for P450 activity in astrocyte neuroprotection.

Since we found a vital role of P450 in chlorpyrifos metabolism in astrocyte, it will be important to further identify subtypes of P450 involved in metabolism. Also P450 activity can be induced in the presences of some chemicals in vivo, identification of P450 expression and activity level pre or post chlorpyrifos treatment could be performed to identify hESC derived astrocyte function. Astrocyte and hepatocyte chlorpyrifos metabolism comparisons is another direction to work toward for chlorpyrifos physiologically based pharmacokinetic modelling study and risk assessment.

Future directions

There are more than 7 million recognized chemicals in existence right now, and approximately 80,000 of them are in common use worldwide (General Accounting Office (GAO)). However, most heavily used chemicals in commerce are largely untested and their safety is a significant concern. Some environmental chemicals result in damage to the developing brain in both humans and animals and also lead to some form of neurodevelopmental abnormality. Therefore, routine testing of all chemicals with potential for human exposure is warranted. In our hESC derived neuronal models, we characterized BPA, estradiol and testosterone long term exposure neurotoxicity in DIV 0 to DIV 14 in vitro neural differentiation model and in the DIV 28 neural cell acute exposure screening model using a an 8 chemical training set. In these models, we confirmed their neurotoxicity on cell viability and neurite outgrowth and found novel mechanism such as estradiol estrogen receptor (ER) independent toxicity. However, to validate the models and apply the model for potential neurotoxins more chemicals need to be used in the assay. Known developmentally neurotoxic chemicals with well-established relationships between exposure and neurological disorders are a good starting point, such as lead, methyl mercury, and ethanol. These well studied neurotoxins have previously been shown to inhibit neurite outgrowth in both primary rodent neural cultures and cell lines and can be standard compounds to evaluate a new assay [9-11]. Also, evaluation of the predictive ability of a new assay requires a set of chemicals that have been shown to alter brain development after in vivo exposure (“test set”). Currently, approximately 100 developmental neurotoxicity test set chemicals were identified, with 22% having evidence of DNT in humans [12].

In order to build adverse outcome (AOP) pathway of each know neurotoxins, molecular initial events should be characterized in our hESC derived neuron models by methodology that

includes metabolomics for signaling pathway analysis or receptor binding assay. Integrating data of molecular initial event and cellular level change with animal data would strongly provide the AOP information for other similar chemical characterization.

Further characterization of electrophysiological activity and synapse formation in DIV28 neuron or neurons co-cultured with astrocyte are necessary for functional analysis. Synaptogenesis is a critical process in nervous system development whereby neurons establish specialized contact sites which facilitate neurotransmission. Synaptogenesis and synapse pruning are associated with autism initiation [13]. Astrocyte provides brain's extracellular matrix and they are involved in regulating the sprouting and pruning of synapses, which represents an important morphological correlate of synaptic plasticity in the adult nervous system [14]. Currently, in vitro rodent primary mixed cortical cultures including neuron and astrocyte has been developed for synapse formation assays [15]. During the first 15 days in vitro culture, cortical neurons developed a network of polarized neurites (i.e., axons and dendrites) and expression of the pre-synaptic protein synapsin increased over time [15]. Measurement of synapsin formation provided greater sensitivity than cell counts in detecting the adverse effects of known synaptogenic inhibitors in this study. The in vitro synapse formation measurement provided specific endpoint and could be an ideal assay to characterize neurotoxins target on synaptogenesis and this morphological changes correlated to electrophysiological activity. Microelectrode arrays (MEAs) have been applied in primary cortex neural culture in rat to explore the toxicological effects of numerous compounds on spontaneous activity of neuronal cell network [16]. The assay of neurite outgrowth and synaptogenesis combined with MEAs will efficiently identify neurotoxins window of susceptibility. Providing astrocytes are required for synaptogenesis, the structural maintenance and proper functioning of synapses. Thus astrocyte

and neuron co-culturing model could potentially be a complex model for not only neurite outgrowth morphology analysis but also for neuron function assay such as synaptogenesis. Human ESC derived neuron and astrocyte could provide defined population for quantification of synapse formation. And the species difference could be an issue, of which hESC could be a solution for in vitro synaptogenesis assay development.

In previous neuron and astrocyte co-culturing model, we found that astrocyte increased neurite elongation which indicate the astrocyte provide growth factors for neuron maturation. Further study focusing on astrocyte secreting factor could further explain the mechanism of its role in neurite elongation.

In the neuron and astrocyte co-culturing model, we identified a neural protective role for astrocytes via P450 enzyme of chlorpyrifos. We found astrocytes metabolized chlorpyrifos to TCP, while little chlorpyrifos was metabolized by neuron cells. The different results indicated the different levels and activity of P450 in CNS cells. Thus characterization of P450 activity in the embryonic stem cells is important to further understand the different subtypes which are involved in different chemical metabolism. Since several P450 enzyme subtypes including CYP1A2, 2C, 2D6, 3A4/5 are involved in chlorpyrifos metabolism to TCP in human hepatocytes [17], it will be important to identify the subtype of P450 in astrocyte and whether this correlates with hepatocyte metabolism. If compound metabolism mechanisms are cell type or organ specific, new more representative DNT analysis of compounds may be required for AOP studies and both astrocytes and hepatocytes may need to be included in larger DNT compound screening campaigns.

References

1. Seki, S., et al., *Bisphenol-A suppresses neurite extension due to inhibition of phosphorylation of mitogen-activated protein kinase in PC12 cells.* Chemico-Biological Interactions, 2011. **194**(1): p. 23-30.
2. Lee, Y.M., et al., *Estrogen receptor independent neurotoxic mechanism of bisphenol A, an environmental estrogen.* Journal of Veterinary Science, 2007. **8**(1): p. 27-38.
3. Masuo, Y. and M. Ishido, *Neurotoxicity of Endocrine Disruptors: Possible Involvement in Brain Development and Neurodegeneration.* Journal of Toxicology and Environmental Health-Part B-Critical Reviews, 2011. **14**(5-7): p. 346-369.
4. Beronius, A., et al., *The influence of study design and sex-differences on results from developmental neurotoxicity studies of bisphenol A: implications for toxicity testing.* Toxicology, 2013. **311**(1-2): p. 13-26.
5. Woehrling, E.K., E.J. Hill, and M.D. Coleman, *Development of a neurotoxicity test-system, using human post-mitotic, astrocytic and neuronal cell lines in co-culture.* Toxicology in Vitro, 2007. **21**(7): p. 1241-1246.
6. Lee, S., et al., *Effects of Nicotine Exposure on In Vitro Metabolism of Chlorpyrifos in Male Sprague-Dawley Rats.* Journal of Toxicology and Environmental Health-Part a-Current Issues, 2009. **72**(2): p. 74-82.
7. Malaplate-Armand, C., B. Leininger-Muller, and A.M. Batt, *Astrocytic cytochromes p450: an enzyme subfamily critical for brain metabolism and neuroprotection.* Revue Neurologique, 2004. **160**(6-7): p. 651-658.
8. Meyer, R.P., et al., *Possible function of astrocyte cytochrome P450 in control of xenobiotic phenytoin in the brain: In vitro studies on murine astrocyte primary cultures.* Experimental Neurology, 2001. **167**(2): p. 376-384.
9. Bearer, C.F., et al., *Ethanol inhibits L1-mediated neurite outgrowth in postnatal rat cerebellar granule cells. (vol 274, pg 13264, 1999).* Journal of Biological Chemistry, 1999. **274**(28): p. 20046-20046.
10. Parran, D.K., S. Barone, and W.R. Mundy, *Methylmercury decreases NGF-induced TrkA autophosphorylation and neurite outgrowth in PC12 cells.* Developmental Brain Research, 2003. **141**(1-2): p. 71-81.
11. Harrill, J.A., et al., *Comparative sensitivity of human and rat neural cultures to chemical-induced inhibition of neurite outgrowth.* Toxicology and Applied Pharmacology, 2011. **256**(3): p. 268-280.
12. Mundy, W.R., et al., *Expanding the test set: Chemicals with potential to disrupt mammalian brain development.* Neurotoxicology and Teratology, 2015. **52**: p. 25-35.
13. Tang, G.M., et al., *Loss of mTOR-Dependent Macroautophagy Causes Autistic-like Synaptic Pruning Deficits (vol 83, pg 1131, 2014).* Neuron, 2014. **83**(6): p. 1482-1482.
14. Faissner, A., et al., *Contributions of astrocytes to synapse formation and maturation - Potential functions of the perisynaptic extracellular matrix.* Brain Res Rev, 2010. **63**(1-2): p. 26-38.
15. Harrill, J.A., B.L. Robinette, and W.R. Mundy, *Use of high content image analysis to detect chemical-induced changes in synaptogenesis in vitro.* Toxicology in Vitro, 2011. **25**(1): p. 368-387.
16. Cotterill, E., et al., *Characterization of Early Cortical Neural Network Development in Multiwell Microelectrode Array Plates.* J Biomol Screen, 2016. **21**(5): p. 510-9.

17. Lee, S., et al., *Effects of nicotine exposure on in vitro metabolism of chlorpyrifos in male Sprague-Dawley rats.* J Toxicol Environ Health A, 2009. **72**(2): p. 74-82.